EXPLORATIONS OF ASPECTS OF MIXOTROPHY USING MATHEMATICAL MODELS

by

KENNETH W. CRANE

Presented to the Faculty of the Graduate School of
The University of Texas at Arlington in Partial Fulfillment
of the Requirements
for the Degree of

DOCTOR OF PHILOSOPHY

THE UNIVERSITY OF TEXAS AT ARLINGTON
August 2010

ACKNOWLEDGEMENTS

This work could not have been completed without the financial support of the Biology Department and the University in the form of teaching assistantships and fellowships. I especially want to thank the Graduate School for providing the Graduate Dean's Dissertation Fellowship that made the completion of this dissertation possible. My supervising professor, James P. Grover, made the completion of this work possible with advice on academics, research topics and methodologies, writing, and the funding of a research assistantship. I would also like to thank the other members of my committee, Thomas Chrzanowski, Laura Gough, Hristo Kojuharov, and Laura Mydalrz, for their time and advice. Finally, the financial and moral support of my family was essential to the completion of this challenge.

July 8, 2010

ABSTRACT

EXPLORATIONS OF ASPECTS

OF MIXOTROPHY USING

MATHEMATICAL

MODELS

Kenneth W. Crane, Ph.D.

The University of Texas at Arlington, 2010

Supervising Professor: James P. Grover

This work examined three theoretical aspects of mixotrophy, the simultaneous use of phototrophic and heterotrophic nutritional modes, and one practical application. The first study addressed the coexistence of microorganisms pursuing diverse nutritional strategies. It was found that in the range of model environments explored that all four types of organisms were predicted to persist for certain parameter combinations. The most successful mixotrophs were predicted to be primarily autotrophic, supplementing photosynthesis with bacterivory. The second study extended the first one by focusing on the effects of environmental parameters governing resource supplies and the responses of populations and ecosystem properties in relation to relative supplies of light and phosphorus. The model generally predicts that mixotrophs are abundant under wide ranges of resource supplies and leave a signature on the properties of aquatic ecosystems, such as phosphorus recycling. The third study further extends the model by incorporating seasonal variations in physiology. The densities of organisms and their growth limitations in response to this seasonal forcing were analyzed, along with the ecosystem

properties of phosphorus flux and the C:P ratios of the organisms. The predictions of this seasonal model suggest that mixotrophs change the growth limitations of other organisms, and increase the recycled P flux in the microbial food web. The final study examined the consequences of adding mixotrophy to a model for *Prymnesium parvum*, a harmful algal species that forms blooms in Texas in the winter. This modified model was unable to account for the winter increase in the *P. parvum* population in Texas. Overall, this work gives insights into the role of mixotrophy in aquatic microbial communities.

TABLE OF CONTENTS

LIST OF FIGURES

LIST OF TABLES

CHAPTER 1

INTRODUCTION

In aquatic systems microbes pursuing different nutritional strategies often coexist. Heterotrophs consume organic matter from the environment. Phototrophs, on the other hand, do not consume organic matter, and instead use the sun's energy to produce their own organic material. Heterotrophs can either consume dissolved matter or they can consume other organisms. Then there is one other curious strategy in which organisms simultaneously mix these two nutritional forms. These organisms, mixotrophs, can simultaneously utilize the sun's energy for photosynthesis while also consuming organic matter from the environment. This strategy would intuitively seem to be better than being a pure heterotroph or a pure autotroph. The ability to pursue these two strategies simultaneously, however, comes at the cost of having to maintain a set of cellular machinery for both of them.

Theoretically, there are situations where maintaining this balance can be advantageous. Troost et al. (2005a) have argued that mixotrophy is advantageous when the environment is oligotrophic, with low resources, and that specialization on heterotrophy or phototrophy is better in eutrophic, high resources, conditions. In fact, eukaryotic phytoplankton are hypothesized to have obtained their plastids through endosymbiosis that likely occurred during a time when the environmental conditions favored mixotrophy (Litchman 2007). This means that phagotrophy in eukaryotic phototrophs is a primary characteristic, and that the inability to phagocytize in some lineages is a derived character (Raven 1997). Sometimes it is advantageous to keep both characteristics. Kamjunke et al. (2007) described the competitive advantage that bacterivory gave a mixotrophic flagellate during the re-oligotrophication of Lake Constance. However, keeping both characteristics comes at a cost. Raven (1997) discusses the cost to benefit ratio of each type of machinery. It takes about 50% of a cell's energy to maintain chloroplasts, while it

takes about 10% to maintain phagotrophy. Therefore, it is more “costly” to be a photosynthetic protozoan than a phagotrophic alga (Stoecker 1998). She notes that this may explain why there is widespread phagotrophy among phytoflagellates, but a rarity of plastids in zooflagellates. In fact, mixotrophy was found to be a widespread phenomenon in the oceans by Zubkoz and Tarran (2008). They found that plastidic cells derive about 25% of their nutritional needs from bacterivory and that these cells make up about 90% of the plankton and account for about 50% of the bacterivory in the oceans. An inevitable consequence of mixotrophy is a complex web of interactions in aquatic communities. For example, Rothaupt (1996) looked at the interactions of an obligate heterotroph, a phototroph, and a mixotroph. His conclusion was that because mixotrophs could use substitutable carbon and phosphorus resources, but could not outcompete specialists on these resources, all three types of microbes could coexist in low resource environments. Tittel et al. (2003) described the complex interactions of mixotrophs, phagotrophs, and prey to explain the deep chlorophyll maximum, where there is an accumulation of phototrophs at subsurface strata, found in oligotrophic lakes. They found that even though mixotrophs were inferior competitors with phagotrophs for prey, in the illuminated surface waters they were able to reduce the prey population to lower levels than those where competing heterotrophic specialists could survive.

H. L. Jones (1997) created a conceptual model of mixotrophs and classified them based on their behavior in their utilization of resources. She placed them into one of four groups (A,B,C,D) based on their primary nutritional mode (heterotrophy or phototrophy) and then by the use of heterotrophy based on light levels. Another attempt to classify mixotrophs was undertaken by Stoecker (1998). In her work, mixotrophs are classified into three types depending on their primary nutritional mode (phagotrophic, photosynthetic, or balanced) and then divided into groups depending on how the nutritional modes are utilized in response to some necessity e.g. light, prey, or limiting nutrient. R. I. Jones (2000) later looked at the role of these mixotrophs in terms of nutrient flux and created a summary of the groups created by H.L. Jones and then looked at the role mixotrophs play in the nutrient flux of planktonic systems.

Sterner and Hessen (1994) described the importance of the mineral content of the prey of herbivores saying that the herbivore's growth was not always limited by the quantity of prey, but often by the quality of the mineral content in the prey. This idea was later extended to include the influence of light on the mineral content of photosynthetic organisms (Sterner et. al. 1997). Photosynthetic organisms utilize light and inorganic carbon to create organic carbon. The mineral content of the photosynthetic organisms was characterized in terms of the ratio of carbon to phosphorus (C:P) and this was described as being directly proportional to the ratio of light available for photosynthesis and the P content of the environment. This is referred to as the light:P hypothesis. Combining the importance of the mineral content of prey and the light:P hypothesis, predictions can be made about the limiting nutrients to growth for organisms in an ecosystem. Chrzanowski and Grover (2001a) extended the light:P hypothesis to include the seasonal variation in light and its impact of the growth limitations of planktonic aquatic organisms and other properties of the ecosystem.

As the seasons change, dark winters change to bright summers. Higher incident light increases photosynthesis and leads to increased C production in photosynthetic organisms. Photosynthetic organisms switch from being light-limited in the dark winter to being P-limited in the summer. The C:P ratio of the organisms should rise with the increase in organic C production by the photosynthetic organisms. Prey organisms with high C:P ratios indicate lower quality food for the herbivores (Sterner 1994). When photosynthetic organisms have excess light in relation to P supply, they produce excess photosynthate that is released into the environment as DOC (Bratbak and Thingstad 1985). With an increase in DOC, which then can be taken up by bacteria, the bacteria then also become more-P limited in the summer. The C:P ratios of the organisms would also be expected to decrease with increasingly eutrophic conditions, as more P became available for microbial uptake. The recycling of P by consumers should also increase as the supply of P relative to light increases. Food richer in P, with lower C:P ratio, is more likely to provide P in excess of consumer assimilation (Elser and Urabe 1999).

There are few theoretical examinations of the role of mixotrophy in these complex interactions with other organisms (Burkholder 2008). Thingstad et al. (1996) created a mathematical model that looked at the interactions of four populations of plankton with different nutritional strategies (specialized autotroph, mixotroph, bacteria, and specialized phototroph) and having differing affinities for nutrients and prey. With this model, they were not able to get all four nutritional types to coexist. However, populations of plankton pursuing these different nutritional strategies are able to coexist in nature, a fact which remains unexplained theoretically. Stickney et. al. (2000) created a model that examined the interactions of a phytoplankton, zooplankton, and mixotroph. In this model the mixotrophs are consumers of the phytoplankton and the zooplankton are consumers of the phytoplankton and mixotrophs. There were two resources of light and a limiting nutrient. With the interactions described, they were able to achieve coexistence of all three organisms. Flynn and Mitra (2009) created a model of the physiology of mixotrophs where he tried to discover the combinations of resource use that would create the "perfect beast" that could combine resources and outcompete all others. In reality, there are costs to trying to do it all. Another model sometimes mentioned in the literature was created by Hammer and Pitchford (2005). In this work, they created a model where they examined different types of mixotrophs and their effects on a phytoplankton and zooplankton system. They concluded that the presence of mixotrophs reduced the potential for bloom formations.

It is the role that mixotrophy plays in bloom formations that has led to the increase in its study. Though the fact that mixotrophy is widespread in the world should make it important to study (Zubkov and Tarran 2008), it is the link to harmful algal blooms (HABs) that has really increased its study. Burkholder (2008) reviewed harmful algal species (HASs) and found that all of the ones reviewed were mixotrophs. One particular HAS has garnered attention in Texas due to its tendency to form HABs and cause large fish kills. *Prymnesium parvum* is a mixotorphic species first described by Carter (1937) and is commonly referred to as "golden algae." Baker et al. (2007) described the growth of *P. parvum* in terms of temperature, light, and salinity. Mathematical models of the growth of *P. parvum* were created by Grover et al. (2010). In these

models, the growth curve that Baker et al. described is used for *P. parvum*, but growth is described in terms of photosynthetic growth only and there are two limiting nutrients. Seasonal inputs of environmental properties are based on field observations made by D. L. Roleke at Lake Granbury in Texas. This model predicts the P. parvum density to be at its minimum in late winter. This is the time of year when the natural population forms HABs. Carvalho and Grane´li (2010) have recently shown that phagotrophy in *P. parvum* is a permanent nutritional adaptation. The lack of phagotrophy in the current model could be a contribution to the inability of the model to make predictions that reflect the natural population.

This dissertation uses mathematical models to explore aspects of mixotrophy. There are four studies developed here. The first study involves a model that includes four dynamic populations of organisms. The populations include phototrophic algae that utilize photosynthesis, heterotrophic bacteria that take up inorganic nutrients from the environment, heterotrophic zooflagellates that consume bacteria, and mixotrophs that combine phototrophy and heterotrophy in response to a parameter α that is the proportion that the mixotroph utilizes photosynthesis. This was the parameter that was varied in this study. The mixotrophs were placed in a variety of environments to explore coexistence with the other nutritional types and the most successful type of mixotroph in terms of the α parameter and the type of environment. The second study uses the previously developed model, but fixed the α parameter and varied the environmental parameters. The simulations were run to a steady state with constant environmental supplies. Results were examined in terms of coexistence of all four nutritional types, growth limiting nutrients, and the ecosystem properties of total C:P of the organisms, excess P released by consumption, and the DOC of the ecosystem. The third study changes this model to include seasonal variation in light and temperature and their effects on nutrient uptake, growth, and attack rates. Variations in P supply were also included. The results of the numerical simulations were examined for seasonal variations in the densities of the organisms, their coexistence, and seasonal effects on the aforementioned ecosystem properties. The fourth and final study creates

a much revised model of *P. parvum* dynamics from one of the current models for *P. parvum* growth that incorporates mixotrophy in terms of a dynamic population of bacterial prey. The seasonal densities of these populations and the effects of altering parameters that affected mixotrophy were explored.

CHAPTER 2

COEXISTENCE OF MIXOTROPHS, AUTOTROPHS, AND HETEROTROPHS IN PLANKTONIC MICROBIAL COMMUNITIES

2.1 Introduction

Mixotrophy is the capability to utilize both autotrophic and heterotrophic modes of nutrition. The best-known and most widely-distributed mixotrophs are relatively small, unicellular flagellates with functional chloroplasts that also ingest particulate matter through phagotrophy (Stoecker 1998). Usually, heterotrophic bacterioplankton or other very small microbes are thus ingested. Such mixotrophic organisms are represented in several algal taxa (Graham and Wilcox 2000), occur widely in inland waters and oceans, and are globally significant consumers of bacteria (Zubkov and Tarran 2008). Often, they co-occur with purely heterotrophic microorganisms that live entirely by consuming particulate matter, again usually bacterial prey (Porter et al. 1985). Mixotrophs and heterotrophs that prey on bacteria also often co-occur with pure autotrophs that photosynthesize and do not consume organic matter. This study focuses on the ecological circumstances under which mixotrophs consuming bacterial prey can coexist with three other, nutritionally distinct types of microorganisms: heterotrophic bacteria that consume dissolved organic matter, heterotrophic zooflagellates consuming bacterial prey, and photosynthetic algal microorganisms.

Although these four types of microorganisms pursue different nutritional strategies, they overlap partially in their resource use (Figure 2.1). Mixotrophs and zooflagellates both consume bacterial prey. Mixotrophs also consume inorganic nutrients and light when growing photosynthetically, as do algae. Thus mixotrophs are generalists competing for resources shared with two different specialists. The bacterial prey of mixotrophs and zooflagellates, like mixotrophs

and algae, consume inorganic nutrients. Bacteria also consume dissolved organic matter, which is often produced as a consequence of photosynthesis by both algae and mixotrophs. Zooflagellates excrete inorganic nutrients that are then consumed by bacteria, mixotrophs, and algae. Thus there is a complex web of competitive, and possibly commensalistic or facilitative, resource-based interactions among mixotrophs and microorganisms pursuing other nutritional strategies (R. I. Jones 2000). As a further complication, the mixotrophic blend of two nutritional strategies (heterotrophic and autotrophic) falls along a spectrum of proportions for different organisms (H. L. J. Jones 1997; Stoecker 1998; R. I. Jones 2000).

Previous theory has addressed some aspects of coexistence of mixotrophs and other microorganisms. Thingstad et al. (1996) examined coexistence of mixotrophs, zooflagellates, bacteria and algae under limitation by a single nutrient resource, using a generalized Lotka-Volterra model. Mixotrophs were modeled with a tradeoff in affinities for heterotrophic and autotrophic resources. Coexistence of all four nutritional types was not possible, and persistence of mixotrophs was favored by high affinity for the nutrient combined with intermediate affinity for bacterial prey. Kooijman and colleagues have used the Dynamic Energy Budget formalism to address evolutionary issues in mixotrophy, though not in the context of a dynamic microbial food web. The symbiotic merger of free-living heterotrophs and autotrophs into a single mixotroph is favored when each uses products excreted by the other (Kooijman et al. 2003, 2004), a transition that took place early in the evolution of bacterivorous mixotrophs (Hackett et al. 2007). Troost et al. (2005a, b) found that intense mixing in a vertical light gradient could promote the opposite transition – the evolutionary divergence of a mixotroph into specialized autotrophs and heterotrophs – which has also been common in the evolution of protists (Fehling et al. 2007).

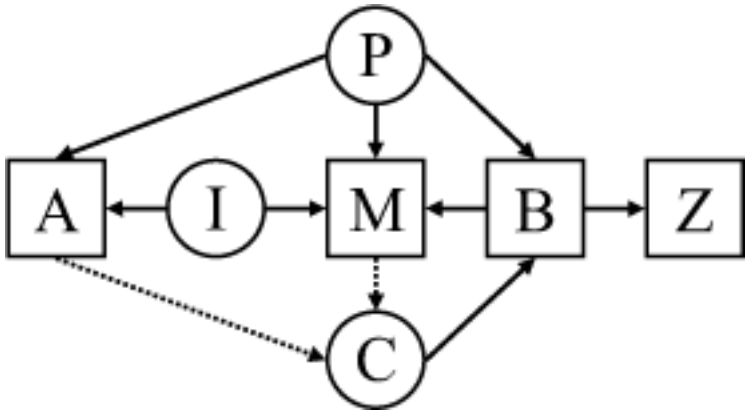

Figure 2.1 Resource interactions involving four microbial nutritional types. The boxes indicate organisms and are labeled A for algae, M for mixotrophs, B for bacteria, and Z for zooflagellates. The circles indicate resources and are labeled I for light, C for organic carbon, and P for inorganic phosphorus. The solid arrows indicate flows of resources. The dashed arrows indicate the release of excess photosynthate that occurs when autotrophs are growing under P limitation. The return of C and P to the resource pools by the organisms occurs but is not shown.

The model we present here goes further than its predecessors in several respects. Like Thingstad et al. (1996), we focus on ecological coexistence of mixotrophs, zooflagellates, bacteria and algae, but allow three basal resources: light, dissolved organic carbon (C), and an inorganic nutrient, taken here to be phosphorus (P). Furthermore, we examine a spectrum of mixotroph types, ranging from heterotrophy to autotrophy as a parameter (α) increases, and a vertical light gradient. We also allow for variable nutrient content of all nutritional types, which was not generally done in previous studies. To accomplish this we build on related models constructed for the specialist nutritional strategies of zooflagellates, bacteria, and algae (Grover 2003, 2004; Berger et al. 2006; Diehl 2007). In common with previous work on mixotrophs, we assume that they are less competitive than specialist zooflagellates for bacterial prey, and less competitive than specialist algae for inorganic resources. This assumption is consistent with observations that mixotrophs tend to dominate over specialist nutritional types only under limitation by multiple resources that favors generalists (Rothhaupt 1996; Tittel et al. 2003; Katechakis and Stibor 2006).

2.2 Model Formulation

We first present the equations governing the specialist strategies of the algae and zooflagellates. Then, we present those for the mixotrophs because they are described by a blend of these equations using a parameter α, the proportion that the mixotroph uses autotrophic means for nutrition. The equations follow for the bacteria that serve as prey for the zooflagellates and mixotrophs. The symbols *A*, *Z*, *M*, and *B* are used both to represent the densities of algae, zooflagellates, mixotrophs, and bacteria respectively, and as indices to distinguish quantities specific to these nutritional types (Table 2.1). Finally, we present the equations that describe the nutrients in the environment.

2.2.1 Algae

The algae utilize photosynthesis for their carbon (C) requirement and take up dissolved phosphorus (P) from the environment. They are described by two differential equations.

$$\frac{dA}{dt} = (\mu_A - D - m_A)\,A \tag{2.1}$$

$$\frac{dQ_{PA}}{dt} = V_{PA}^{max}\left(\frac{P}{k_{PA}+P}\right)\left(\frac{Q_{PA}^{max}-Q_{PA}}{Q_{PA}^{max}-Q_{PA}^{min}}\right) - \mu_A Q_{PA} \tag{2.2}$$

The per capita rate of change of the density of the algae (*A*) (Eq.(2.1)) is the balance of growth (μ_A) minus dilution (*D*) and mortality (m_A). The rate of change of the algal P quota (Q_{PA}; Eq.(2.2)) is the balance of uptake from the environment minus the dilution due to reproduction ($\mu_A Q_{PA}$). The uptake rate in relation to dissolved phosphorus (*P*) follows a Michaelis-Menten equation with V_{PA}^{max} being the maximum uptake rate and k_{PA} the half-saturation constant. The uptake rate also decreases linearly as the phosphorus quota increases from the minimal value of Q_{PA}^{min} to the maximum value of Q_{PA}^{max}, where uptake ceases.

The growth rate of the algae (μ_A) (Eq. (2.3)) is the minimum of their potential C-dependent growth (μ_{CA}) or their potential P-dependent growth (μ_{PA}).

$$\mu_A = \min(\mu_{CA}, \mu_{PA}) = \min\left(\frac{\rho_A^{max}}{\omega z}\ln\left(\frac{k_{CA}+I_{in}}{k_{CA}+I_{out}}\right), \mu_A^{max}\left(1-\frac{Q_{PA}^{min}}{Q_{PA}}\right)\right) \tag{2.3}$$

$$\omega = k_{bg} + k_B B Q_{CB} + k_A A Q_{CA} + k_M M Q_{CM} + k_Z Z Q_{CZ} \tag{2.4}$$

$$I_{out} = I_{in}\, e^{-\omega z} \tag{2.5}$$

In equation(2.3), ω is the sum of all the shading that occurs in the water column. Shading (Eq.(2.4)) occurs from background turbidity (k_{bg}) and from organisms, proportional to their population density and C quota through a factor k_x, where the subscript *x* indicates the type of organism. The C quota thus indicates how dark an organism is due to its cellular mass, and the parameter k_x indicates the absorptive quality of cellular mass. Multiplying k_x by C quota and population density gives the total shading for each population. These are summed and then added to the background turbidity of the water (k_{bg}). I_{out} is calculated from equation (2.5).

Table 2.1 Notation and Parameter Values

Definition	Symbol	Value	Units
Algae:			
concentration	A	variable	cells m^{-3}
growth rate	μ_A	variable	d^{-1}
P-dependent growth rate	μ_{PA}	variable	d^{-1}
C-dependent growth rate	μ_{CA}	variable	d^{-1}
quota of P	Q_{PA}	variable	mol P $cell^{-1}$
uptake rate of dissolved P	V_{PA}	variable	mol P $cell^{-1}$ d^{-1}
maximal uptake rate for P	V_{PA}^{max}	2.0×10^{13}	mol P $cell^{-1}$ d^{-1}
minimal cell quota of P	Q_{PA}^{min}	2.7×10^{-15}	mol P $cell^{-1}$
maximal cell quota of P	Q_{PA}^{max}	3.2×10^{13}	mol P $cell^{-1}$
quota of C	Q_{CA}	3.8×10^{-12}	mol C $cell^{-1}$
half-saturation constant for P	k_{PA}	1.9×10^{-3}	mol P m^{-3}
half-saturation constant for light	k_{CA}	5.4	J s^{-1} m^{-2}
maximal growth rate	μ_A^{max}	1.0	d^{-1}
mortality rate	m_A	0.1	d^{-1}
shading coefficient	k_A	18	m^2 (mol C)$^{-1}$
maximum rate of photosynthesis	ρ_A^{max}	1.0	d^{-1}
efficiency at which photosynthate is lost	e_A	0.25	none
Zooflagellates:			
concentration	Z	variable	cells m^{-3}
growth rate	μ_Z	variable	d^{-1}
P-dependent growth rate	μ_{PZ}	variable	d^{-1}
C-dependent growth rate	μ_{CZ}	variable	d^{-1}
quota of P	Q_{PZ}	variable	mol P $cell^{-1}$
minimal cell quota of P	Q_{PZ}^{min}	3.0×10^{-15}	mol P $cell^{-1}$
maximal cell quota of P	Q_{PZ}^{max}	30.0×10^{-15}	mol P $cell^{-1}$
quota of C	Q_{CZ}	3.75×10^{-12}	mol C $cell^{-1}$
attack rate on bacteria	a_{BZ}	1.0×10^{-9}	m^3 $cell^{-1}$ d^{-1}
efficiency at which prey C is utilized	e_Z	0.6	none
maximal growth rate	μ_Z^{max}	6.0	d^{-1}
mortality rate	m_Z	0.1	d^{-1}
shading coefficient	k_Z	18	m^2 (mol C)$^{-1}$
Mixotrophs:			
proportion that mixotroph is photosynthetic	α	various	none
concentration	M	variable	cells m^{-3}
growth rate	μ_M	variable	d^{-1}
P-dependent growth rate	μ_{PM}	variable	d^{-1}
C-dependent growth rate	μ_{CM}	variable	d^{-1}
quota of P	Q_{PM}	variable	mol P $cell^{-1}$
uptake rate of dissolved P	V_{PM}	variable	mol P $cell^{-1}$ d^{-1}
maximal uptake rate for P	V_{PM}^{max}	2.0×10^{-13}	mol P $cell^{-1}$ d^{-1}

Table 2.1 - *Continued*

minimal cell quota of P	Q_{PM}^{min}	3.6×10^{-15}	mol P cell^{-1}
maximal cell quota of P	Q_{PM}^{max}	36.0×10^{-15}	mol P cell^{-1}
quota of C	Q_{CM}	4.56×10^{-12}	mol C cell^{-1}
half-saturation constant for P	k_{PM}	1.9×10^{-3}	mol P m^{-3}
half-saturation constant for light	k_{CM}	5.4	J s^{-1} m^{-2}
attack rate on bacteria	a_{BM}	1.0×10^{-9}	m^3 cell^{-1} d^{-1}
efficiency at which prey C is utilized	e_M	0.6	none
maximal growth rate	μ_M^{max}	1.0	d^{-1}
mortality rate	m_M	0.1	d^{-1}
shading coefficient	k_M	18	m^2 (mol C)$^{-1}$
maximum rate of photosynthesis	ρ_M^{max}	1.0	d^{-1}
efficiency at which photosynthate is lost	e_{MA}	0.25	none
Bacteria:			
population density	B	variable	cells m^{-3}
growth rate	μ_B	variable	d^{-1}
P-dependent growth rate	μ_{PB}	variable	d^{-1}
C-dependent growth rate	μ_{CB}	variable	d^{-1}
uptake rate of dissolved P	V_{PB}	variable	mol P cell^{-1} d^{-1}
quota of P	Q_{PB}	variable	mol P cell^{-1}
uptake rate of labile DOC	V_{CB}	variable	mol C cell^{-1} d^{-1}
maximal uptake rate for P	V_{PB}^{max}	4.8×10^{-16}	mol P cell^{-1} d^{-1}
maximal uptake rate for labile DOC	V_{CB}^{max}	9.54×10^{-15}	mol C cell^{-1} d^{-1}
minimal cell quota for P	Q_{PB}^{min}	1.0×10^{-17}	mol P cell^{-1}
maximal cell quota for P	Q_{PB}^{max}	2.0×10^{-17}	mol P cell^{-1}
quota of C	Q_{CB}	1.59×10^{-15}	mol C cell^{-1}
half-saturation constant for P	k_{PB}	1.0×10^{-5}	mol P m^{-3}
half-saturation constant for C	k_{CB}	1.0×10^{-3}	mol C m^{-3}
maximal growth rate	μ_B^{max}	6.0	d^{-1}
mortality rate	m_B	0.1	d^{-1}
shading coefficient	k_B	18	m^2 (mol C)$^{-1}$
gross growth efficiency	e_B	0.5	none
Environment:			
light intensity into the water column	I_{in}	various	J s^{-1} m^{-2}
supplied organic C	C_{in}	various	mol m^{-3}
supplied inorganic P	P_{in}	various	mol m^{-3}
background turbidity	k_{bg}	various	m^{-1}
depth	z	various	m
concentration of dissolved organic C	C	variable	mol m^{-3}
light intensity out of the water column	I_{out}	variable	J s^{-1} m^{-2}
total shading due to organisms and turbidity	ω	variable	m^{-1}
concentration of dissolved inorganic P	P	variable	mol m^{-3}
dilution rate	D	0.25	d^{-1}

$$\rho(I(s)) = \frac{\rho_A^{max} I(s)}{k_{CA} + I(s)} \tag{2.6}$$

$$\int_0^z \rho(I(s))ds = \frac{\rho_A^{max}}{\omega} \ln\left(\frac{k_{CA} + I_{in}}{k_{CA} + I_{out}}\right) \tag{2.7}$$

Photosynthesis at a given light level (Eq.(2.6)) is formulated as a Michaelis-Menten function of irradiance at a given depth (*s*), with ρ_A^{max} being the maximum C-specific rate of photosynthesis and k_{CA} the half saturation constant for light. The total photosynthesis (Eq.(2.7)) from the surface (*s*=0) to depth *s*=*z* is then found using a change in the variable of integration from depth to irradiance following Huisman and Weissing (1994), with I_{in} being the light intensity at the top of the water column and I_{out} the light intensity that leaves it at the bottom. Equation (2.7) is then divided by depth to make μ_{CA} the depth averaged photosynthesis. The parameter μ_{PA} depends on the quota of P contained in the cells with μ_A^{max} being the maximum growth rate for the algae that would occur if the P quota was infinite.

2.2.2 Zooflagellates

The zooflagellates obtain all of their nutrients from the consumption of the bacteria. They are also described by two differential equations.

$$\frac{dZ}{dt} = (\mu_Z - D - m_Z)Z \tag{2.8}$$

$$\frac{dQ_{PZ}}{dt} = a_{BZ} B Q_{PB} \frac{Q_{PZ}^{max} - Q_{PZ}}{Q_{PZ}^{max} - Q_{PZ}^{min}} - \mu_Z Q_{PZ} \tag{2.9}$$

The per capita rate of change in the density of the zooflagellates (Eq. (2.8)) is the balance of their reproductive growth (μ_Z) minus dilution (*D*) and mortality (m_Z). The rate of change in P quota (Q_{PZ}) is the gain from the predation of bacteria minus the dilution due to reproduction (Eq. (2.9)). The rate of predation depends on the attack rate of the bacteria by the zooflagellates (a_{BZ}) and the rate of P assimilation depends linearly on the quota of P in the

zooflagellates, decreasing as the quota goes from its minimal value ($Q_{PZ}^{\min}$) to its maximal value ($Q_{PZ}^{\max}$). The assumption of a variable P quota for zooflagellates was introduced by Grover (2003) based on the evolutionary affinity of phagotrophic flagellates with autotrophs known to have variable quotas. Here, the assumption of variable P quotas for autotrophs, heterotrophs, and mixotrophs enables the physiological properties of the latter to be smoothly related to the former.

$$\mu_Z = \min(\mu_{CZ}, \mu_{PZ}) = \min\left(a_{BZ}\, e_Z\, B\frac{Q_{CB}}{Q_{CZ}}, \mu_Z^{max}(1-\frac{Q_{PZ}^{min}}{Q_{PZ}})\right) \tag{2.10}$$

The growth rate of the zooflagellates (μ_Z) (Eq. (2.10)) is the minimum of their potential C-dependent growth (μ_{CZ}) or their potential P-dependent growth (μ_{PZ}). The C-dependent growth rate of the zooflagellates is the ingestion rate (the product $a_{BZ}B$) times the efficiency (e_Z) of zooflagellate assimilation of C times the ratio of the C quota in bacteria to the C quota in zooflagellates. The parameter μ_{PZ} is defined similarly to P-dependent growth for algae.

2.2.3 Mixotrophs

Since mixotrophy is the ability to use both heterotrophic and autotrophic modes of nutrition simultaneously, the parameter α is introduced to designate the proportion of autotrophic nutrition. The mixotrophs' total consumption of resources is a linear combination of consumption terms resembling the autotrophic terms of algae (with coefficient α) and the heterotrophic terms of zooflagellates (with coefficient 1 - α).

The mixotroph is assumed to have higher nutrient requirements than either the algae or the zooflagellates, because of its need to carry both autotrophic and heterotrophic machinery (Raven 1997), leading to a larger C quota and a larger minimal P quota. Otherwise, the consumption and growth terms used to represent mixotrophs are equivalent to the corresponding terms for algae and zooflagellates. The mixotrophs are governed by two differential equations.

$$\frac{dM}{dt} = (\mu_M - D - m_M)\, M \tag{2.11}$$

Equation (2.11) describes the per capita rate of change in the density of mixotrophs (*M*) as the balance of growth (μ_M) minus dilution and mortality (m_M).

$$\frac{dQ_{PM}}{dt} = \alpha V_{PM}^{max} \frac{P}{k_{PM}+P} \frac{Q_{PM}^{max}-Q_{PM}}{Q_{PM}^{max}-Q_{PM}^{min}} + (1-\alpha)\, a_{BM}\, B Q_{PB} \frac{Q_{PM}^{max}-Q_{PM}}{Q_{PM}^{max}-Q_{PM}^{min}} - \mu_M\, Q_{PM} \quad (2.12)$$

The rate of change in the P quota (Eq. (2.12)) is the sum of the gain from the uptake of dissolved P and the gain from predation on bacteria minus that diluted due to reproduction.

$$\mu_M = \min(\mu_{CM}, \mu_{PM}) = \min\Big(\alpha \frac{\rho_M^{max}}{\omega z} \ln\Big(\frac{k_{CM}+I_{in}}{k_{CM}+I_{out}}\Big) + (1-\alpha)\, a_{BM}\, e_M\, B \frac{Q_{CB}}{Q_{CM}}, \mu_M^{max}\Big(1-\frac{Q_{PM}^{min}}{Q_{PM}}\Big)\Big) \quad (2.13)$$

The growth rate of the mixotrophs (μ_M) (Eq. (2.13)) is the minimum of their potential C-dependent growth rate (μ_{CM}) or their potential P-dependent growth rate (μ_{PM}). The potential C-dependent growth rate of the mixotroph is the sum of terms relating to photosynthesis and consumption of bacteria. These are defined similarly to corresponding terms for algae and zooflagellates, respectively. The mixotrophs' autotrophic fraction of C-dependent growth depends on photosynthesis, which in turn depends on light intensity and shading. The mixotrophs' heterotrophic fraction of C-dependent growth depends on assimilation of C obtained from ingestion of bacteria. The parameter μ_{PM} is defined similarly to that of the algae and zooflagellates.

There is an important consequence of assigning higher minimal and maximal quotas to the mixotrophs, than those assigned to algae and zooflagellates, while sharing other terms related to consumption and growth. When the parameter α is 0 or 1, so that the mixotroph is actually a specialist autotroph or heterotroph, respectively, its growth rate is lower than that of algae or zooflagellates. This makes highly specialized mixotrophs (α near 0 or near 1) poorer competitors than the specialist types, algae and zooflagellates.

2.2.4 *Bacteria*

The bacteria obtain all of their nutrients by taking up labile dissolved organic carbon and dissolved phosphorus from the environment (Figure 2.1). They serve as prey for the zooflagellates and potentially the mixotrophs, and are governed by two differential equations.

$$\frac{dB}{dt} = \left(\mu_B - D - m_B - (1-\alpha)\, a_{BM}\, M - a_{BZ}\, Z \right) B \tag{2.14}$$

$$\frac{dQ_{PB}}{dt} = V_{PB}^{max} \left(\frac{P}{k_{PB} + P}\right) \left(\frac{Q_{PB}^{max} - Q_{PB}}{Q_{PB}^{max} - Q_{PB}^{min}}\right) - \mu_B\, Q_{PB} \tag{2.15}$$

Equation (2.14) describes the per capita rate of change in the density of bacteria (*B*) as the balance of reproductive growth (μ_B) minus dilution (*D*), mortality (m_B), and the losses to predation by the mixotrophs and the zooflagellates at densities *M* and *Z*, respectively which assumes linear functional responses with attack rates a_{BM} and a_{BZ}. The attack rate of the mixotrophs is decreased by the α parameter. Equation (2.15) describes the rate of change in the phosphorous quota of bacteria (Q_{PB}) as the balance between uptake and dilution due to reproduction. The uptake rate for P is defined similarly to that of the algae.

$$\mu_B = \min(\mu_{CB}, \mu_{PB}) = \min\left(e_B \mu_B^{max} \left(\frac{C}{k_{CB} + C}\right), \mu_B^{max} \left(1 - \frac{Q_{PB}^{min}}{Q_{PB}}\right)\right) \tag{2.16}$$

Equation (2.16) describes the growth rate of the bacteria (μ_B) as the minimum of their potential C-dependent growth rate (μ_{CB}) or their potential P-dependent growth rate (μ_{PB}). Carbon-dependent growth depends directly on the concentration of labile, dissolved organic C in the environment, while P dependent growth is determined by the quota of P contained in cells. Bacterial uptake of labile, dissolved organic carbon from the environment follows a Michaelis-Menten equation with the maximum uptake rate μ_B^{max}, and k_{CB} the half-saturation constant. In equation (2.16), a gross growth efficiency, e_B determines the proportion of carbon taken from the environment that is used for growth under C limitation. The proportion (1- e_B) is lost due to

respiration. When bacterial growth is limited by P, there is additional C taken up but not assimilated into growth that is implicitly lost to respiration

2.2.5 Environment

The environment has two differential equations that track labile dissolved organic C and inorganic P.

$$\begin{aligned}\frac{dC}{dt} &= D(C_{in} - C) - \frac{\mu_B B Q_{CB}}{e_B} \\ &+ e_A \max(0, \mu_{CA} - \mu_{PA}) A Q_{CA} + e_{MA} \max(0, \mu_{CM} - \mu_{PM}) M Q_{CM} \\ &+ m_B B Q_{CB} + m_M M Q_{CM} + m_A A Q_{CA} + m_Z Z Q_{CZ}\end{aligned} \tag{2.17}$$

The rate of change of dissolved organic C depends on several factors (Eq. (2.17)). The first term is a standard chemostat supply term: the net supply of dissolved organic C is the dilution rate D times the difference between the supply concentration C_{in} and current concentration C. The second term represents consumption by bacteria during their growth; e_B is the proportion of organic carbon removed from the environment that is used for growth, and the rest is respired. The next two terms are rates of release to the environment due to excess photosynthesis by algae and mixotrophs when their growth is P-limited (Bratbak and Thingstad 1985). When growth of either algae or mixotrophs is P-limited ($\mu_{PA} < \mu_{CA}$ or $\mu_{PM} < \mu_{CM}$, respectively), there is excess C production by photosynthesis that is not incorporated in growth. A fraction of this excess is released as dissolved organic C, governed by proportions e_A and e_{MA} for algae and mixotrophs, respectively. Implicitly, the fraction of excess production not released as dissolved organic C is respired away. The final terms track the return of C to the environment by mortality of the organisms, assuming that the entire C content of dead organisms recycles to the dissolved phase.

$$\begin{aligned}\frac{dP}{dt} &= D(P_{in} - P) - B V_{PB} - A V_{PA} - \alpha M V_{PM} \\ &+ m_B B Q_{PB} + m_M M Q_{PM} + m_A A Q_{PA} + m_Z Z Q_{PZ} \\ &+ (1-\alpha) a_{BM} B M Q_{PB} \left(\frac{Q_{PM} - Q_{PM}^{min}}{Q_{PM}^{max} - Q_{PM}^{min}}\right) + a_{BZ} B Z Q_{PB} \left(\frac{Q_{PZ} - Q_{PZ}^{min}}{Q_{PZ}^{max} - Q_{PZ}^{min}}\right)\end{aligned} \tag{2.18}$$

The rate of change of dissolved P in the environment again has a chemostat supply term with supply concentration P_{in} (Eq. (2.18)). The next three terms represent uptake by bacteria, autotrophs, and mixotrophs. Then, four terms denote the rates returned by mortality of the organisms, assuming that the entire P content of dead organisms recycles to the dissolved phase. Finally, the rates recycled by the mixotroph and the zooflagellates are added, which involve P in bacterial prey ingested but not assimilated.

2.3 Parameter Values

2.3.1 Algae

Parameters for the algae are based on the green alga *Scenedesmus*, widely used in experiments on resource-limited growth (e.g. Gotham and Rhee 1981, Huisman et. al. 1999). The data collected by Huisman et. al. (1999) on light-limited growth do not tightly constrain the parameter ρ_A^{max} which was arbitrarily set to 1.0 d^{-1}, the value assigned to μ_A^{max}. The shading coefficient for the algae (k_A) was chosen to produce shading per cell consistent with data of Huisman et al. (1999), when using the C quota adopted. All of the other organisms were then given the same shading coefficient per unit cellular C. The fraction of excess C fixation that is excreted is (e_A) is not well constrained by available data and was adjusted to 0.25 so that a P-limited chemostat would produce a dissolved organic C concentration similar to that observed in experiments (Grover 2000, Codeço and Grover 2001). The mortality rate was arbitrarily set to 0.1 d^{-1}, the same as all of the other organisms.

2.3.2 Zooflagellates

Parameters for the zooflagellates are derived from a prior model (Grover 2003) and reflect assumptions that many zooflagellates are taxonomically affiliated to mixotrophic algae such as chrysophytes (Porter et. al. 1985), and are thought to recycle P at high rates (Dolan 1997). Zooflagellates grow rapidly so a high value of μ_Z^{max} was assigned (Fenchel 1986). The attack rate of the zooflagellates on the bacteria was set to control the population of bacteria at

population densities of about 10^6 cells ml^{-1}, when zooflagellates are the only consumers of bacteria.

2.3.3 Mixotrophs

Parameters for the mixotrophs are a mixture of the values used for the algae and the zooflagellates. Parameters having to do with bacterivory, the attack rate and the efficiency at which prey C is utilized, were assigned the same values as those for the zooflagellates. Parameters having to do with autotrophy, the efficiency at which C from photosynthesis is lost, the half-saturation constant for light, the uptake rate for P, and the maximum rate of photosynthesis, were assigned the same values as those for the algae. The maximal growth rate was also set to that of the algae to produce slower growth than the zooflagellates. The minimal and maximal quotas for P were set to be 20% higher than that for the zooflagellates, which is in turn higher than that for algae, to reflect the need to carry the machinery for both photosynthesis and bacterivory. The C quota for the mixotroph was also set to be 20% larger than that of the algae for the same reason.

2.3.4 Bacteria

Most of the parameters follow Thingstad (1987) for a marine *Pseudomonas* species. The maximal growth rate μ_B^{max} was lowered to 6.0 d^{-1} to better reflect slower growth of bacteria noted by field observations (Chrzanowski and Grover 2001b). The mortality rate m_B was arbitrarily set to 0.1 d^{-1}. The gross growth efficiency for carbon, e_B, was set to 0.5, a representative value for labile organic substrates (Goldman and Dennett 2000).

2.4 Numerical Simulations

After the initial assignments, parameters were not tuned to produce any particular ecological or mathematical outcome, and yielded widely varying characteristic rates for the processes represented in this model, e.g. bacterial uptake of dissolved P is very rapid, while recycling through mortality is much slower. Thus the ten simultaneous differential equations are stiff, and require appropriate numerical methods. The MATLAB ode23s solver was used, which is

based on a modified Rosenbrock triple and is a one step method that forms a new Jacobian at every time step (Shampine and Reichelt 1997). Equations were numerically integrated for 2000 days, or until asymptotic behavior (point equilibrium or limit cycle) was attained. After 1500 days, any organism that had a concentration less than 10^{-5} cells/m^3 was removed. Dynamics of such organisms were examined to ensure that these removals were for organisms going extinct and not just displaying transient periods of low density.

Numerical exploration focused on the potential coexistence of the four nutritional types in relation to the variation of physical and chemical environment, represented by the parameters describing P supply (P_{in}), organic C supply (C_{in}), light intensity at the surface (I_{in}), background turbidity (k_{bg}), and depth of the habitat (z). The parameter I_{in} was given high and low values to correspond to summer and winter light conditions near 30° latitude, while k_{bg} was chosen to produce background shading comparable to that produced by the organisms and then one-tenth of that for the low value. Depth was arbitrarily chosen to be one and ten meters to explore shallow and deep photic zones; P_{in} was chosen to represent oligotrophic and eutrophic lakes; and C_{in} was chosen to represent habitats with no external organic carbon supply and those with substantial supply. These five conditions were given high and low values (Table 2.2), and all thirty-two resulting combinations of environmental situations were explored with variations of the mixotrophs' α parameter from zero to one in increments of 0.05 or 0.01. Thus a wide range of mixotrophic strategies, ranging from virtual autotrophy to virtual heterotrophy was examined over widely differing environmental conditions. For selected environments, a much finer grid of α values was used to construct one-dimensional bifurcation diagrams showing asymptotic dynamics of the four nutritional types. These runs were continued for 4000 days.

Table 2.2 Low and high values for environmental parameters governing resource supply.

Quantity	Low	High	Units
Phosphorus (P_{in})	0.0001	0.001	mol m^{-3}
Carbon (C_{in})	0	0.6	mol m^{-3}
Light (I_{in})	400	900	J s^{-1} m^{-2}
Turbidity (k_{bg})	0.07	0.7	m^{-1}
Depth (z)	1	10	m

2.5 Results

First, the persisting organisms from the thirty-two environments used for the coarse gradation are presented. The sequences of persisting organisms (Table 2.3) were examined as α increased from 0 to 1. For α values of 0 and 1, very slow (nearly neutral) dynamics arose due to competition between very similar organisms, two heterotrophs when α is 0 and two autotrophs when α is 1, so we report results exclusive of these values. Sequences of persisting organisms mostly fell into two groups defined by low P versus high P environments.

The low P environments had persisting mixotrophs over wider ranges of α values than the high P environments. Thus more varied types of mixotrophs were persistent with lower P supply. There were two main sequences in both the high and low P environments. The low P environment had sequences that were AZB-AMB-MB-ZMB, and AZB-MB-AMB-MB-ZMB, which differed only in the elimination of algae at α = 0.1. There were four other sequences in the very challenging low P environments with high turbidity and high depth – low light – that did not resemble the two more common sequences.

The high P environments favored persistence of zooflagellates at the expense of mixotrophs. In these environments, the algae, zooflagellates, and bacteria always persisted with the mixotrophs also persisting only at some of the higher α values near 1. It was in these environments, all with high surface light intensity and shallow depth, where coexistence of all four organisms occurred.

Table 2.3 Sequences of persisting organisms in relation to α.

Sequence of coexisting populations as α increases	Phosphorus (P_{in})	Carbon (C_{in})	Light (I_{in})	Turbidity (k_{bg})	Depth (z)
AZB-AMB-MB-ZMB	Low	Low	Low	Low	Low
	Low	Low	Low	Low	High
	Low	Low	Low	High	Low
	Low	Low	High	Low	Low
	Low	Low	High	Low	High
	Low	Low	High	High	Low
	Low	High	Low	Low	Low
	Low	High	Low	Low	High
AZB-MB-AMB-MB-ZMB	Low	High	Low	High	Low
	Low	*High*	*High*	*Low*	*Low*
	Low	High	High	Low	High
	Low	High	High	High	Low
AZB AZB-AMB-AZB AZB-ZMB AZB-ZMB-MB-ZMB	Low	Low	Low	High	High
	Low	Low	High	High	High
	Low	High	Low	High	High
	Low	High	High	High	High
AZB-AZMB-AZB	High	Low	High	Low	Low
	High	Low	High	High	Low
	High	*High*	*High*	*Low*	*Low*
	High	High	High	High	Low
AZB	High	Low	Low	Low	Low
	High	Low	Low	Low	High
	High	Low	Low	High	Low
	High	Low	Low	High	High
	High	Low	High	Low	High
	High	Low	High	High	High
	High	High	Low	Low	Low
	High	High	Low	Low	High
	High	High	Low	High	Low
	High	High	Low	High	High
	High	High	High	Low	High
	High	High	High	High	High

Three environments were simulated with a fine gradation of α to illustrate associated bifurcations. Logarithmic graphs were needed to show the full ranges of population densities, so plots are blank whenever a nutritional type went extinct.

The first environment (Figure 2.2) had high light, high organic C supply, and high depth, with low P and low turbidity, characteristics defining many lakes conventionally classified as oligotrophic. Here limit cycles of the algae, mixotrophs, and bacteria extended for α from about 0.3 to 0.8. The algae showed a flattened parabola in relation to α with densities averaging around 10^{10} cells/m^3 during their limit cycles. The zooflagellates were eliminated everywhere except for the extreme values of α. The mixotrophs showed a steady increase in density through values of α from about 0.1 to 0.9. The bacteria were always present with an average density independent of α at about 10^{12} cells/m^3.

The second environment was the same as the last one except that P supply is high, representing a eutrophic lake. In this environment, the mixotrophs were not able to persist and the other organisms showed damped cycles with very slow convergence. These simulations were run for 8000 days and did not reach a steady state or limit cycle of constant amplitude. The algae, zooflagellates, and bacteria had average densities near 1.7×10^{10}, 2.4×10^{9}, and 1.4×10^{12} cells/m^3 respectively. It appeared that a steady state would be reached at values near these averages, but this was not confirmed. There were no surviving mixotrophs and thus the densities of other organisms were constant across α.

The last environment (Figure 2.3) was the same as the previous eutrophic habitat, except that it had low depth. This increased the available light and allowed the mixotrophs to persist when they had high α values. The algae, zooflagellates, and bacteria had constant densities across α when the mixotrophs were absent. However, when all four organisms persisted, they were all in limit cycles. In these cycles, the zooflagellates were C-limited and the bacteria were P-limited, but the algae and mixotrophs were cycling between C- and P-limitation. When all four

organisms coexisted, there were slight decreases in the average densities of algae and zooflagellates.

In summary, mixotrophs with a wide range of α values persisted in the oligotrophic environment and those with high values of α persisted in the shallow, eutrophic environment. In both of these environments, mixotroph densities were greatest when α was near 0.9. Algae persisted in the three environments illustrated except for the oligotrophic environment around α = 0.1 and at higher values of α near 0.9. Zooflagellates persisted in the oligotrophic environment only when mixotrophs were parameterized with extremes of α near 0 or 1. Bacteria always persisted and although they displayed large-amplitude limit cycles for some parameter sets, their average density was always around 10^{12} cells/m^3. The persistence of all four organisms was observed only with all four organisms in limit cycles and dynamically changing nutrient limitations.

2.6 Discussion

This study addressed the coexistence of microorganisms pursuing diverse nutritional strategies, using the first model of mixotrophs that embeds these organisms in a realistic, dynamic microbial food web and explicitly represents the categories of resources minimally required for autotrophic and heterotrophic growth. It is perhaps not surprising that coexistence of three or four species representing different strategies was found. The model used here has three basal resources, and potentially two species, zooflagellates and mixotrophs that prey upon a consumer of the basal resources. Thus the number of limiting factors (resources and predators) is as high as five, so finding three or four coexisting species does not violate general constraints on coexistence at steady state (Levin 1970; Tilman 1982).

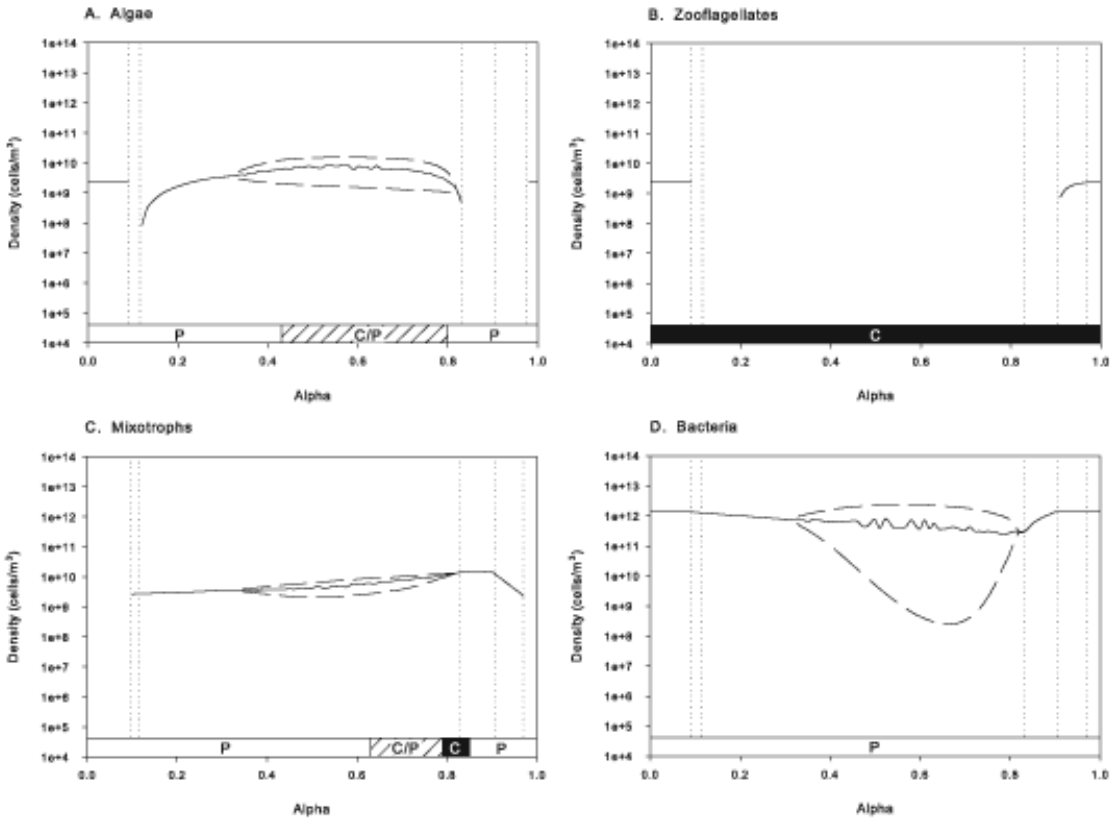

Figure 2.2 Bifurcations of organism densities in relation to α for a low P environment representing an oligotrophic lake. Solid lines indicate equilibrium values, or average values over limit cycles. Dashed lines indicate minimum and maximum values of limit cycles. Vertical dotted lines indicate bifurcations where organisms gain or lose persistence. Bars across the bottom of each panel indicate the limiting nutrient for organism growth: solid for C- or light-limitation; open for P-limitation; cross-hatched for dynamic shifts between C- and P-limitation during limit cycles.

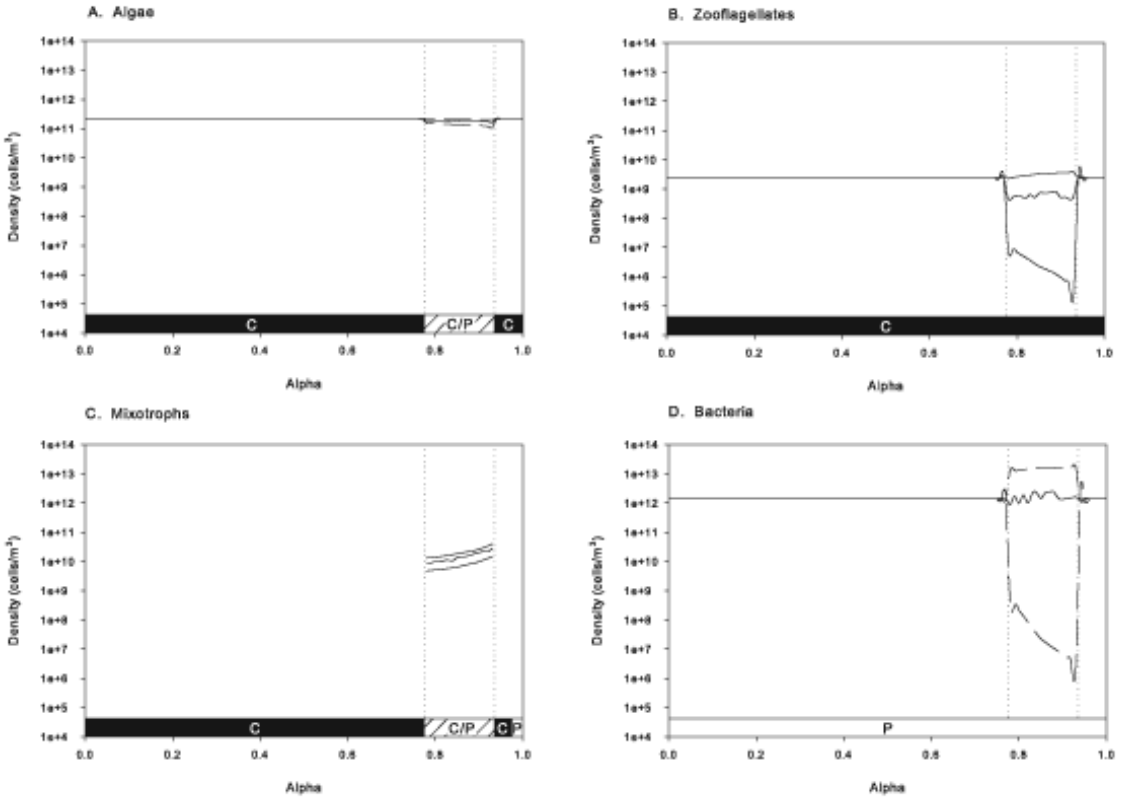

Figure 2.3 Bifurcations of organism densities in relation to α for a low-depth, eutrophic environment with all four organisms coexisting. Solid lines indicate equilibrium values, or average values over limit cycles. Dashed lines indicate minimum and maximum values of limit cycles. Vertical dotted lines indicate bifurcations where organisms gain or lose persistence. Bars across the bottom of each panel indicate the limiting nutrient for organism growth: solid for C- or light-limitation; open for P-limitation; cross-hatched for dynamic shifts between C- and P-limitation during limit cycles.

Despite factors that allow the coexistence of the four nutritional types represented, it is not a foregone conclusion that this potential coexistence will be achieved. The joint action of predation and competition, both present in the microbial web modeled here, can sometimes lead to coexistence, but it can also lead to exclusion of populations in ways that depend strongly on context (Chase et al. 2002). Moreover, the microbial web has complex interactions involving carbon excretion, nutrient recycling and consumption (Figure 2.1), whose implications for coexistence are poorly understood. Finally, the organisms represented here are prone to have periodic, limit-cycle dynamics, which in other theoretical contexts can produce either competitive exclusion or coexistence (Abrams 1999; Abrams and Holt 2002).

In most natural planktonic environments, microorganisms pursuing several nutritional strategies coexist (Porter et. al. 1985). In the range of model environments explored here, at least three different types of organisms were predicted to persist, and with high supply of both P and light, all four types of organisms were predicted to persist for some ranges of the mixotrophy parameter α.

To illuminate factors promoting coexistence, the proximate limitation on growth rate was examined for all populations. The algae, mixotrophs, and bacteria were generally P-limited in environments with low P supply and C-limited otherwise. However, the algae and mixotrophs also showed oscillations between C- and P-limitation when in limit cycles. When the algae were P-limited and at a stable equilibrium, they controlled the dissolved P concentration at their R^* level (sensu Tilman 1982). The zooflagellates were always C-limited. Given the relatively high P content of planktonic bacteria compared to many other, mostly eukaryotic microorganisms (Vadstein 2000), it is reasonable to portray zooflagellates as being C-limited. Bacteria were always predicted to persist and since bacteria are found in all aquatic habitats, predicting their extinction would have indicated a serious theoretical flaw. Beyond this, their predicted abundance of about 10^6 cells/ml on average across all habitats modeled agrees well with observations from a variety of aquatic ecosystems (Azam et al. 1983).

Although bacteria were modeled here as better competitors than algae for dissolved P, they can be removed by the zooflagellates and the mixotrophs at rates sufficient to decrease their competitive impact on algae. This reduction of bacteria also benefits mixotrophs in competition for dissolved P. And because mixotrophs are not entirely dependent upon their bacterial prey, their competition with zooflagellates for prey is mitigated. The balance between predation and competition, along with partitioning of partially overlapping resources, potentially allows for coexistence even when several species are simultaneously limited by the same nutrient. In fact, the model predicts that under low P supply, bacteria and algae will both be P-limited, an outcome that has been observed in inland waters (Chrzanowski and Grover 2001b). It is also possible that non-equilibrium dynamics contributed to coexistence, since persistence of all four modeled organisms was observed only when limit cycles occurred.

The results presented here suggest that mixotrophy is especially favored by nutrient limitation. Persistence of mixotrophs was predicted predominantly when P supply was low, or when high P supply was accompanied by environmental characteristics producing high light supply. Moreover, predicted population densities of mixotrophs increased as α increased, peaking near α of 0.9. Thus, in terms of abundance, the most successful mixotrophs were predicted to be primarily autotrophic, supplementing photosynthesis with a small proportion of nutrition obtained by preying on bacteria. Such mixotrophs appear to occur frequently and abundantly in many natural aquatic ecosystems (Stoecker 1998).

Some of these results could have been produced by particular parameter choices adopted here. The large number of parameters and problems of stiffness noted for this model prevented an exhaustive study of parameter values. Nevertheless, variations were explored for four important parameter choices, the C and P quotas of the mixotrophs, the growth efficiency of bacteria for C, and the shading coefficients.

The first parameter choices explored are those of the C and P quotas for mixotrophs. By default, these were assumed to exceed corresponding values for algae and zooflagellates by a

factor of 1.2, to reflect the presence of both autotrophic and heterotrophic cellular machinery. This produced a competitive disadvantage for highly specialized mixotrophs (α near 0 or 1) competing against the true specialist types, zooflagellates or algae. Exploring alternative assumptions for these quota parameters is complicated by stiffness: the dynamic bacterial population can go through rapid changes while the quotas of eukaryotic organisms change slowly.

A range of alternative assignments for mixotroph quota parameters was examined by setting these to factors of algae and zooflagellate quotas ranging from 1.3 to 0.8. Thus mixotrophs were assigned various levels of both competitive disadvantage and advantage over specialist types. Although outcomes under some parameter assignments could not be solved numerically, some general patterns could be found for the 32 environments considered before (Table 2.2). For environments with low P supply, more competitive mixotrophs with lower quota parameters displace the zooflagellates for low α values, and bacterial oscillations of unrealistic amplitude occurred, especially in shallow environments with high α values. For environments with high P supply, the least competitive mixotrophs with highest quota parameters could not persist. As mixotrophs became more competitive with lower quota parameters they were more likely to persist, but bacterial oscillations of unrealistic amplitude again occurred for shallow environments and high α, and in the worst cases the numerical algorithm failed. As expected, sufficiently competitive mixotrophs with low enough quota parameters (multiple of 0.9) outcompeted the zooflagellates in most of the environments where numerical solutions were obtained, and those that also had higher α values outcompeted the algae in some environments. Fortuitously, the competitive disadvantage assigned to mixotrophs through the default parameterization of quota parameters both favored coexistence with other nutritional types of microbes, and reduced stiffness to a level consistent with mathematical tractability.

Further parameter explorations examined the growth efficiency of bacteria for C (e_B). In this model, dissolved organic C was assumed to be relatively labile, consisting of substances

produced by algae and mixotrophs as exuded photosynthate. We used a value of 0.5, to represent the gross growth efficiency for such labile substrates (Goldman and Dennett 2000). Reducing this parameter to 0.4 gave similar results, though the range of α values where all four organisms coexisted decreased and some environments showed bacterial oscillations of unrealistic amplitude. Lowering efficiency further to 0.3 gave more environments with bacterial oscillations of unrealistic amplitude and several that could not be numerically solved, and no environments were found where all four organisms coexisted. Higher values of e_B up to 1.0 produced similar results to those of 0.5.

Since the amount of light plays an important role in this model, we also examined the lowering of the shading coefficient for the organisms. The shading coefficients for all organisms were lowered to 75, 50, and 25 percent of their original values. The lowering of the shading coefficient has negligible impact in the low P environments, but had a dramatic effect in the high P environments. As the shading percentage dropped, coexistence of all four organisms occurred in the low depth environments and the range of α values where this happened expanded. Therefore the coexistence of all four organisms in this model was generally predicted with enough available light. Though we tried to choose realistic parameters, those necessary for all four organisms to coexist may not be entirely realistic, and some of our parameter choices may need to be refined as further research more realistically restrains them.

The model studied here potentially falls short of realism in many other respects. None of the nutritional types is described in full physiological detail, and for mixotrophs in particular, some interesting possibilities are neglected, such as the short term sequestration of plastids from small algae that have been ingested (Stoecker 1998). A more complete model of mixotroph physiology has recently been constructed (Flynn and Mitra 2009), but has yet to be explored when coupled to a suite of competitor types. The dissolved resources represented here (dissolved P and organic C) are not single resource pools but are instead complex mixtures of multiple substrates (Riemann and Sondergaard 1986; Vadstein 2000). Finally, the model environment is well mixed and has constant supplies of light, organic C, and P, which is clearly unrealistic.

Though we cannot recreate the complexity of a natural system in the model we studied, we have extended the reach of theoretical models commonly applied to microbial food webs, and specifically to mixotrophs. This model thus lays a foundation for addressing open questions concerning the ecosystem and geochemical roles of mixotrophs. Further examination of potential combinations and tradeoffs between autotrophic and heterotrophic nutritional modes characterizing mixotrophs would seem to be one among many interesting issues to explore.

CHAPTER 3

STEADY STATE ANALYSIS OF ENVIRONMENTAL PARAMETERS AND IMPLICATIONS FOR ECOSYSTEM PROPERTIES IN A MODEL INCLUDING MIXOTROPHY

3.1 Introduction

Mixotrophy is a nutritional strategy that blends autotrophy and heterotrophy. Traditionally, it has been regarded primarily as a coping strategy for nutritionally poor environments (Nygaard and Tobiessen 1993). Recently, mixotrophy has been found to be a very widespread nutritional strategy that is an important component of microbial ecosystems (Zubkov and Tarran 2008). Further interest in mixotrophy comes about from the increase in harmful algal blooms (HABs) and the association of mixotrophic species with bloom dynamics (Burkholder 2008). Despite the prevalence and importance of mixotrophy, mathematical models that incorporate mixotrophs as distinct species are not very prevalent.

Crane and Grover (2010) created a model that includes mixotrophs as a distinct population along with three other dynamic populations pursuing different nutritional modes. This model was used to examine the coexistence of four types of organisms, phototrophic algae, heterotrophic bacteria, and two types of bacterivores, heterotrophic zooflagellates and mixotrophs combining the nutritional strategies of algae and zooflagellates. The combination of these nutritional modes was handled as a linear tradeoff between the two forms as the type of mixotroph was varied from one that was mostly heterotrophic to one that was mostly autotrophic. Coexistence was examined in several model aquatic environments differing in the amount of P supply, organic C supply, surface irradiance, turbidity, and mixing depth. This was done primarily to look for the types of mixotrophs and environments that led to coexistence.

In this study, we want to examine how varying environmental parameters affects community and ecosystem structures with two alternative types of mixotrophs, those that are primarily autotrophic and those that are primarily heterotrophic. In the previous study, there was no focus on the geochemical cycling of nutrients taking place in the microbial ecosystems. Modeling affords us a unique opportunity to examine these processes since we can know exactly the makeup of the organisms and the environment, and thus can predict ecosystem properties and how mixotrophs affect them.

This provides opportunities to begin addressing the ecosystem and geochemical roles of mixotrophs. For example, Sterner et al. (1997) took a stoichiometric approach to pelagic food web and ecosystem structure in inland waters, and proposed that the supply ratio of light to P is critical. A low ratio, found in eutrophic lakes for example, produces a microbial community dominated by algae and other microorganisms containing high P content (low C:P ratio), which in turn provides high quality food for crustacean herbivores and a metazoan food chain. A high supply ratio of light to P, found in oligotrophic lakes, produces a microbial community that is more heterotrophic and deficient in P (high C:P ratio), providing poor quality food for crustaceans and limiting the metazoan food chain. Chrzanowski and Grover (2001a) extended this view of spatial variation among lake ecosystems to seasonal variations, and verified some of its underlying assumptions. But neither study explicitly addressed the role of mixotrophs in these patterns.

3.2 Model Description

This study further explores the model presented in Crane and Grover (2010), which models growth of interacting populations in a chemostat environment. Notation follows that used previously (Table 2.1). The four organisms each have equations governing their population densities and P-quotas. The rate of change of the population density (X), where X also indexes the type of organism, is the balance of the per capita growth rate (μ_X) minus dilution (D) and mortality (m_X) rates.

$$\frac{dX}{dt} = (\mu_X - D - m_X) X \tag{3.1}$$

These three equations specify dynamics of the phototrophic algae (*A*), phagotrophic zooflagellates (*Z*), and mixotrophs (*M*). For the fourth type of organism, heterotrophic bacteria (*B*), additional mortality terms specify predation by zooflagellates and mixotrophs.

$$\frac{dB}{dt} = \left(\mu_B - D - m_B - (1-\alpha)\, a_{BM}\, M - a_{BZ}\, Z \right) B \tag{3.2}$$

The predation terms assume linear functional responses with attack rates a_{BM}.and a_{BZ} by mixotrophs and zooflagellates, respectively. The parameter α is the proportion of mixotroph growth that is supported by phototrophy.

For all four types of organisms, the rates of change for quotas of phosphorus depend on the balance between consumption of resources and use in population growth.

$$\frac{dQ_{PA}}{dt} = V_{PA}^{max} \left(\frac{P}{k_{PA} + P}\right) \left(\frac{Q_{PA}^{max} - Q_{PA}}{Q_{PA}^{max} - Q_{PA}^{min}}\right) - \mu_A\, Q_{PA} \tag{3.3}$$

$$\frac{dQ_{PZ}}{dt} = a_{BZ}\, B Q_{PB} \frac{Q_{PZ}^{max} - Q_{PZ}}{Q_{PZ}^{max} - Q_{PZ}^{min}} - \mu_Z\, Q_{PZ} \tag{3.4}$$

$$\frac{dQ_{PM}}{dt} = \alpha V_{PM}^{max} \frac{P}{k_{PM} + P} \frac{Q_{PM}^{max} - Q_{PM}}{Q_{PM}^{max} - Q_{PM}^{min}} + (1-\alpha)\, a_{BM}\, B Q_{PB} \frac{Q_{PM}^{max} - Q_{PM}}{Q_{PM}^{max} - Q_{PM}^{min}} - \mu_M\, Q_{PM} \tag{3.5}$$

$$\frac{dQ_{PB}}{dt} = V_{PB}^{max} \left(\frac{P}{k_{PB} + P}\right) \left(\frac{Q_{PB}^{max} - Q_{PB}}{Q_{PB}^{max} - Q_{PB}^{min}}\right) - \mu_B\, Q_{PB} \tag{3.6}$$

The rate of change of the algal P quota (Q_{PA}; Eq.(3.3)) is the balance of uptake from the environment minus use in population growth ($\mu_A\, Q_{PA}$). The uptake rate in relation to dissolved phosphorus (*P*) follows a Michaelis-Menten equation with V_{PA}^{max} being the maximum uptake rate and k_{PA} the half-saturation constant. The uptake rate also decreases linearly as the phosphorus

quota increases from the minimum value of Q_{PA}^{min} to the maximum value of Q_{PA}^{max}, where uptake ceases. The rate of change in P quota for the zooflagellates (Q_{PZ}) is the gain from the predation of bacteria minus use in population growth (Eq.(3.4)). The rate of predation depends on the attack rate on bacteria by the zooflagellates (a_{BZ}), and the rate of P assimilation depends linearly on the quota of P in the zooflagellates, decreasing as the phosphorus quota increases from the minimum value of Q_{PZ}^{min} to the maximum value of Q_{PZ}^{max}. The rate of change in the P quota for the mixotrophs (Q_{PM}) is the sum of the gain from the uptake of dissolved P, like the algae, and the gain from predation on bacteria, like the zooflagellates, minus use in population growth (Eq.(3.5)). For mixotrophs, the proportion of P obtained by uptake from the dissolved pool versus predation on bacteria is governed by the parameter α, the proportion of phototrophic versus phagotrophic growth. The rate of change in the phosphorous quota of bacteria (Q_{PB}; Eq. (3.6)) is similar to that of the algae.

The per capita growth rates of the organisms (μ_X) are the minimum of their potential C-dependent growth (μ_{CX}) or their potential P-dependent growth (μ_{PX}). For the algae

$$\mu_A = \min(\mu_{CA}, \mu_{PA}) = \min\left(\frac{\rho_A^{max}}{\omega z}\ \ln\left(\frac{k_{CA}+I_{in}}{k_{CA}+I_{out}}\right), \mu_A^{max}\left(1-\frac{Q_{PA}^{min}}{Q_{PA}}\right)\right) \tag{3.7}$$

$$\omega = k_{bg} + k_B B Q_{CB} + k_A A Q_{CA} + k_M M Q_{CM} + k_Z Z Q_{CZ} \tag{3.8}$$

$$I_{out} = I_{in}\, e^{-\omega z} \tag{3.9}$$

where $\mu_A^{\max}$ is the maximal rate for phosphorus-limited growth and $Q_{PA}^{\min}$ is the minimal quota at which growth rate is zero. It is assumed that C-limited growth for algae is determined by the specific rate of photosynthesis integrated over a well-mixed water column of depth *z*. The specific rate of photosynthesis is assumed to be a Michaelis-Menten function of irradiance with $\rho_A^{\max}$

being the maximal specific rate of photosynthesis, and k_{CA} is the half-saturating irradiance. In equation(3.7), ω is the total shading that occurs in the water column. Shading (Eq.(3.8)) occurs from background turbidity (k_{bg}) and from organisms, proportional to their population density and C quota through a factor k_x. The C quota thus indicates how dark an organism is due to its cellular mass, and the parameter k_x indicates the absorptive quality of cellular mass. Multiplying k_x by C quota and population density gives the total shading for each population. These are summed and then added to the background turbidity of the water (k_{bg}). Light at the bottom of the water column (I_{out}) is calculated from equation (3.9), given light at the surface (I_{in}).

For the zooflagellates, the per capita rate of growth is

$$\mu_Z = \min(\mu_{CZ}, \mu_{PZ}) = \min\left(a_{BZ}\, e_Z\, B\frac{Q_{CB}}{Q_{CZ}}, \mu_Z^{max}(1-\frac{Q_{PZ}^{min}}{Q_{PZ}})\right) \tag{3.10}$$

where $\mu_Z^{\max}$ is the maximal rate for phosphorus-limited growth and $Q_{PZ}^{\min}$ is the minimal quota at which growth rate is zero. The potential C-limited growth rate of zooflagellates is determined by the C flux ingested from predation on bacteria in relation to a fixed C quota for zooflagellates (Q_{CZ}) and assimilation efficiency e_Z. The ingested *C* flux is the product of the attack rate a_{BZ}, the bacterial density *B*, and the fixed bacterial C quota (Q_{CB}).

For mixotrophs, the per capita growth rate is again the minimum of the potential C-limited growth rate and the potential P-limited growth rate:

$$\mu_M = \min\left(\alpha\frac{\rho_M^{max}}{\omega z}\ln(\frac{k_{CM}+I_{in}}{k_{CM}+I_{out}}) + (1-\alpha)\, a_{BM}\, e_M\, B\frac{Q_{CB}}{Q_{CM}}, \mu_M^{max}(1-\frac{Q_{PM}^{min}}{Q_{PM}})\right) \tag{3.11}$$

where $\mu_Z^{\max}$ is the maximal rate for phosphorus-limited growth and $Q_{PZ}^{\min}$ is the minimal quota at which growth rate is zero. The potential C-limited growth rate of mixotrophs has a term similar to the light dependent term describing this rate for algae, and a term similar to the predation term

describing the rate for zooflagellates. These terms are added in proportion to α, the extent to which the mixotroph is phototrophic.

For the bacteria, the per capita rate of growth is

$$\mu_B = \min(\mu_{CB}, \mu_{PB}) = \min\left(e_B \mu_B^{max}\left(\frac{C}{k_{CB}+C}\right), \mu_B^{max}\left(1-\frac{Q_{PB}^{min}}{Q_{PB}}\right)\right) \tag{3.12}$$

where $\mu_Z^{\max}$ is the maximal growth rate and $Q_{PZ}^{\min}$ is the minimal quota at which growth rate is zero. The potential C-limited growth rate of bacteria is a Monod function of external dissolved organic C concentration, with maximal rate $\mu_B^{\max}$, half-saturation constant k_{CB} and growth efficiency e_B.

Two differential equations specify rates of change for labile dissolved organic C and inorganic P. For dissolved organic C:

$$\begin{aligned}\frac{dC}{dt} &= D(C_{in}-C) - \frac{\mu_B B Q_{CB}}{e_B} \\ &+ e_A \max(0, \mu_{CA}-\mu_{PA}) A Q_{CA} + e_M \max(0, \mu_{CM}-\mu_{PM}) M Q_{CM} \\ &+ m_B B Q_{CB} + m_M M Q_{CM} + m_A A Q_{CA} + m_Z Z Q_{CZ}\end{aligned} \tag{3.13}$$

This rate depends on several factors. The first term is a standard chemostat supply term: the net supply of dissolved organic C is the dilution rate D times the difference between the supply concentration C_{in} and current concentration C. The second term specifies consumption by bacteria during their growth; given growth efficiency $e_B < 1$, some of the organic C removed from the environment is respired. The next two terms are rates of release to the environment due to excess photosynthesis by algae and mixotrophs when their growth is P-limited (Bratbak and Thingstad 1985), which depends on their potential P-limited growth rates (μ_{PX}) and potential C-limited growth rates (μ_{CX}). When $\mu_{PA} < \mu_{CA}$ or $\mu_{PM} < \mu_{CM}$, there is excess C production by photosynthesis of algae or mixotrophs, respectively, that is not incorporated in growth, and fractions e_A and e_M of these excesses are released as dissolved organic C. The fraction of excess production not released as dissolved organic C is assumed to be respired. The final

terms specify the return of C to the dissolved pool by mortality, assuming that the entire C content of dead organisms recycles to the dissolved phase.

For dissolved P:

$$\begin{aligned}\frac{dP}{dt} &= D(P_{in} - P) - BV_{PB} - AV_{PA} - \alpha M V_{PM} \\ &+ m_B B Q_{PB} + m_M M Q_{PM} + m_A A Q_{PA} + m_Z Z Q_{PZ} \\ &+ (1-\alpha) a_{BM} B M Q_{PB} \left(\frac{Q_{PM} - Q_{PM}^{min}}{Q_{PM}^{max} - Q_{PM}^{min}}\right) + a_{BZ} B Z Q_{PB} \left(\frac{Q_{PZ} - Q_{PZ}^{min}}{Q_{PZ}^{max} - Q_{PZ}^{min}}\right)\end{aligned} \tag{3.14}$$

The rate of change of dissolved P in the environment again has a chemostat supply term with supply concentration P_{in}. The next three terms represent uptake by bacteria, autotrophs, and mixotrophs, with

$$V_{PX} = V_{PX}^{max} \left(\frac{P}{k_{PX} + P}\right) \left(\frac{Q_{PX}^{max} - Q_{PX}}{Q_{PX}^{max} - Q_{PX}^{min}}\right) \tag{3.15}$$

Then, four terms denote the rates of P recycling due to mortality, assuming that the entire P content of dead organisms recycles to the dissolved phase. Finally, the rates recycled by the mixotroph and the zooflagellates appear, which are calculated by mass balance as the P fluxes ingested from bacterial prey but not assimilated.

3.3 Numerical Calculations

All biological parameters were set to the values used previously (Table 2.1). Environmental parameters were assigned the values in Table 3.1, except when varied for exploration. P supply (P_{in}) was varied from a low value of 0.0001 to 0.001 mol m^{-3} in nineteen increments. For the other four environmental parameters, two values (0.0003 and 0.0008 mol m^{-3}) were chosen for P supply to represent more oligotrophic and more eutrophic habitats, respectively.

Table 3.1 Environmental Parameter Values

Parameter	Value	Units
C_{in}	0.6	mol m^{-3}
I_{in}	900	J s^{-1} m^{-2}
k_{bg}	0.07	m^{-1}
depth	1.0	m

As parameterized, this model includes processes with very different rates, resulting in stiff equations. Therefore, numerical calculations were done using MATLAB's ode23s solver for stiff differential equations (Shampine and Reichlet 1997). Simulations were run for 4000 days, saving the results from days 3000 to 4000. Populations below 10^{-3} cells m^{-3} were removed after day 3500. Simulations with populations removed were checked to see whether such populations were truly declining or were removed because they were in limit cycles with very large amplitudes.

After using numerical simulation to obtain predicted population and nutrient dynamics, the growth-limitation status was determined for each persisting population (C-limited, P-limited, or cycling dynamically between the two) and three predicted ecosystem properties were computed: C:P ratio, dissolved organic carbon (DOC) production, and the rate of phosphorus (P) recycling by consumers (excluding recycling due to mortality). The molar C:P ratio of the microbial seston is the ratio of the total carbon in the organisms to the total phosphorus in the organisms and is calculated

$$\frac{AQ_{CA} + ZQ_{CZ} + MQ_{CM} + BQ_{CB}}{AQ_{PA} + ZQ_{PZ} + MQ_{PM} + BQ_{PB}} \tag{3.16}$$

DOC production (Eq. (3.17)) is the amount of excess photosynthate excreted by the algae and mixotrophs per day as a proportion of primary production. The specific photosynthesis rate μ_{CX} (1/d) is multiplied by the constant carbon quota (Q_{CX} ; mol C/cell), and by the population density (cells m^{-3}) for both algae and mixotrophs. The respective productivities for each organism

are then summed in the numerator and denominator. Note that the model predicts DOC release only by P-limited populations.

$$\frac{e_A \max(0, \mu_{CA} - \mu_{PA})\, AQ_{CA} + e_M \max(0, \mu_{CM} - \mu_{PM})\, M\, Q_{CM}}{\mu_{CA} AQ_{CA} + \alpha \mu_{CM} MQ_{CM}} \tag{3.17}$$

The recycled P flux is P that is returned to the environment by the mixotroph and the zooflagellates due to P in bacterial prey ingested, but not assimilated, and is calculated as the last two terms from equation (3.14):

$$(1-\alpha)\, a_{BM}\, BM\, Q_{PB} \left(\frac{Q_{PM} - Q_{PM}^{min}}{Q_{PM}^{max} - Q_{PM}^{min}}\right) + a_{BZ}\, BZ\, Q_{PB} \left(\frac{Q_{PZ} - Q_{PZ}^{min}}{Q_{PZ}^{max} - Q_{PZ}^{min}}\right) \tag{3.18}$$

3.4 Results

The first set of results involves steady states in relation to environmental parameters governing resource supply while the second set of results involves ecosystem properties. Simulations were done using two types of mixotrophs, one that is mostly heterotrophic (α = 0.2), and one that is mostly phototrophic (α = 0.9). For each type of mixotroph, two mortality scenarios were explored, equal mortality rates for all organisms at a low value of 0.1 d^{-1}, and differing mortality rates (0.3 d^{-1} for *A*, 0.1 d^{-1} for *Z*, 0.3 d^{-1} for *M*, and 0.6 d^{-1} for *B*). These rates were found in exploratory work to be consistent with persistence of mixotrophs of at least one type over wide ranges of environmental parameters. For each combination of mixotroph type and mortality scenario, parameters governing resource supply were varied from low to high values through nineteen increments one at a time.

3.4.1 Population Persistence and Dynamics

3.4.1.1 Phosphorus Supply (P_{in})

Phosphorus supply (P_{in}) was varied from 0.0001 to 0.001 mol m^{-3}, representing oligotrophic to eutrophic habitats. The mortality scenarios give similar results depending on

whether the mixotrophs were mostly heterotrophic or mostly autotrophic. When the mixotroph was mostly heterotrophic (α = 0.2) in the equal mortality scenario (Figure 3.1 C), predominantly heterotrophic mixotrophs not predicted to persist at any P supply.

Table 3.2 Persisting organisms as Pin increases from its low to high value. Values are either 0.2 or 0.9 for α, and the mortality scenarios for the organisms are either "Equal" and set to all be 0.1, or they have "Different" values. Persisting organisms indicated in regular type are P-limited, those in bold are C-limited, and those in italics switch dynamically between P- and C-limited growth. Blanks indicate when an organism was predicted to go extinct. Pin values 0.0003 and 0.0008 are in bold because they were chosen for use in exploring the other environmental parameters.

P Supply (P_{in})	α = 0.2				α = 0.9			
	Equal		Different		Equal		Different	
0.0001	A **M** B		A **Z** B		**Z** M B		**Z** M B	
0.00015	A **M** B		A **Z** B		M B		**Z** M B	
0.0002	A **M** B		A **Z** B		A M B		**Z** M B	
0.00025	A **M** B		A **Z** B		A M B		A M B	
0.0003	A **M** B		A **Z** B		A M B		A **Z** M B	
0.00035	A **M** B		A **Z** B		A M B		A **Z** M B	
0.0004	A **M** B		A **Z** B		A M B		A **Z** M B	
0.00045	A **M** B		A **Z** B		A **Z** M B		A **Z** M B	
0.0005	A **M** B		A **Z** B		A **Z** M B		A **Z** M B	
0.00055	A **M** B		A **Z** B		A **Z** M B		A **Z** M B	
0.0006	A **Z** B		A **Z** B		A **Z** M B		A **Z** M B	
0.00065	A **Z** B		A **Z** B		A **Z** M B		A **Z** M B	
0.0007	A **Z** B		A **Z** B		A **Z** *M* B		A **Z** M B	
0.00075	A **Z** B		A **Z** B		A **Z** *M* B		A **Z** *M* B	
0.0008	A **Z** B		A **Z** B		A **Z** *M* B		A **Z** *M* B	
0.00085	A **Z** B		A **Z** B		A **Z** *M* B		A **Z** **M** B	
0.0009	A **Z** B		A **Z** B		*A* **Z** *M* B		**A** **Z** B	
0.00095	A **Z** B		A **Z** B		*A* **Z** *M* B		**A** **Z** B	
0.001	A **Z** B		A **Z** B		**A** **Z** **M** B		**A** **Z** B	

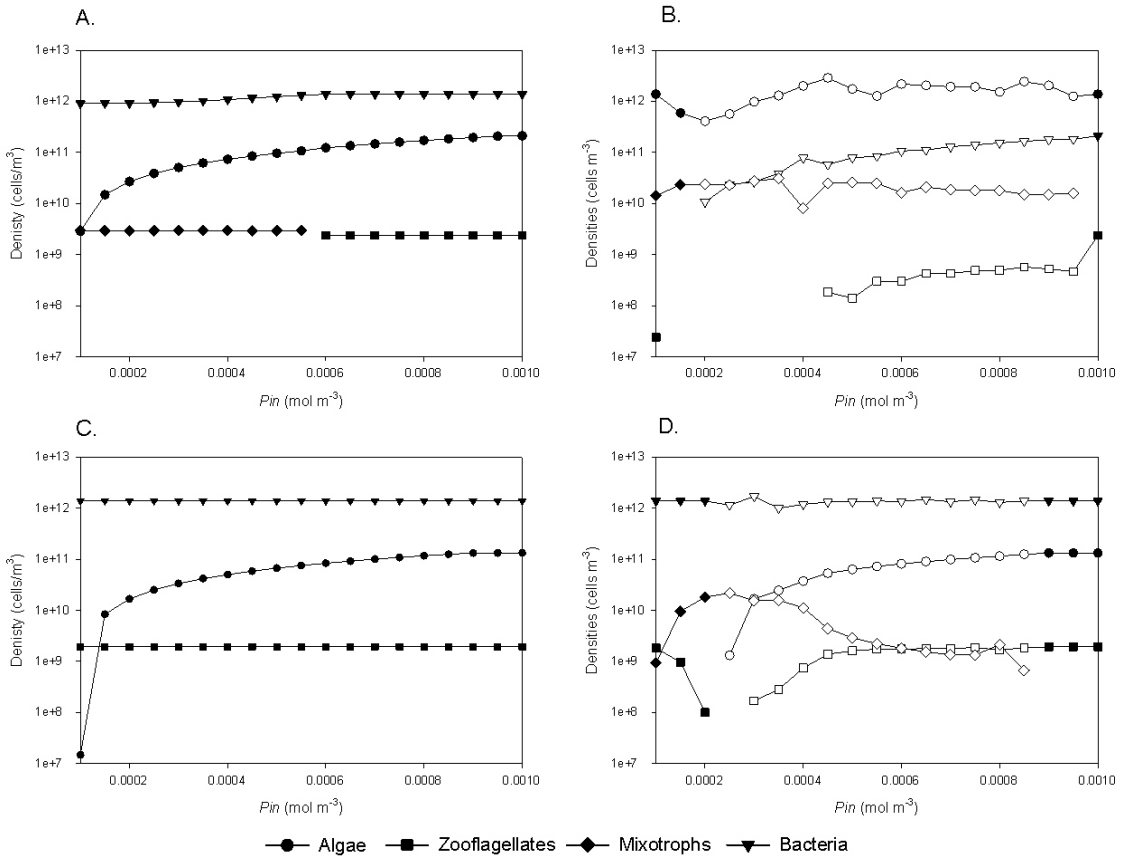

Figure 3.1 Population density average values as P supply (P_{in}) increases from low to high values. Open symbols indicate populations in limit cycles. A) α = 0.2 and equal mortalities B) α = 0.9 and equal mortalities C) α = 0.2 and different mortalities D) α = 0.9 and different mortalities

When the mixotroph is mostly autotrophic (α = 0.9) in the equal mortalities scenario (Table 3.2), the algae were not predicted to persist at low P supply, though mixotrophs were. With higher P supply, algae did persist, and switched from being P-limited to C-limited when P_{in} approached the highest values examined. Limit cycles of algal population density were predicted (Figure 3.1 B) with about a tenfold increase in time-averaged density over the range of P supply tested. The zooflagellates were not present for some values in the low end of the P supply range and when present displayed limit cycles and time-averaged densities largely independent of P supply. Mixotrophs were predicted to persist at all P supplies, switching from P-limited to C-limited growth at the higher end of the P supply range. Mixotroph population densities were in limit cycles with time-averaged densities independent of P supply. The bacteria were predicted to persist with P-limited growth at all P supplies, but were also predicted to have limit cycles with extremely large amplitudes. The results are similar for all of the organisms in the differing mortalities scenario (Table 3.2), however, all of the limit cycles have much lower amplitudes (Figure 3.1 D) and there were no values of P_{in} where algae were predicted to switch dynamically between P- and C-limitation.

3.4.1.2 Mixing Depth

The influence of mixing depth was explored for eight cases, with two values for P supply (P_{in}), two values for α, and two mortality scenarios. With high P supply (0.0008 mol m^{-3}, the results for the four combinations are similar (Table 3.3). The algae were always predicted to persist, switching from P-limitation to C-limitation for depths greater than one meter. They decreased in population density (Figure 3.2) as the depth increased by about tenfold. The zooflagellates are also predicted to persist, and be C-limited with population densities independent of depth. Mixotrophs were only predicted to persist at a depth of one meter when mostly autotrophic (α = 0.9). The bacteria are always predicted to persist and be P-limited with population densities independent of depth.

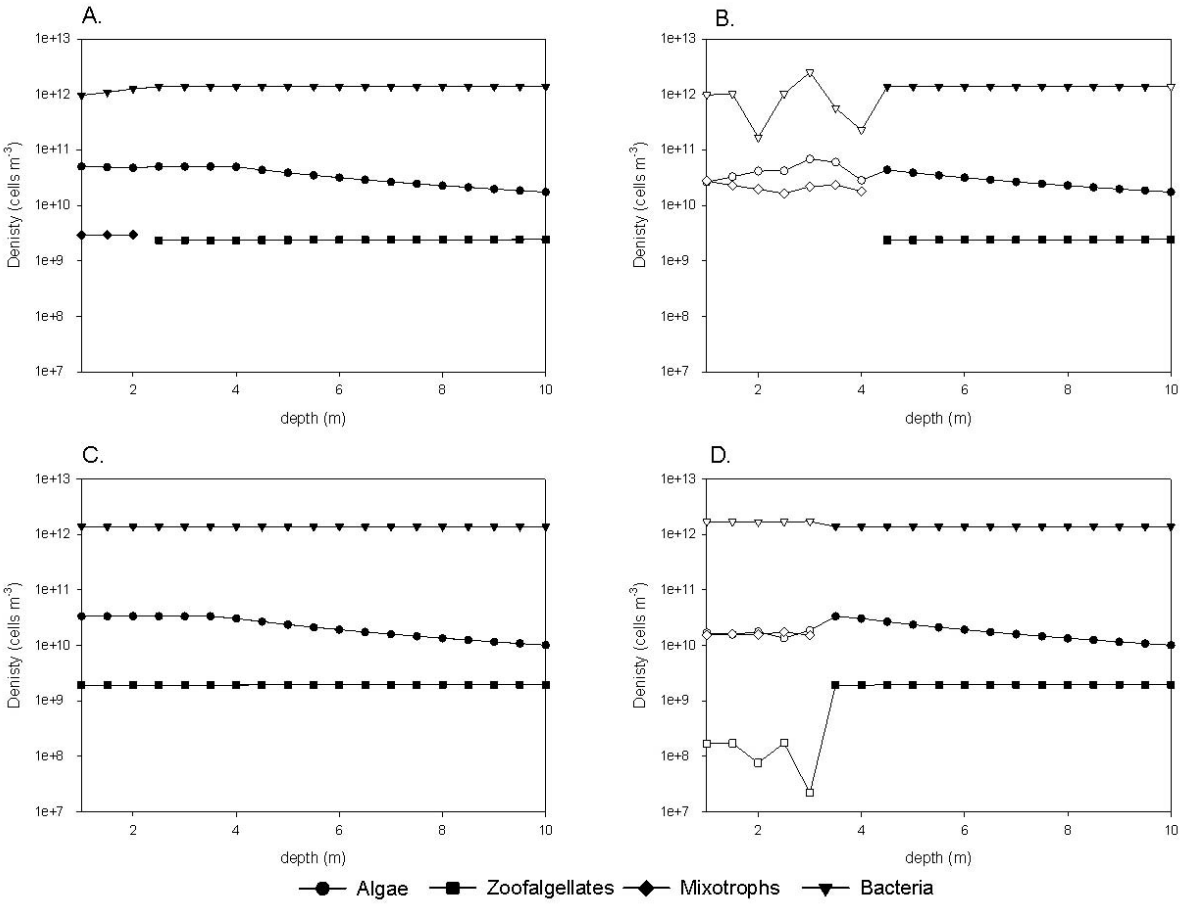

Figure 3.2 Population density average values as depth changes from low to high values for low P supply (P_{in} = 0.0003). Open symbols indicated populations in limit cycles. A) α = 0.2 with equal mortalities B) α = 0.9 with equal mortalities C) α = 0.2 with differing mortalities D) α = 0.9 with differing mortalities.

Table 3.3 Persisting organisms as depth changes from its lowest to highest value. Values are either 0.2 or 0.9 for α, and the mortality scenarios for the organisms are either "Equal" and set to all be 0.1, or they have "Different" values. Persisting organisms indicated in regular type are P-limited, those in **bold** are C-limited, and those in *italics* switch dynamically between P- and C-limited growth. Blanks indicate when an organism was predicted to go extinct.

	P_{in} = 0.0003				P_{in} = 0.0008			
	α = 0.2		α = 0.9		α = 0.2		α = 0.9	
depth	Equal	Different	Equal	Different	Equal	Different	Equal	Different
1.0	A **M** B	A **Z** B	A M B	A **Z** M B	A **Z** B	A **Z** B	A **Z** *M* B	A **Z** *M* B
1.5	A **M** B	A **Z** B	A M B	A **Z** M B	**A Z** B	**A Z** B	**A Z** B	**A Z** B
2.0	A **M** B	A **Z** B	A M B	A **Z** M B	**A Z** B	**A Z** B	**A Z** B	**A Z** B
2.5	A **Z** B	A **Z** B	A *M* B	A **Z** M B	**A Z** B	**A Z** B	**A Z** B	**A Z** B
3.0	A **Z** B	A **Z** B	*A* *M* B	*A* **Z** M B	**A Z** B	**A Z** B	**A Z** B	**A Z** B
3.5	A **Z** B	A **Z** B	*A* *M* B	A **Z** B	**A Z** B	**A Z** B	**A Z** B	**A Z** B
4.0	**A Z** B	**A Z** B	*A* **M** B	**A Z** B	**A Z** B	**A Z** B	**A Z** B	**A Z** B
4.5	**A Z** B	**A Z** B	**A Z** B	**A Z** B	**A Z** B	**A Z** B	**A Z** B	**A Z** B
5.0	**A Z** B	**A Z** B	**A Z** B	**A Z** B	**A Z** B	**A Z** B	**A Z** B	**A Z** B
5.5	**A Z** B	**A Z** B	**A Z** B	**A Z** B	**A Z** B	**A Z** B	**A Z** B	**A Z** B
6.0	**A Z** B	**A Z** B	**A Z** B	**A Z** B	**A Z** B	**A Z** B	**A Z** B	**A Z** B
6.5	**A Z** B	**A Z** B	**A Z** B	**A Z** B	**A Z** B	**A Z** B	**A Z** B	**A Z** B
7.0	**A Z** B	**A Z** B	**A Z** B	**A Z** B	**A Z** B	**A Z** B	**A Z** B	**A Z** B
7.5	**A Z** B	**A Z** B	**A Z** B	**A Z** B	**A Z** B	**A Z** B	**A Z** B	**A Z** B
8.0	**A Z** B	**A Z** B	**A Z** B	**A Z** B	**A Z** B	**A Z** B	**A Z** B	**A Z** B
8.5	**A Z** B	**A Z** B	**A Z** B	**A Z** B	**A Z** B	**A Z** B	**A Z** B	**A Z** B
9.0	**A Z** B	**A Z** B	**A Z** B	**A Z** B	**A Z** B	**A Z** B	**A Z** B	**A Z** B
9.5	**A Z** B	**A Z** B	**A Z** B	**A Z** B	**A Z** B	**A Z** B	**A Z** B	**A Z** B
10.0	**A Z** B	**A Z** B	**A Z** B	**A Z** B	**A Z** B	**A Z** B	**A Z** B	**A Z** B

With low P supply (0.0003 mol m^{-3}), bacteria were again always predicted to persist and be P-limited (Table 3.3). Algae were also always predicted to persist, and to switch from P- to C-limitation for depths greater than about 3.5 meters. When the mixotrophs were mostly autotrophic (α = 0.9), they had a small range of depths, 2.5 to 3.5 meters, where they switched dynamically between C- and P-limitation during limit cycles. Primarily autotrophic mixotrophs were predicted to be C-limited at 4 meters, and to go extinct in deeper habitats. When the mixotrophs were mostly heterotrophic (α = 0.2) and in the equal mortality scenario, they were predicted to persist and C-limited for depths up to two meters, but to go extinct for deeper habitats. In the differing mortality scenario, mixotrophs were not predicted to persist for any depth. The zooflagellates were predicted to persist and be C-limited whenever mixotrophs were absent, except when the mixotrophs were mostly autotrophic and in the differing mortalities scenario where zooflagellates coexisted with the mixotrophs for habitats up to three meters deep. In this coexistence range all of the organisms exhibited limit cycles (Figure 3.2 B).

3.4.1.3 Surface Irradiance (I_{in})

Eight cases were again examined with varying surface irradiance (I_{in}) -- two types of mixotrophs, two P supplies, and two mortality scenarios. For the four environments with low P supply (0.0003 mol m^{-3}), results are similar (Table 3.4). For primarily phototrophic mixotrophs (α = 0.9) and the differing mortality scenario, persistence of all four organisms was predicted at all surface irradiances, with zooflagellates C-limited and other organisms P-limited. With equal mortality, zooflagellates were predicted to go extinct with primarily autotrophic mixotrophs. Primarily heterotrophic mixotrophs (α = 0.2) were predicted to persist and be C-limited with equal mortality, while zooflagellates went extinct. With differing mortality, primarily heterotrophic mixotrophs were not predicted to persist, but were replaced by C-limited zooflagellates. Apart from these instances of C-limitation, organisms were predicted to be P-limited in low P supply habitats. For all organisms predicted to persist, time-averaged populations densities did not

Table 3.4 Persisting organisms as light changes from its lowest to highest value. Values are either 0.2 or 0.9 for α, and the mortality scenarios for the organisms are either "Equal" and set to all be 0.1, or they have "Different" values. Persisting organisms indicated in regular type are P-limited, those in **bold** are C-limited, and those in ***italics*** switch dynamically between P- and C-limited growth. Blanks indicate when an organism was predicted to go extinct.

Light Supply (I_{in})	P_{in} = 0.0003								P_{in} = 0.0008							
	α = 0.2				α = 0.9				α = 0.2				α = 0.9			
	Equal		Different		Equal		Different		Equal		Different		Equal		Different	
400	A **M** B		A **Z** B		A M B		A **Z** M B		A **Z** B		**A Z** B		***A*** **Z** ***M*** B		**A Z** B	
430	A **M** B		A **Z** B		A M B		A **Z** M B		A **Z** B		**A Z** B		***A*** **Z** ***M*** B		**A Z** B	
460	A **M** B		A **Z** B		A M B		A **Z** M B		A **Z** B		**A Z** B		***A*** **Z** ***M*** B		**A Z** B	
480	A **M** B		A **Z** B		A M B		A **Z** M B		A **Z** B		**A Z** B		***A*** **Z** ***M*** B		**A Z** B	
510	A **M** B		A **Z** B		A M B		A **Z** M B		A **Z** B		A **Z** B		***A*** **Z** ***M*** B		A **Z** B	
540	A **M** B		A **Z** B		A M B		A **Z** M B		A **Z** B		A **Z** B		***A*** **Z** ***M*** B		A **Z** B	
570	A **M** B		A **Z** B		A M B		A **Z** M B		A **Z** B		A **Z** B		***A*** **Z** ***M*** B		A **Z** B	
590	A **M** B		A **Z** B		A M B		A **Z** M B		A **Z** B		A **Z** B		***A*** **Z** ***M*** B		A **Z** B	
620	A **M** B		A **Z** B		A M B		A **Z** M B		A **Z** B		A **Z** B		A **Z** ***M*** B		A **Z** B	
650	A **M** B		A **Z** B		A M B		A **Z** M B		A **Z** B		A **Z** B		A **Z** ***M*** B		A **Z** **M** B	
680	A **M** B		A **Z** B		A M B		A **Z** M B		A **Z** B		A **Z** B		A **Z** ***M*** B		A **Z** ***M*** B	
700	A **M** B		A **Z** B		A M B		A **Z** M B		A **Z** B		A **Z** B		A **Z** ***M*** B		A **Z** ***M*** B	
730	A **M** B		A **Z** B		A M B		A **Z** M B		A **Z** B		A **Z** B		A **Z** ***M*** B		A **Z** ***M*** B	
760	A **M** B		A **Z** B		A M B		A **Z** M B		A **Z** B		A **Z** B		A **Z** ***M*** B		A **Z** ***M*** B	
790	A **M** B		A **Z** B		A M B		A **Z** M B		A **Z** B		A **Z** B		A **Z** ***M*** B		A **Z** ***M*** B	
820	A **M** B		A **Z** B		A M B		A **Z** M B		A **Z** B		A **Z** B		A **Z** ***M*** B		A **Z** ***M*** B	
840	A **M** B		A **Z** B		A M B		A **Z** M B		A **Z** B		A **Z** B		A **Z** ***M*** B		A **Z** ***M*** B	
870	A **M** B		A **Z** B		A M B		A **Z** M B		A **Z** B		A **Z** B		A **Z** ***M*** B		A **Z** ***M*** B	
900	A **M** B		A **Z** B		A M B		A **Z** M B		A **Z** B		A **Z** B		A **Z** ***M*** B		A **Z** ***M*** B	

change with surface irradiance (results not shown). When mixotrophs are predicted to persist, population densities displayed limit cycles.

For the four environments with high P (P_{in} = 0.0008 mol m^{-3}), the results differ (Table 3.4). When the mixotroph is mostly heterotrophic (α = 0.2) it is not predicted to persist. In the equal mortalities scenario, P-limited algae and bacteria persisted with C-limited zooflagellates for all irradiances examined. When the mortalities differ, the results were similar to the equal mortalities scenario, but the algae switched from C-limited to P-limited at higher light levels. All of the persisting organisms had predicted population densities independent of light supply (not shown). When the mixotrophs were mostly autotrophic (α = 0.9), coexistence of all four organisms was predicted. For the equal mortalities scenario, the time-averaged population densities were independent of light supply and exhibited limit cycles (not shown). During these cycles, mixotrophs shifted dynamically between C- and P-limitation. Algae and bacteria were predicted to be P-limited, with C-limited zooflagellates. For the different mortalities scenario, mixotrophs were predicted to persist and coexist with the other organisms only at higher surface irradiances. They were predicted to be C-limited at 650 W/m^2, with dynamically switching limitations during limit cycles for higher irradiances. Algae were predicted to be C-limited for low irradiances and P-limited otherwise, Bacteria were predicted always to be P-limited and zooflagellates to be C-limited.

3.4.1.4 Organic C supply (C_{in}) and turbidity (k_{bg})

For both of these parameters (C_{in}, k_{bg}), there is no change in community structure over the ranges explored and results depend on mixotrophy type and mortality scenario in the same way (Table 3.5, Table 3.6). For the low P supply (P_{in} = 0.0003 mol m^{-3}) environments, there are four patterns. When the mixotrophs were mostly heterotrophic (α = 0.2), the results differ depending on the mortality scenario. With equal mortalities, C-limited mixotrophs were predicted to persist with P-limited algae and bacteria, with zooflagellates going extinct. With different mortalities, primarily heterotrophic mixotrophs were not predicted to persist, but C-limited

Table 3.5 Persisting organisms as organic C supply (C_{in}) changes from its lowest to highest value. Values are either 0.2 or 0.9 for α, and the mortality scenarios for the organisms are either "Equal" and set to all be 0.1, or they have "Different" values. Persisting organisms indicated in regular type are P-limited, those in **bold** are C-limited, and those in *italics* switch dynamically between P- and C-limited growth. Blanks indicate when an organism was predicted to go extinct.

C supply (C_{in})	P_{in} = 0.0003				P_{in} = 0.0008			
	α = 0.2		α = 0.9		α = 0.2		α = 0.9	
	Equal	Different	Equal	Different	Equal	Different	Equal	Different
0	A **M** B	A **Z** B	A M B	A **Z** M B	A **Z** B	A **Z** B	A **Z** *M* B	A **Z** *M* B
0.033	A **M** B	A **Z** B	A M B	A **Z** M B	A **Z** B	A **Z** B	A **Z** *M* B	A **Z** *M* B
0.067	A **M** B	A **Z** B	A M B	A **Z** M B	A **Z** B	A **Z** B	A **Z** *M* B	A **Z** *M* B
0.100	A **M** B	A **Z** B	A M B	A **Z** M B	A **Z** B	A **Z** B	A **Z** *M* B	A **Z** *M* B
0.133	A **M** B	A **Z** B	A M B	A **Z** M B	A **Z** B	A **Z** B	A **Z** *M* B	A **Z** *M* B
0.167	A **M** B	A **Z** B	A M B	A **Z** M B	A **Z** B	A **Z** B	A **Z** *M* B	A **Z** *M* B
0.200	A **M** B	A **Z** B	A M B	A **Z** M B	A **Z** B	A **Z** B	A **Z** *M* B	A **Z** *M* B
0.233	A **M** B	A **Z** B	A M B	A **Z** M B	A **Z** B	A **Z** B	A **Z** *M* B	A **Z** *M* B
0.267	A **M** B	A **Z** B	A M B	A **Z** M B	A **Z** B	A **Z** B	A **Z** *M* B	A **Z** *M* B
0.300	A **M** B	A **Z** B	A M B	A **Z** M B	A **Z** B	A **Z** B	A **Z** *M* B	A **Z** *M* B
0.333	A **M** B	A **Z** B	A M B	A **Z** M B	A **Z** B	A **Z** B	A **Z** *M* B	A **Z** *M* B
0.367	A **M** B	A **Z** B	A M B	A **Z** M B	A **Z** B	A **Z** B	A **Z** *M* B	A **Z** *M* B
0.400	A **M** B	A **Z** B	A M B	A **Z** M B	A **Z** B	A **Z** B	A **Z** *M* B	A **Z** *M* B
0.433	A **M** B	A **Z** B	A M B	A **Z** M B	A **Z** B	A **Z** B	A **Z** *M* B	A **Z** *M* B
0.467	A **M** B	A **Z** B	A M B	A **Z** M B	A **Z** B	A **Z** B	A **Z** *M* B	A **Z** *M* B
0.500	A **M** B	A **Z** B	A M B	A **Z** M B	A **Z** B	A **Z** B	A **Z** *M* B	A **Z** *M* B
0.533	A **M** B	A **Z** B	A M B	A **Z** M B	A **Z** B	A **Z** B	A **Z** *M* B	A **Z** *M* B
0.567	A **M** B	A **Z** B	A M B	A **Z** M B	A **Z** B	A **Z** B	A **Z** *M* B	A **Z** *M* B
0.600	A **M** B	A **Z** B	A M B	A **Z** M B	A **Z** B	A **Z** B	A **Z** *M* B	A **Z** *M* B

Table 3.6 Persisting organisms as turbidity (k_{bg}) changes from its lowest to highest value. Values are either 0.2 or 0.9 for α, and the mortality scenarios for the organisms are either "Equal" and set to all be 0.1, or they have "Different" values. Persisting organisms indicated in regular type are P-limited, those in **bold** are C-limited, and those in *italics* switch dynamically between P- and C-limited growth. Blanks indicate when an organism was predicted to go extinct.

turbidity (k_{bg})	P_{in} = 0.0003				P_{in} = 0.0008			
	α = 0.2		α = 0.9		α = 0.2		α = 0.9	
	Equal	Different	Equal	Different	Equal	Different	Equal	Different
0.070	A **M** B	A **Z** B	A M B	A **Z** M B	A **Z** B	A **Z** B	A **Z** *M* B	A **Z** *M* B
0.105	A **M** B	A **Z** B	A M B	A **Z** M B	A **Z** B	A **Z** B	A **Z** *M* B	A **Z** *M* B
0.140	A **M** B	A **Z** B	A M B	A **Z** M B	A **Z** B	A **Z** B	A **Z** *M* B	A **Z** *M* B
0.175	A **M** B	A **Z** B	A M B	A **Z** M B	A **Z** B	A **Z** B	A **Z** *M* B	A **Z** *M* B
0.210	A **M** B	A **Z** B	A M B	A **Z** M B	A **Z** B	A **Z** B	A **Z** *M* B	A **Z** *M* B
0.245	A **M** B	A **Z** B	A M B	A **Z** M B	A **Z** B	A **Z** B	A **Z** *M* B	A **Z** *M* B
0.280	A **M** B	A **Z** B	A M B	A **Z** M B	A **Z** B	A **Z** B	A **Z** *M* B	A **Z** *M* B
0.315	A **M** B	A **Z** B	A M B	A **Z** M B	A **Z** B	A **Z** B	A **Z** *M* B	A **Z** *M* B
0.350	A **M** B	A **Z** B	A M B	A **Z** M B	A **Z** B	A **Z** B	A **Z** *M* B	A **Z** *M* B
0.385	A **M** B	A **Z** B	A M B	A **Z** M B	A **Z** B	A **Z** B	A **Z** *M* B	A **Z** *M* B
0.420	A **M** B	A **Z** B	A M B	A **Z** M B	A **Z** B	A **Z** B	A **Z** *M* B	A **Z** *M* B
0.455	A **M** B	A **Z** B	A M B	A **Z** M B	A **Z** B	A **Z** B	A **Z** *M* B	A **Z** *M* B
0.490	A **M** B	A **Z** B	A M B	A **Z** M B	A **Z** B	A **Z** B	A **Z** *M* B	A **Z** *M* B
0.525	A **M** B	A **Z** B	A M B	A **Z** M B	A **Z** B	A **Z** B	A **Z** *M* B	A **Z** *M* B
0.560	A **M** B	A **Z** B	A M B	A **Z** M B	A **Z** B	A **Z** B	A **Z** *M* B	A **Z** *M* B
0.595	A **M** B	A **Z** B	A M B	A **Z** M B	A **Z** B	A **Z** B	A **Z** *M* B	A **Z** *M* B
0.630	A **M** B	A **Z** B	A M B	A **Z** M B	A **Z** B	A **Z** B	A **Z** *M* B	A **Z** **M** B
0.665	A **M** B	A **Z** B	A M B	A **Z** M B	A **Z** B	A **Z** B	A **Z** *M* B	A **Z** **M** B
0.700	A **M** B	A **Z** B	A M B	A **Z** M B	A **Z** B	A **Z** B	A **Z** *M* B	A **Z** **M** B

zooflagellates were predicted to persist with P-limited algae and bacteria. Population densities were predicted to be independent of organic C supply or turbidity (results not shown). When the mixotrophs were mostly autotrophic (α = 0.9) and the mortalities equal, algae, mixotrophs, and bacteria were predicted to coexist with P-limitation, and zooflagellates were predicted to go extinct. Densities of persisting populations were independent of C supply or turbidity, and in limit cycles. With different mortalities, the C-limited zooflagellates were predicted to coexist with P-limited mixotrophs, algae and bacteria, with all four populations in limit cycles.

For the high P supply (0.0008 mol m^{-3}) environments, there were no differences between the two mortality scenarios tested. Primarily heterotrophic mixotrophs (α = 0.2) were not predicted to persist. C-limited zooflagellates were predicted to persist with P-limited algae and bacteria. Densities of all persisting populations were predicted to be independent of C supply or turbidity. Primarily autotrophic mixotrophs were predicted to coexist with zooflagellates, algae and bacteria, switching dynamically between C- and P-limitation during limit cycles. Zooflagellates were predicted to be C-limited, and algae and bateria P-limited. All of population densities were in limit cycles and and independent of C supply or turbidity.

3.4.2 Ecosystem Properties

3.4.2.1 Phosphorus Supply (P_{in})

There were general trends for the ecosystem properties that developed as a consequence of increasing the P supply. The predicted C:P ratio (Figure 3.3 A) increased rapidly until the P supply reached about 0.0003 mol m^{-3} and then became constant as the P supply increased. The predicted C:P ratios are higher for the equal mortality scenario than for different mortalities. The recycled P flux (Figure 3.3 B) generally increased as the P supply increased when the mixotrophs were mostly autotrophic (α = 0.2). When the mortalities were different, the P flux became constant as P supply increased. When the mortalities were equal, P flux increased until the P supply reached 0.0006 mol m^{-3} and then became constant for increasing P

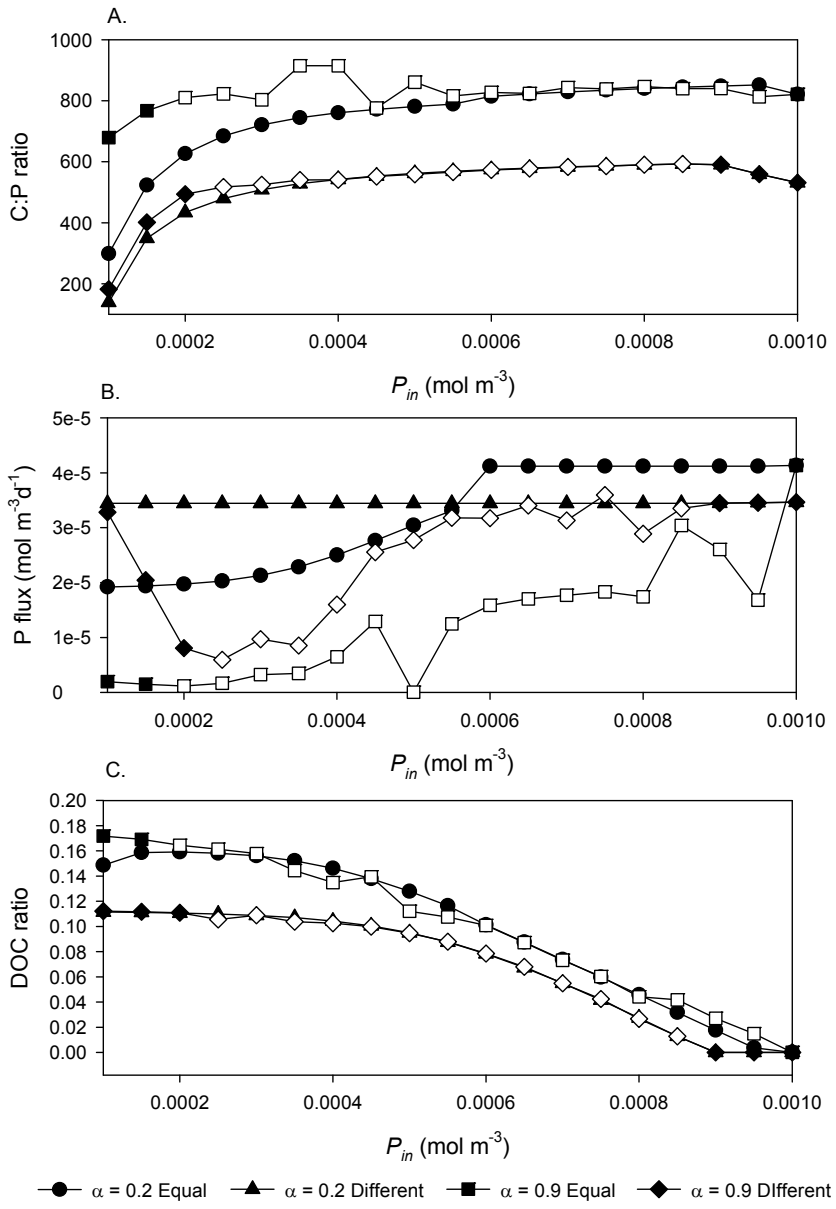

Figure 3.3 Predicted ecosystem properties for the four combinations of α and mortality scenarios as P supply (P_{in}) increases. Time averages are shown when populations were in limit cycles (open symbols).

supply. For the different mortalities scenario, P flux was always independent of P supply. For all conditions examined, the predicted DOC flux (Figure 3.3 C) decreased as the P supply increased.

3.4.2.2 Mixing Depth

As depth increased, the C:P ratio response depended on the level of P supply. For low P supply (P_{in} = 0.0003 mol m^{-3}), the C:P ratios did not change with increasing depth until around three meters and then slowly decreased (Figure 3.4 A). For the high P supply (P_{in} = 0.0008 mol m^{-3}), the ratios continually decreased as depth increased (Figure 3.5 A). P flux generally increased as depth increased and then became unchanging (Figure 3.4 B). For the two combinations of low P supply (P_{in} = 0.0003 mol m^{-3}) and high α (0.9), P flux was relatively low until around 3 meters and then increased rapidly and became unchanging with increasing depth (Figure 3.5 B). For the two combinations of low α (0.2) and differing mortalities, the P flux remained fairly constant. DOC segregated depending on P supply. For the four combinations with low P supply (P_{in} = 0.0003 mol m^{-3}), there was a gradual decline with depth until about four meters and then DOC became zero (Figure 3.4 C). For the four combinations with high P supply (P_{in} = 0.0008 mol m^{-3}), DOC began low (5%) and became zero after one meter (Figure 3.5 C).

3.4.2.3 Surface Irradiance (I_{in})

The effect of surface irradiance was examined for eight combinations of P supply, mortality scenario, and mixotroph type (α). As the incident light increased from the low value of 400 W/m^2 to the high value of 900 W/m^2, the predicted C:P ratio showed a slight increase of about 5% for all combinations (results not shown). The predicted recycled P flux (results not shown) was unchanging as surface irradiance (I_{in}) increased. The predicted DOC flux was slightly more complicated. DOC flux increased slightly as incident light increased in the low P supply (P_{in}) environments (Figure 3.6 A) with the equal mortalities scenario being much higher overall than the different mortality scenario. In the high P supply (P_{in}) environments (Figure 3.6 B), the increase in predicted DOC flux was more pronounced with the equal mortality scenarios again giving higher values.

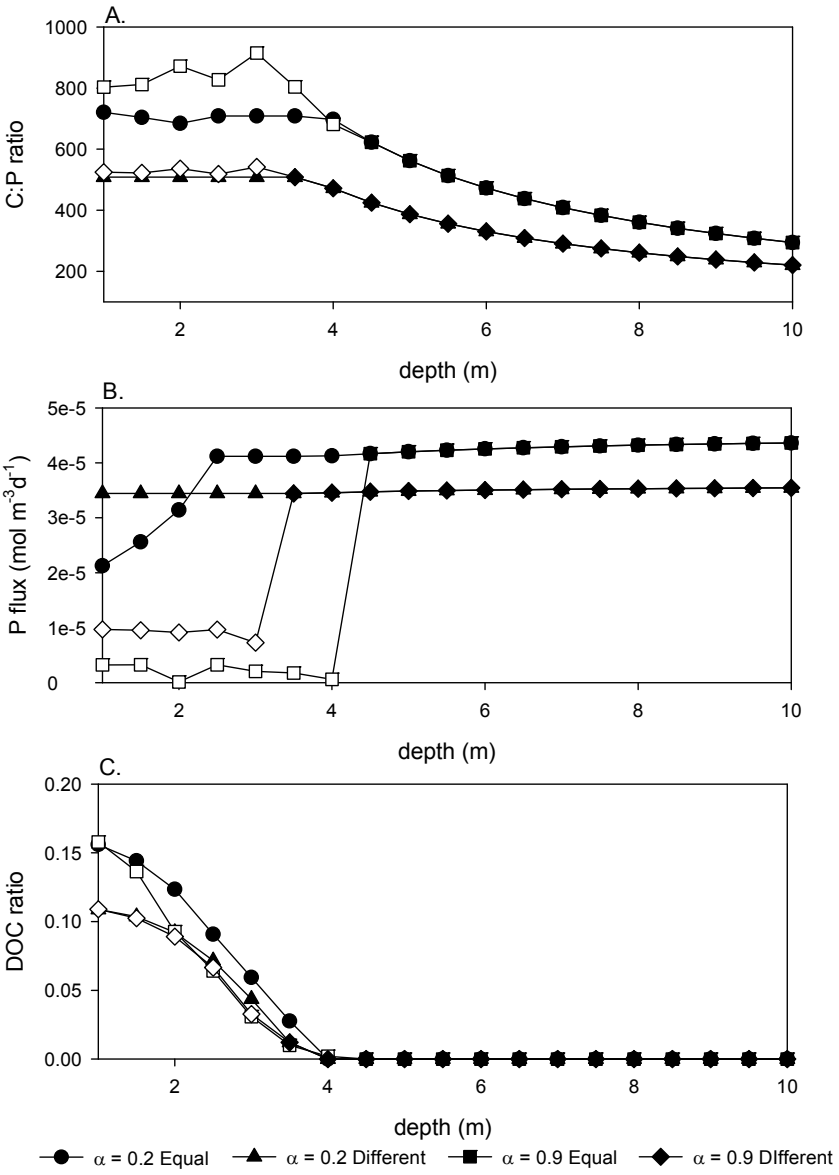

Figure 3.4 Ecosystem properties for the four combinations of α, and mortality scenarios as depth increases for the low P supply (P_{in} = 0.0003 mol m^{-3}) environments. Time averages are shown when populations were in limit cycles (open symbols).

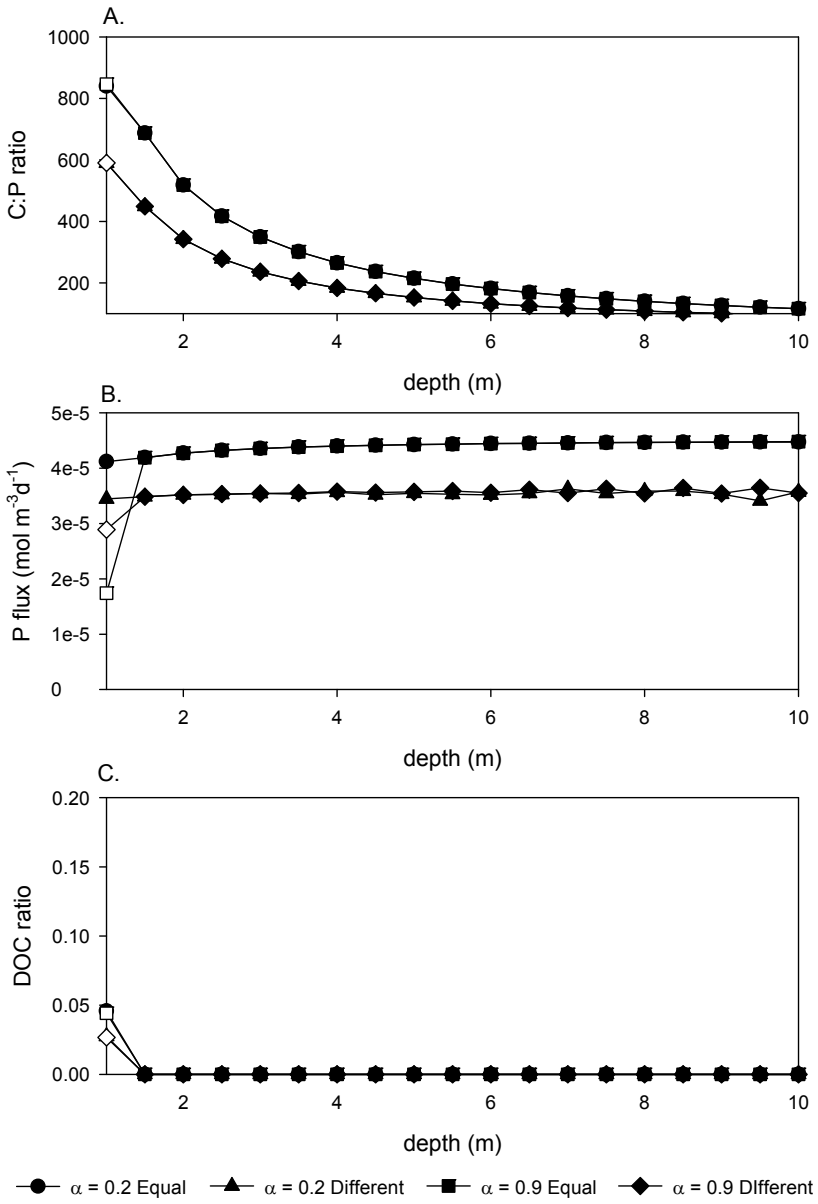

Figure 3.5 Ecosystem properties for the four combinations of α, and mortality scenarios as depth increases for the high P supply (P_{in} = 0.0008 mol m^{-3}) environments. Time averages are shown when populations were in limit cycles (open symbols).

3.4.2.4 Organic Carbon Supply (C_{in}) and turbidity (k_{bg})

Predicted ecosystem properties did not change in response to carbon supply (C_{in}) or turbidity (k_{bg}).

3.5 Discussion

This study explored the role of mixotrophs in aquatic ecosystems using a mathematical model of a simple microbial food web with mixotrophs, specialist phototrophs, and two types of specialist heterotrophs, osmotrophic bacteria and phagotrophic zooflagellates preying upon them. This study focused on the effects of environmental parameters governing resource supplies and the responses of populations and ecosystem properties. The previous chapter used the same model, but focused on the properties of the mixotroph, exploring a range of values portraying it as ranging from heterotrophic (α = 0) to autotrophic (α = 1). That work found that coexistence of mixotrophs with the other microbial types was favored by high supplies of P and light. This study also predicted that the mixotrophs that were most successful in terms of achieving high density were those that were mostly autotrophic. This chapter extends the previous one by focusing more on the environmental parameters governing resource supplies for two distinct types of mixotrophs, primarily heterotrophic and primarily phototrophic. We again found that coexistence of all four organisms was possible and even likely, and we further predict that coexistence is favored when mostly autotrophic mixotrophs reside in shallow environments. This study also examined ecosystem properties, especially as they pertain to the light:P hypothesis (Sterner et al. 1997), which did not explicitly address the role of mixotrophs in aquatic ecosystems in its original formulation. We found that the model generally reflects the predictions of this hypothesis as long as the P supply is not profoundly limiting.

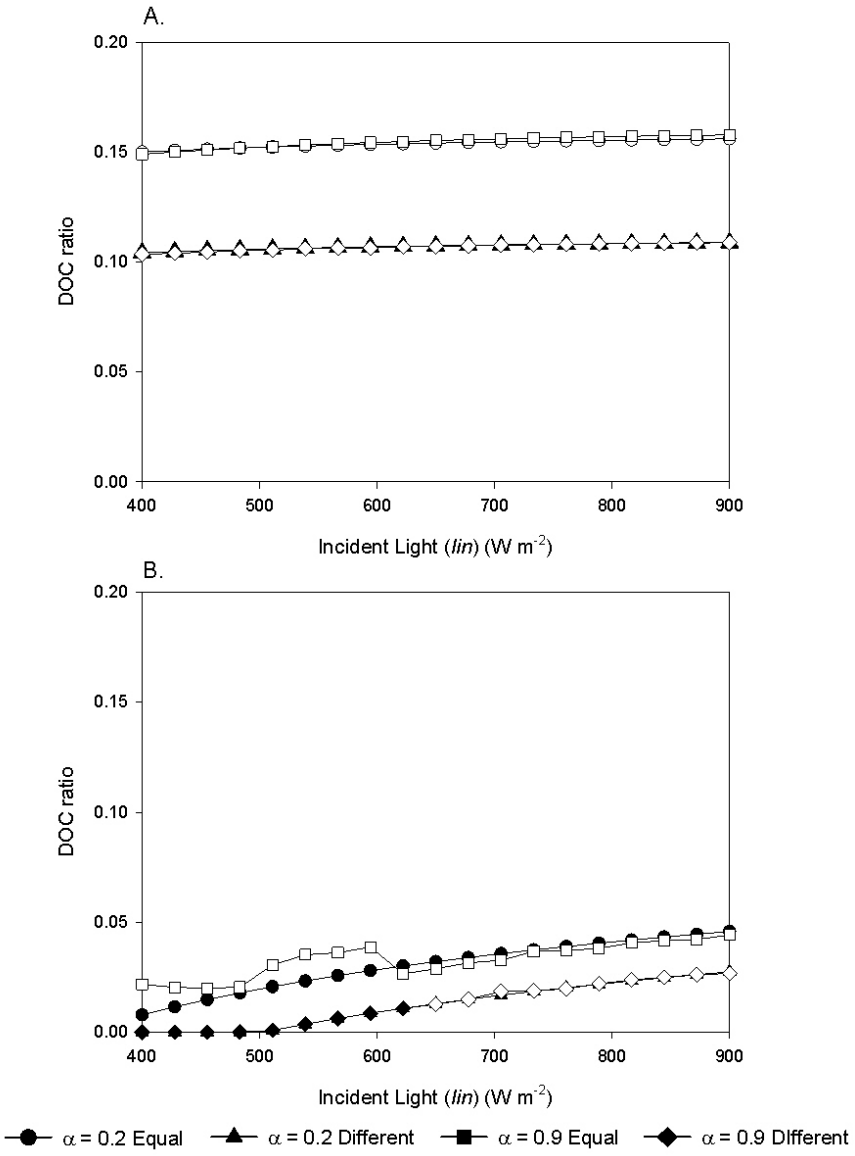

Figure 3.6 DOC as incident light (I_{in}) increases from its low to high values for the four combinations of α and mortality scenarios in the A) low P supply (P_{in} = 0.0003) environments and B) high P supply (P_{in} = 0.0008) environments. Time average values are used when populations are in limit cycles (open symbols).

A principal comparison for the predictions elaborated here is the Thingstad et al. (1996) model, which used Lotka-Voltera equations with a single basal nutrient resource. That study examined a mixotroph with differing affinities for the resource and for bacterial prey. It did not predict coexistence of the four species modeled (bacteria, the mixotroph, and specialized phagotrophs and phototrophs) under any conditions. Using another model with one basal nutrient resource, Stickney (2000) predicted coexistence of mixotrophs consuming phytoplankton, their phototrophic phytoplankton prey, and heterotrophs consuming both mixotrophs and phytoplankton. Compared to these prior models, the one presented here (and in Chapter 2) has two basal resources (light and a nutrient), with internal storage of the nutrient modeled with Droop equations and attenuation of light in a well-mixed water column. Thus species interactions are represented in greater mechanistic detail. The resulting model often predicts coexistence of mixotrophs with other microbial types in a variety of environments. One striking prediction is that coexistence is more likely when the mixotroph is mostly autotrophic. Primarily phototrophic plankton were noted to supplement their nutritional needs with phagotrophy (Stoecker 1999). Coexistence was possible across the range of incident light examined, and across a broad range of higher values for P supply. However, coexistence was only predicted at shallow depths, at most four meters. Primarily phototrophic mixotrophs are found widespread in shallow waters in freshwater and marine environments where they compete well with phytoplankton (Tittel et al. 2003, Zubkov and Tarran 2008).

This study also predicted how seston C:P, proportion of photosynthesis released as DOC, and recycling of P by phagotrophic consumers would respond to environmental parameters governing resource supplies, in microbial food webs with mixotrophs. The light:P hypothesis is a broader framework predicting how these ecosystem properties vary in pelagic ecosystems (Sterner et al. 1997), which did not address the role of mixotrophs, but did emphasize these and other ecosystem properties that connect microbial food webs to the metazoa of higher trophic levels. According to the light:P hypothesis, the C:P of the seston should show a direct correspondence with light:P (Sterner et. al. 1997). Increasing light over the range used (400-900

W m^{-2}) and holding P supply constant did slightly increase the predicted bulk C:P ratio of the organisms, a proxy for seston, and the predicted C:P ratio also decreased with increasing depth (decreasing light and P supply constant). These results agree with the light:P hypothesis. However, when light is held constant and P supply is increased (decreasing the light:P ratio), the C:P ratio predicted by this model did not decrease, contradiction the expectations of the light:P hypothesis. The C:P ratio did increase for the lowest P supplies examined, and then decreased for the highest levels. This increase, which contradicts the light:P hypothesis, occurs when the algae are predicted to be P-limited. P-limited algae can achieve high C:P ratios when P-limited (Sterner and Hessen 1994), a property allowed by the parameters of this model. In severely P-limited conditions, a small increase in P supply increases the abundance of algae without much reducing their C:P ratio, and with a higher contribution of algae to seston, its C:P accordingly rises. Once P-supply increases sufficiently, decreasing C:P of algae compensates for the increase of their abundance, and predicted seston C:P varies little P-supply (see the range P_{in} = 0.0004 – 0.0008 mol m^{-3}, Fig. 3.3A). With higher P-supply, algae become light-limited, and the predicted C:P ratios decline, in agreement with the light:P hypothesis. The range of P_{in} (0.0001 to 0.001 mol m^{-3}) used here only leads the algae to become light limited for the highest values (P_{in} > 0.0008 mol m^{-3}). If this range was continued, the predicted seston C:P ratio would likely follow the expectations of the light:P hypothesis.

As the light:P ratio increases, organisms other than bacteria also become P-limited. For the low P supply environments (P_{in} = 0.0003 mol m^{-3}) when light was increased (increasing light:P) , there was no change in prediction limitations for the different types of organisms and most were P-limited (Table 3.4). However, in the high P supply environments (P_{in} = 0.0008 mol m^{-3}) when light was increased (again, increasing light:P), switches from C-limitation to P-limitation were predicted for most types of organisms as the light levels rose (Table 3.4). The expectations of the light:P hypothesis are largely based on switches in the growth-limitation status of aquatic organisms as relative supplies of these resources vary. For the mechanistic model of microbial food webs developed here, similar predictions arise when supply conditions vary through ranges

where similar switches in growth-limitation occur, but contrary predictions are sometimes observed in extremely P-limited conditions where no such switches occur.

In discussing phagotrophy by phototrophs, Raven (1997) described the mixed use of resources by these organisms as having an effect on biogeochemical cycling that is out of proportion to their representation in the community of phototrophs (both specialized and mixotrophic). The mixotrophs modeled here were predicted to have a profound influence on the P flux recycled during bacterivory. When mixotrophs and algae are both present, this P flux is low and inversely related to light:P. In the few cases where mixotrophs were not present with algae, the recycled P flux was directly related to light:P. This model thus suggests that the composition of nutritional strategies in microbial ecosystems can have a profound influence on this measure of ecosystem properties.

Models by their nature have some limitations. All of the numerical calculations presented here arise from simulations run for very long periods of time with constant nutrient inputs, generating predictions that might apply as long-term averages to natural ecosystems, but which also neglect transient dynamics and responses to temporal environmental variability. Perfect mixing of the aquatic habitat has also been assumed, which limits the scope of the predictions but also avoids computational difficulties involved in modeling growth that depends on internal stores in poorly mixed conditions (Grover 2009), and light-limited growth in such conditions (Huisman and Sommeijer 2002). Possibly more important, comparison of two mortality scenarios suggests that many predictions of the model presented here are sensitive to assumptions about mortality rates. In broad terms, the predictions of coexistence and ecosystem properties emphasized here were similar for the two mortality scenarios modeled. Clearly, further exploration of the influence of mortality rates would better delimit the predictions of this model. Technically, this model suffers from intrinsic difficulties of stiffness to the point that some systems could not be resolved even though a solver for stiff systems was used (Shampine and Reichelt 1997).

Even with the limitations of the model, some useful insights were obtained that were reasonably robust within the parameter settings explored. Coexistence of microbial populations

pursuing different nutritional strategies was commonly predicted. Moreover, the ecosystem properties expected under the light:P hypothesis were supported by the predictions of this model, with a few notable exceptions involving severely P-limited habitats. This study shows the hypothesis remains a reasonable way to look at aquatic ecosystems, when mixotrophs and their mechanisms of interaction with other microorganisms are explicitly incorporated. More generally, this study suggests theoretically that mixotrophs are abundant under wide ranges of resource supplies and leave a signature on the properties of aquatic ecosystems.

CHAPTER 4

SEASONAL VARIATION OF COMMUNITY COMPOSITION AND ECOSYSTEM PROPERTIES

4.1 Introduction

This chapter extends the theoretical investigation of mixotrophy undertaken in the previous chapters, by incorporating idealized seasonal variation in critical parameters. These previous investigations considered the interactions of mixotrophs with microorganisms pursing autotrophic and heterotrophic nutritional strategies. These included algae (pure autotrophs), bacteria (pure heterotrophs consuming dissolved organic carbon, DOC), and zooflagellates (pure heterotrophs consuming bacterial prey).

Model equations previously introduced were modified here to describe seasonal changes in temperature and available light and consequent variation in population growth. The previous models dealt with constant environments and were analyzed at steady state. However, to model organisms in nature, we must take in to account the changing environment. Models that explicitly deal with mixotrophy are not common, and models that deal with it in a seasonal environment seem to be completely lacking even though we know that mixotrophs are important bacterial consumers that vary seasonally (Domaizon et al. 2003). This lack of attention to seasonal dynamics of mixotrophy may not merely reflect lack of effort. Even relatively simple models with seasonal forcing can result in limit cycles or chaos depending on the strength of the forcing (Huppert 2005). Therefore models that provide transparent results for constant environments can have results that are chaotic and difficult to interpret after adding seasonal forcing (Gao et al. 2009). For example, Cropp and Norbury (2009) working with a moderately complex plankton ecosystem model found that adding a seasonal forcing to the phytoplankton led to a mildly chaotic system.

The model of mixotrophy we have developed is not a simple model, since it describes the nutritional strategy of blending autotrophy and heterotrophy and places mixotrophs in a food web context where they interact with other microorganisms pursuing purely autotrophic and heterotrophic nutrition. The model has the additional technical difficulty of stiff equations, once realistically parameterized. However, we pursue the goal of understanding mixotrophs in a seasonal context in part because they make up many of the species that form harmful algal blooms (Burkholder 2008) and being able to model them in realistic environments may give us insights into amelioration of this problem. On a more basic level, while there is considerable study of the succession of photosynthetic organisms in planktonic ecosystems (e.g. Hutchinson 1944, Reynolds 1980, Sommer et al. 1986), there has not been much theoretical attention on how mixotrophs impact planktonic succession.

In Chapter 3, our model of mixotrophs and other microbial populations was used to generate predictions of microbial food web composition and ecosystem properties, such as the seston C:P ratio, primary productivity, production of dissolved organic carbon (DOC) and recycling of P during microbial consumption of prey. The results of steady state analyses were used to evaluate the light:P hypothesis of pelagic ecosystem structure advanced by Sterner et al. (1997). This proposal portrayed how the relative supply of light and the critical mineral nutrient P might influence these properties of microbial communities, which in turn would influence higher trophic structure through feedbacks with zooplankton nutrition and dynamics.

The light:P hypothesis was originally based on observations of spatial differences between lakes in conditions affecting light and P supply (Sterner et al. 1997). The hypothesis was extended to also reflect seasonal differences by Chrzanowski and Grover (2001b), who contrasted patterns of microbial nutrient limitation during warm and cool seasons in Texas lakes, verifying that P limitation was more intense during the well-lit, warm summer season. By extending our model of mixotrophs to reflect seasonal variation, we can approach issues of the seasonality of ecosystem properties. When photosynthetic organisms have excess light in relation to P supply, they produce excess photosynthate that is released into the environment as

DOC (Bratbak and Thingstad 1985). As seasons change from dark winter to bright summer, we would expect to see that photosynthetic organisms switch from being light-limited in the dark winter to being P-limited in the summer. This should also allow for an increase in DOC which then can be taken up by bacteria which should then also become more-P limited in the summer, exactly the pattern found by Chrzanowski and Grover (2001b).

Other ecosystem properties are hypothesized to change with the relative supplies of light and P in aquatic ecosystems (Sterner et al. 1997). For example, higher incident light should increase the seston C:P ratio as photosynthesis leads to increased C production. Seston C:P ratios would also be expected to decrease with increasingly eutrophic conditions, as more P became available for microbial uptake. Seston with high C:P ratios indicates lower quality food for higher organisms such as zooplankton (Sterner 1993). The recycling of P by consumers should also increase as the supply of P relative to light increases. Food richer in P, with lower C:P ratio, is more likely to provide P in excess of consumer assimilation (Elser and Urabe 1999). The goal of this chapter is to assess theoretical support for these expectations in a seasonal context, using the model of mixotrophs embedded in a microbial food web developed in earlier chapters.

4.2 Model Formulation

The model used for this study is the same one as presented in Chapter 3, except that modifications have been made to rate processes and light supply to allow for seasonal variation. Only the details of necessary modifications are presented in this chapter; full descriptions of the original model are presented in Chapters 2 and 3.

To provide a realistic context, light and temperature data were collected intermittently over a year at Lake Granbury, Texas. In order to simulate the observed season variation, these light and temperature data were used to create sinusoidal functions that were similar to the light and temperature measurements. These functions were then used to assign daily values that could be used in numerical simulations of the model. These functions were created with minimized differences with the interpolated values from measurements in Texas (Grover et al.

2010). The values in these functions could be adjusted to reflect light and temperature values for a variety of locations.

$$I_{in} = 270\sin(\frac{2\pi}{365}(day - 80)) + 650$$

$$temperature = 10\sin(\frac{2\pi}{365}day + 4.275) + 20$$

The model uses an equation modified from Huisman and Weissing (1994), in which available light determines rates of photosynthesis for the phototrophic algae and the mixotroph. It also uses Michaelis-Menten equations for P uptake, Droop equations for P-limited growth, Monod equations for DOC-limited growth, and Holling type I functional response equations for predation rates. The maximal photosynthesis rates, maximal rates of P uptake, maximal growth rates, and attack rates on prey all depend on temperature in the seasonal model. The temperature adjustment assumed that growth and other rates of heterotrophic bacteria and phototrophic algae are most rapid in warm conditions (e.g. Chrzanowski and Grover, 2001b). In contrast, many of the flagellated protists that consume bacteria, both heterotrophic and mixotrophic, display peak growth rates at moderate temperatures and reduced growth at high temperatures (Butterwick et al., 2005, Baker et al., 2007).

Rate adjustments for the bacteria and the algae use an Arrhenius equation where the rate at a given temperature T depends on the rate at a reference temperature T_{ref} of 20° C,

$$\text{rate}(T) = \text{rate}(T_{ref})\exp(k(T - T_{ref})),$$

where coefficient k = 0.1 $\log_e$ 2, equivalent to a Q_{10} of two, close to the values of 1.88 found by Eppley (1972) for phytoplankton and 1.86 found for bacterioplankton by Morris and Lewis (1992). The rate at T_{ref} was taken as the rate previously parameterized in Chapters 2 and 3. The temperature adjustment for the mixotrophs and zooflagellates (Figure 4.1) is based on a modified form of an equation applied to the mixotrophic flagellate *Prymnesium parvum* (Baker et al., 2007) of the form:

$$\text{adjustment}(T) = \mathrm{k}_0 + \mathrm{k}_1 \exp(\theta \frac{T - T_{ref}}{T}) + \mathrm{k}_2 \exp(2\theta \frac{T - T_{ref}}{T}) .$$

The parameters k_0, k_1 and k_2 were chosen to give the function a peak value of 1 at 28° C and a value of 0 at 35° C; T_{ref} was again 20° C. The adjustment thus calculated was then multiplied by the value of the rate parameter previously used in Chapters 2 and 3. The rate adjustments were calculated based on temperature and then sent to the solver for each day (Figure 4.2).

4.3 Numerical Solutions

The model equations were integrated numerically using MatLab's ode23s solver for stiff ordinary differential equations (Shampine and Reichelt 1997). To increase computational efficiency, the simulation is run one day at a time, and light and temperature are sent to the solver for each day of the year (rather than attempting to resolve and simulate within-day variation of light and temperature). The same yearly data was used repeatedly for five years of simulated time. By year three, most (>80%) of the runs had settled into their seasonal cycles, and by year four almost all had. All of the output data were saved, but the results presented are just for year five.

4.4 Results

4.4.1 Temporal dynamics

All of the simulations were run with the combinations of low and high P supply (P_{in} = 0.0003 and 0.0008 mol m^{-3}) used in Chapter 3, with the same mortality scenarios used in Chapter 3: equal and low rates (all 0.1), different and higher mortality rates (m_A = 0.3, m_Z = 0.1, m_M = 0.3, m_B = 0.6; mortality rates of algae, zooflagellates, mixotrophs, and bacteria respectively). These were also combined with either low or high values (0.2 and 0.9) of the parameter α describing mixotrophy – the lower value portraying primarily heterotrophic nutrition, and the higher value primarily autotrophic nutrition. Coexistence of all four organisms (algae, bacteria, zooflagellates, and mixotrophs) was not predicted in any seasonal environment examined. Therefore, different groupings of organisms predicted to persist under various environmental conditions were run to examine their dynamics and interactions.

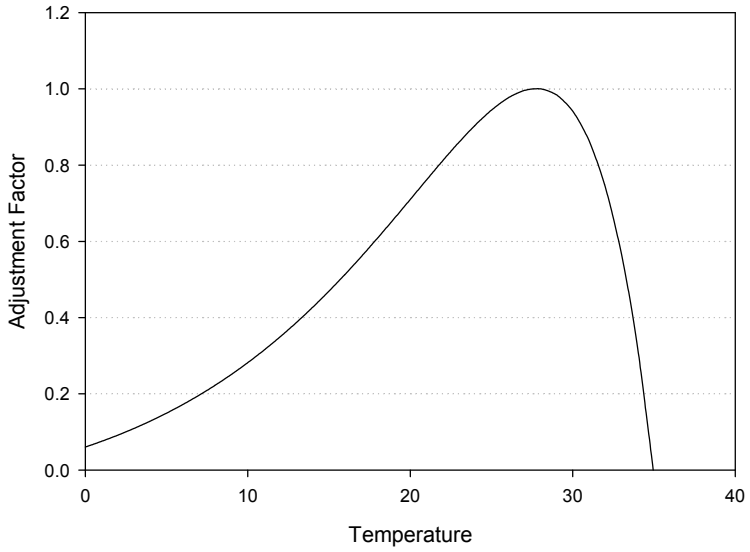

Figure 4.1 Rate adjustment as a fraction of maximum rate for mixotrophs and zooflagellates due to temperature. The rate increases until the maximum rate occurs at 28° C and decreases to 0 at 35° C.

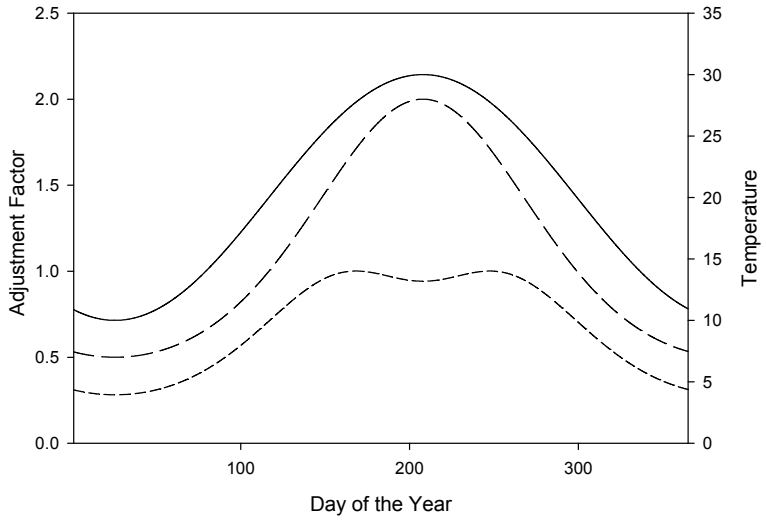

Figure 4.2 Daily rate adjustments due to temperature (solid line) in relation to rates at 20° C for bacteria and algae (long dash) and in relation to maximal rates for mixotrophs and zooflagellates (short dash).

4.4.1.1 Algae

The first groupings examined were particular organisms alone, or with only bacteria for the heterotrophic zooflagellates. The algae alone showed a strong seasonal pattern, high in density in the summer and low in the winter (Figure 4.3). Since results from low and high P supply conditions overlapped, the predicted algal population density was independent of P supply. The runs with low and equal mortality had higher predicted algal densities overall and a greater seasonal amplitude than the runs with high and differing mortalities.

4.4.1.2 Bacteria

The bacteria alone showed four different responses to the combinations of P supply and mortality scenarios (Figure 4.3). Only the combination of high P supply (P_{in} = 0.008 mol m^{-3}) and differing mortalities showed a seasonal response with amplitude comparable to that of the algae. Overall bacterial density was predicted to be higher for the low, equal mortality scenario than the high and different mortality scenario. Overall bacterial density was also predicted to be higher for higher P supply.

4.4.1.3 Zooflagellates and Bacteria

The zooflagellates could not persist without their bacterial prey. The zooflagellates and the bacteria coexisted with oscillations (Figure 4.4 A) of larger amplitudes (Figure 4.4 B) in the differing mortalities scenario than the equal mortality scenario. The seasonal cycle was more apparent in the minima than in the maxima of the relatively high-frequency, predator-prey oscillations predicted for bacteria and zooflagellates. The overlapping results for low and high P supplies showed that densities of these populations were independent of P supply. On average, population densities were predicted to be higher for the equal mortality scenario than for the differing mortality scenario, which assigned higher mortality rates to both bacteria and zooflagellates.

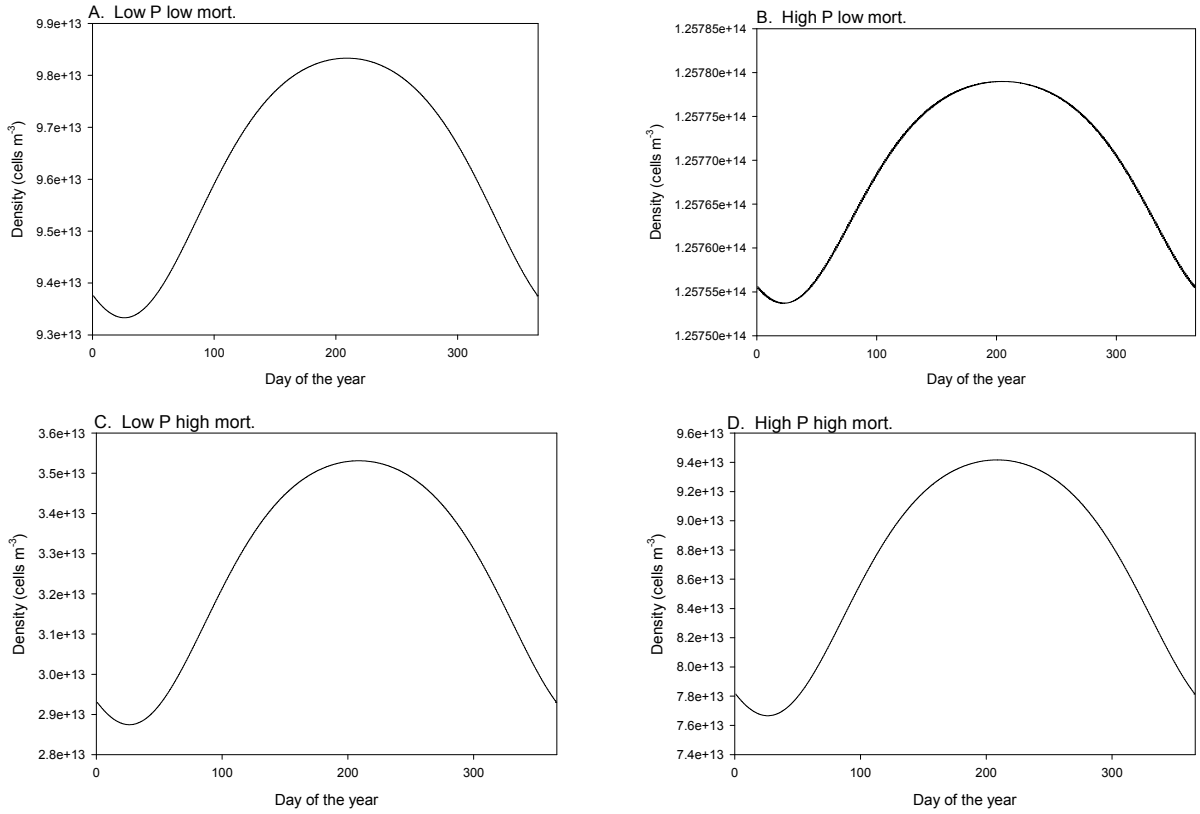

Figure 4.3 Predicted bacterial densities for the four combinations of P supply and mortality scenarios through the year. The densities first depend on mortality scenario with the two lower equal mortality simulations having the highest two densities, and then by P supply with the higher P supply having greater densities.

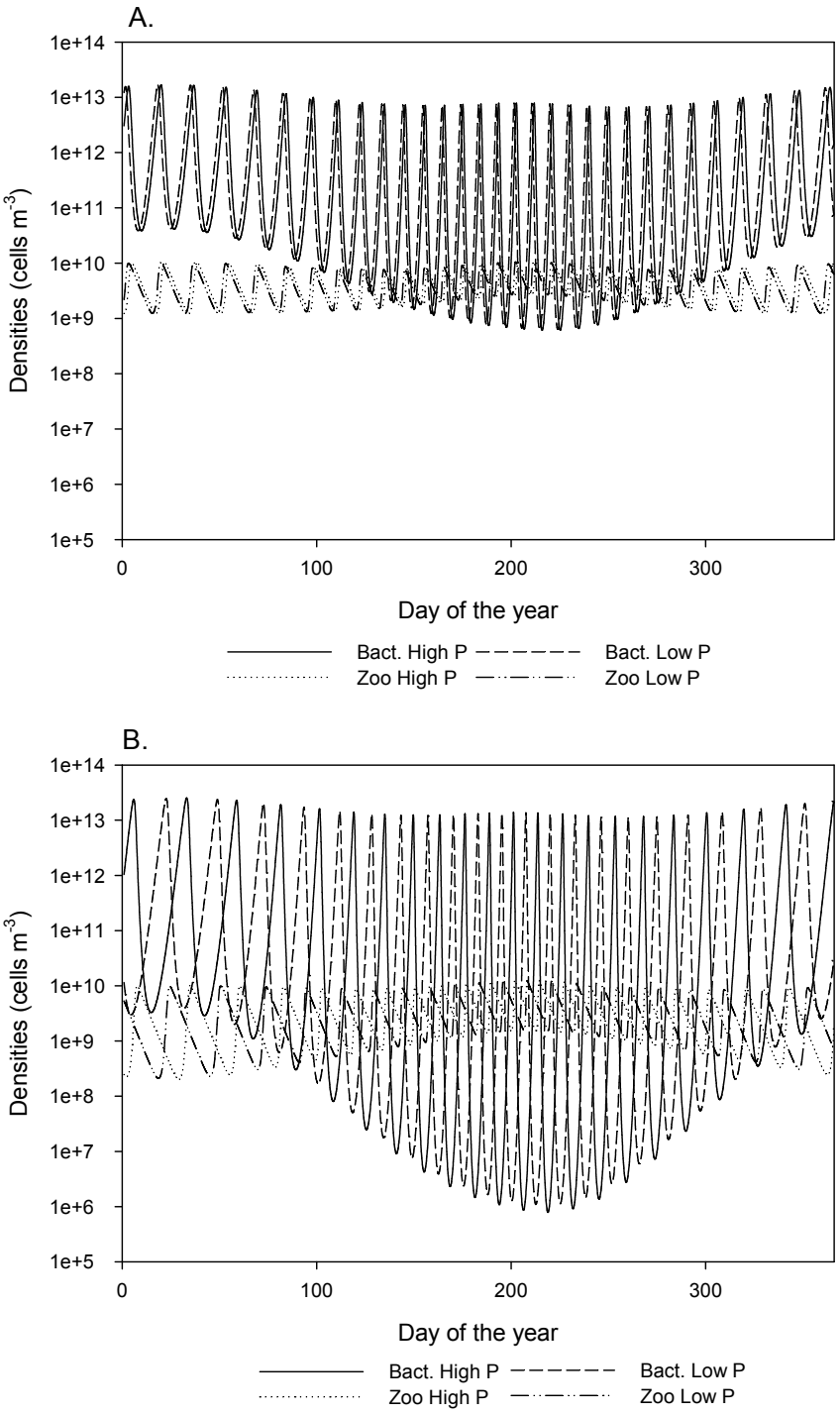

Figure 4.4 Predicted densities of bacteria and zooflagellates for the four combinations of mortality scenarios and P supply through the year. A. Equal and low mortalities B. Different and higher mortalities.

4.4.1.4 Mixotrophs

The mixotrophs were not predicted to persist when they were alone and mostly heterotrophic (α = 0.2), without bacteria upon which to prey. When the P supply was low (0.0003 mol m^{-3}) and all the mortalities were equal, the numerical calculations could not be resolved due to excessive stiffness of the differential equations. For the remaining three combinations (Figure 4.5), the differing mortality scenario predicted a major decline of mixotroph density over the winter while the equal mortality scenario showed a seasonal response that was similar in shape to the rate adjustment graph for the mixotrophs (Figure 4.2). Mixotroph densities were lower in the winter and higher in the summer with a period in the summer with decreased densities. The higher mortality rate of the differing mortality scenario reduced the overall population density of mixotrophs growing alone.

4.4.1.5 Mixotrophs and Bacteria

Since the mixotrophs did not persist when they were mostly heterotrophic (α = 0.2) and without their bacterial prey, bacteria and heterotrophic mixotrophs were simulated together. For the differing mortality scenario, the mixotrophs again showed a decline in the winter, but it was not as severe as when they were mostly heterotrophic (Figure 4.6 A). The bacterial population density was stable during the winter and then oscillating along with the mixotrophs during the summer. For the equal mortality scenario, the bacteria had an unrealistic population decline at the end of the summer. The simulation for high P supply (P_{in} = 0.0008 mol m^{-3}) could not be calculated for the equal mortalities scenario, due to excessive stiffness of the differential equations.

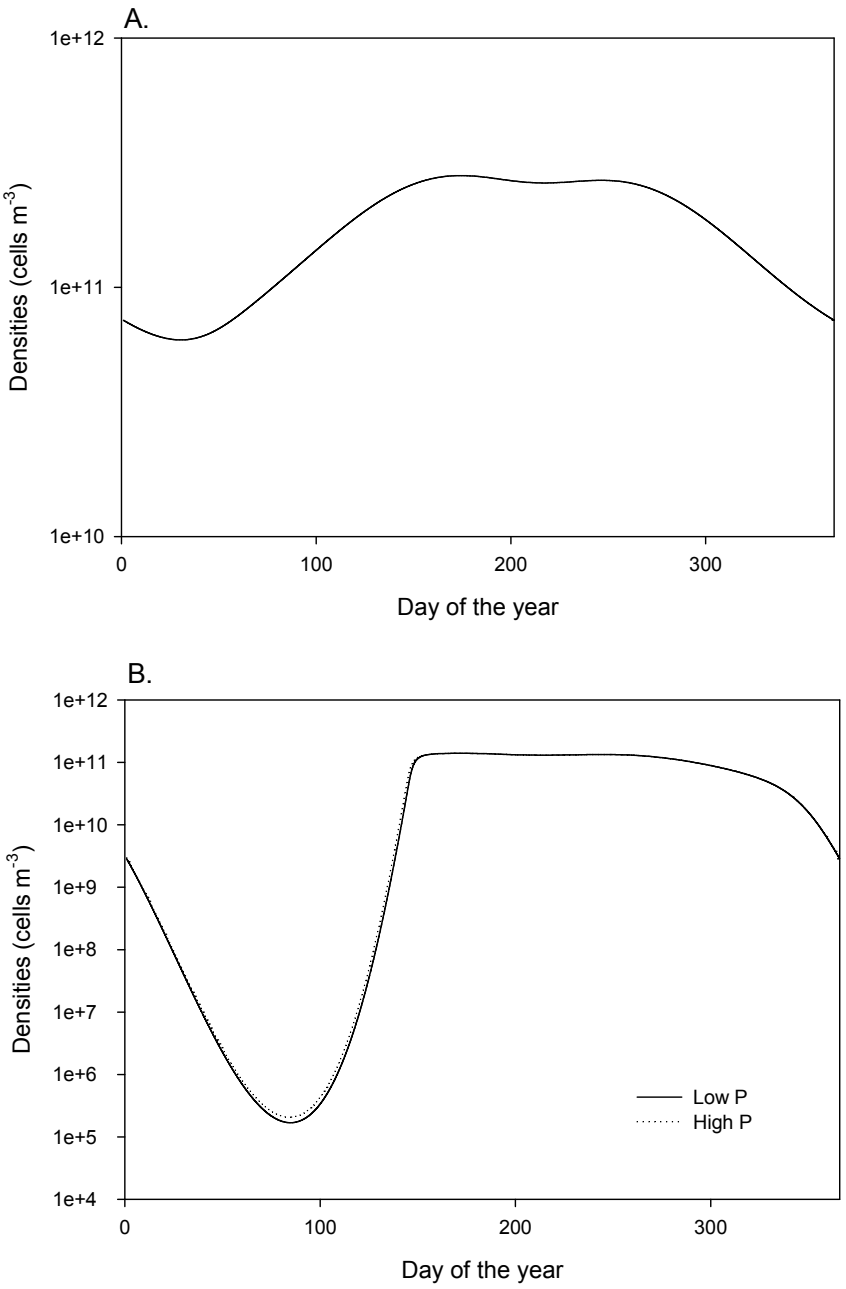

Figure 4.5 Densities of mostly autotrophic mixotrophs alone through the year. A. Low mortality. B. Higher mortality. Note that scales are different for densities and are log scales.

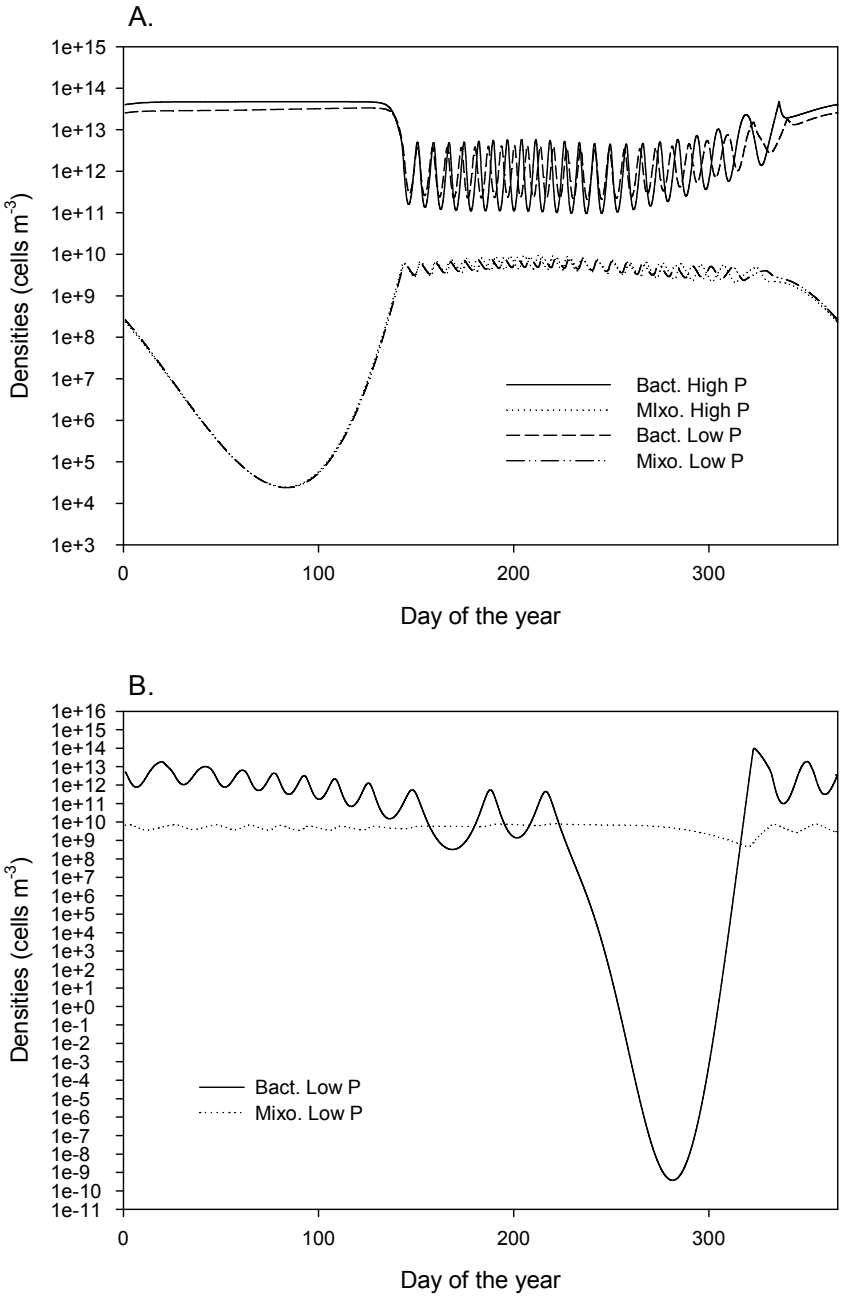

Figure 4.6 Predicted densities of bacteria and heterotrophic mixotrophs through the year for the A. differing mortalities and B. equal mortalities scenarios.

4.4.1.6 Algae, Bacteria, and Zooflagellates

Algae, bacteria, and zooflagellates were simulated without mixotrophs (Figure 4.7 and Figure 4.8), using four combinations of P supply (P_{in} = 0.0003 and 0.0008 mol m^{-3}) and mortality scenario (equal vs. different). Time-averaged population densities were similar for all four combinations. The algae were predicted to increase in density in the summer and decrease in the winter. The predicted zooflagellate densities varied less throughout the seasons, and the predicted bacterial populations decreased in the summer and increased in the winter. For the equal and low mortality scenario, the bacteria and zooflagellates showed small amplitude, high-frequency oscillations at the higher P (P_{in} = 0.0008 mol m^{-3}) supply (Figure 4.7 B). For the different and high mortalities scenario with high P supply, the bacteria and zooflagellates had more pronounced oscillations (Figure 4.8 B).

4.4.1.7 Algae, Mixotrophs, and Bacteria

Mixotrophs were simulated with algae and bacteria, with eight combinations of P supply (0.0003 vs. 0.0008 mol m^{-3}), mortality scenario (equal vs. different), and mixotroph type (α = 0.2 and α = 0.9). Results were different depending on the mortality scenario. There were also two simulations, one from each mortality scenario, which could not be included in the results due to numerical difficulties.

The three combinations of equal mortality scenario simulations had similar patterns to those of the algae, zooflagellates, and bacteria discussed in the previous section (Figure 4.9). The bacterial densities showed a summer decrease and winter increase. In contrast, the densities of the algae showed a summer increase and a winter decrease. The predicted mixotroph densities varied little throughout the year. Higher densities of mixotrophs were found when the mixotrophs were mostly autotrophic (α = 0.9) than when they were mostly heterotrophic (α = 0.2). When the P supply was low (P_{in} = 0.0003 mol m^{-3}) and the mixotrophs were mostly autotrophic (α = 0.9), oscillations on top of the seasonal variation ensued (Figure 4.9 B). The

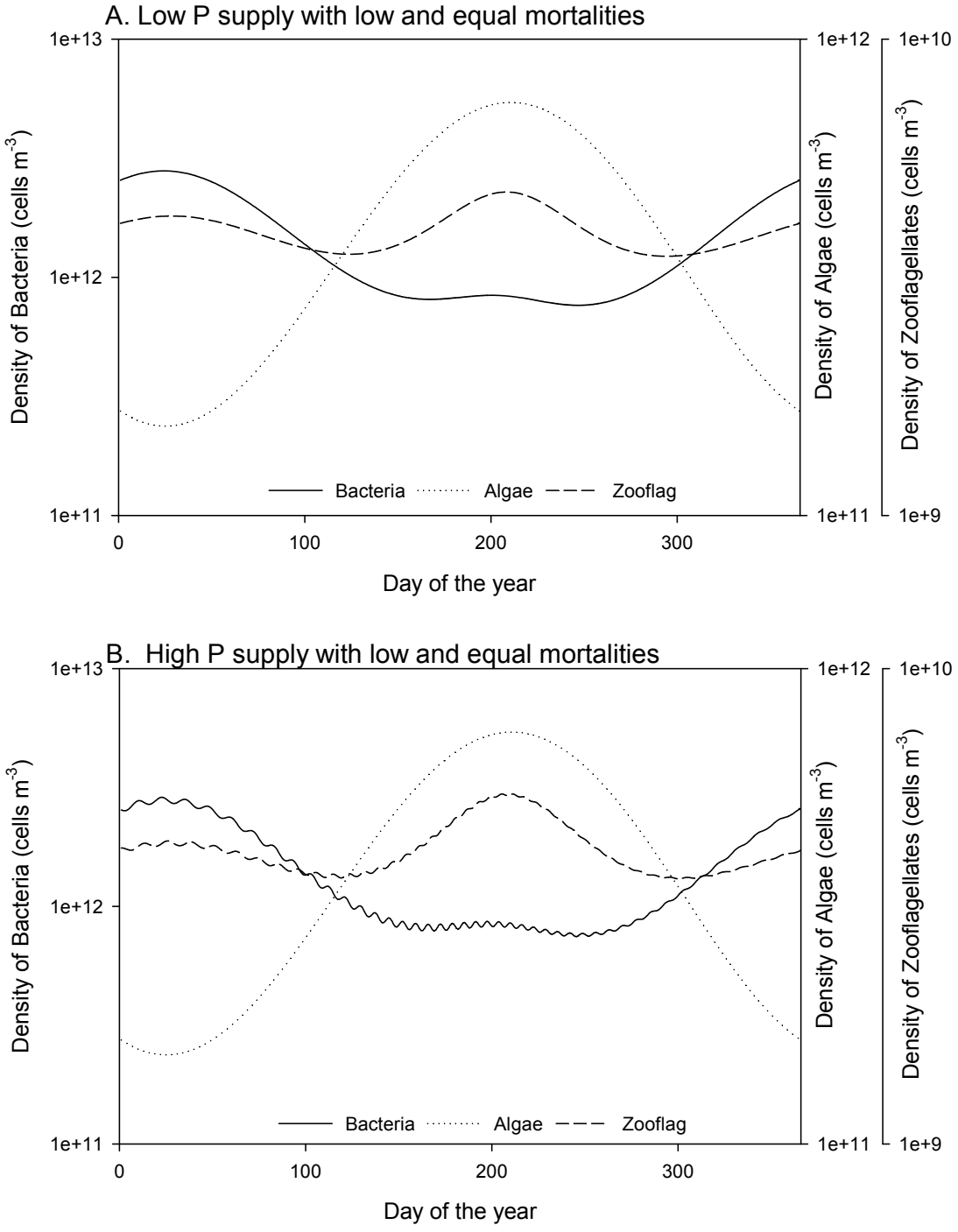

Figure 4.7 Predicted densities of bacteria, algae, and zooflagellates through the year for the equal mortalities scenario. A. Low P. B. High P.

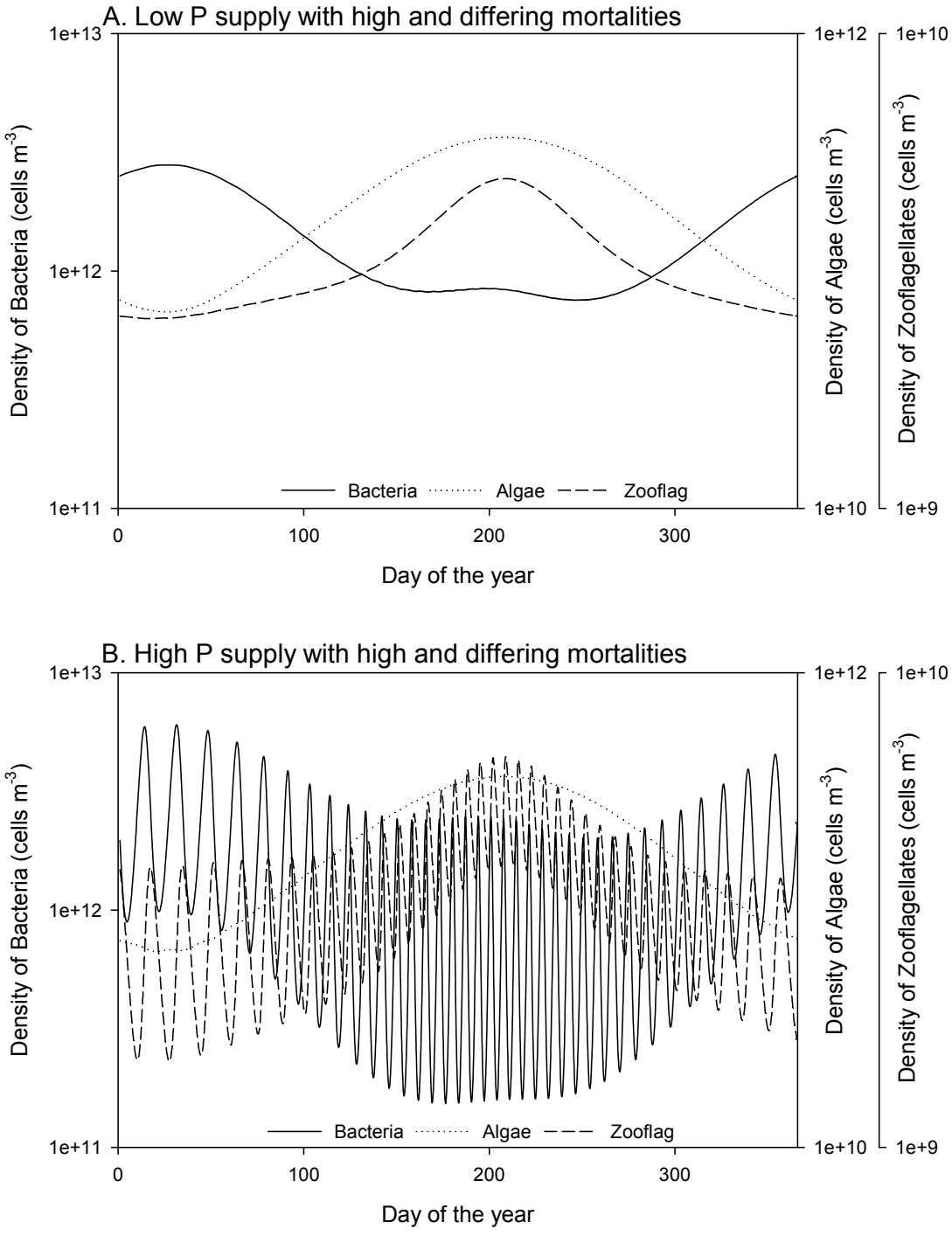

Figure 4.8 Predicted densities of bacteria, algae, and zooflagellates for the differing and high mortalities scenarios through the year. A. Low P. B. High P

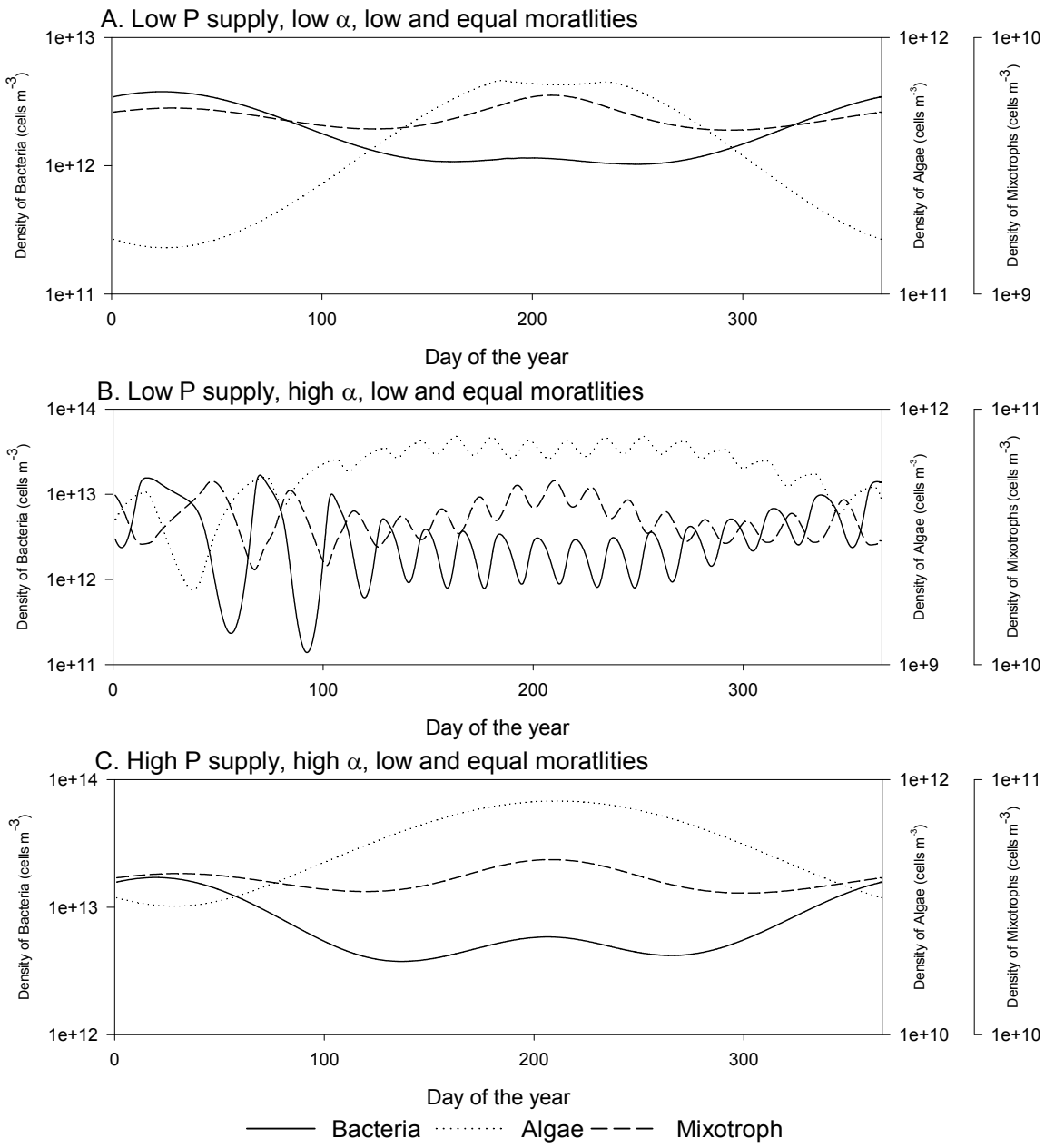

Figure 4.9 Predicted densities of algae, mixotrophs, and bacteria with equal mortalities scenario through the year. A. Low P and low α. B. Low P and high α. C. High P and high α. Note that one combination is missing due to numerical difficulties.

combination of high P supply (P_{in} = 0.0008 mol m^{-3}) and low alpha (α = 0.2) could not be calculated due to stiffness issues.

The simulations using the differing mortality scenario had very different patterns than those using equal mortalities (Figure 4.10). The bacterial densities were again predicted to decrease in the summer and increase in the winter, but during the summer they had high-frequency oscillations. For high P supply (P_{in} = 0.0008 mol m^{-3}) and primarily autotrophic mixotrophs (α = 0.9), a clearing of the bacteria was predicted at the beginning of the summer, with the onset of increased mixotroph and algal densities from winter minima (Figure 4.10 B). The mixotrophs have a winter minimum and then increased in density for the summer where they underwent high-frequency oscillations with the bacteria until the mixotrophs declined in density during the winter. The algae increased in density from their winter minimum into the summer where they showed oscillations in density. For high P supply (P_{in} = 0.0008 mol m^{-3}) and primarily autotrophic mixotrophs (α = 0.9), oscillations of the bacteria and mixotrophs occurred in the summer (Figure 4.10 B). For low P supply (P_{in} = 0.0003 mol m^{-3}) and primarily autotrophic mixotrophs (α = 0.2), algae were predicted to go extinct (Figure 4.10 C). This left only the mixotrophs and bacteria, and they followed the same pattern previously described (Figure 4.6 A). The bacteria show a summer decline with high-frequency oscillations and an increase in the winter without oscillations. The mixotrophs showed a winter minimum and increased in density for the summer where they also exhibited high-frequency oscillations. For low P supply (P_{in} = 0.0003 mol m^{-3}) and primarily autotrophic mixotrophs (α = 0.9), bacteria were predicted to go extinct during a precipitous summer decline and only the algae were predicted to persist (results not shown).

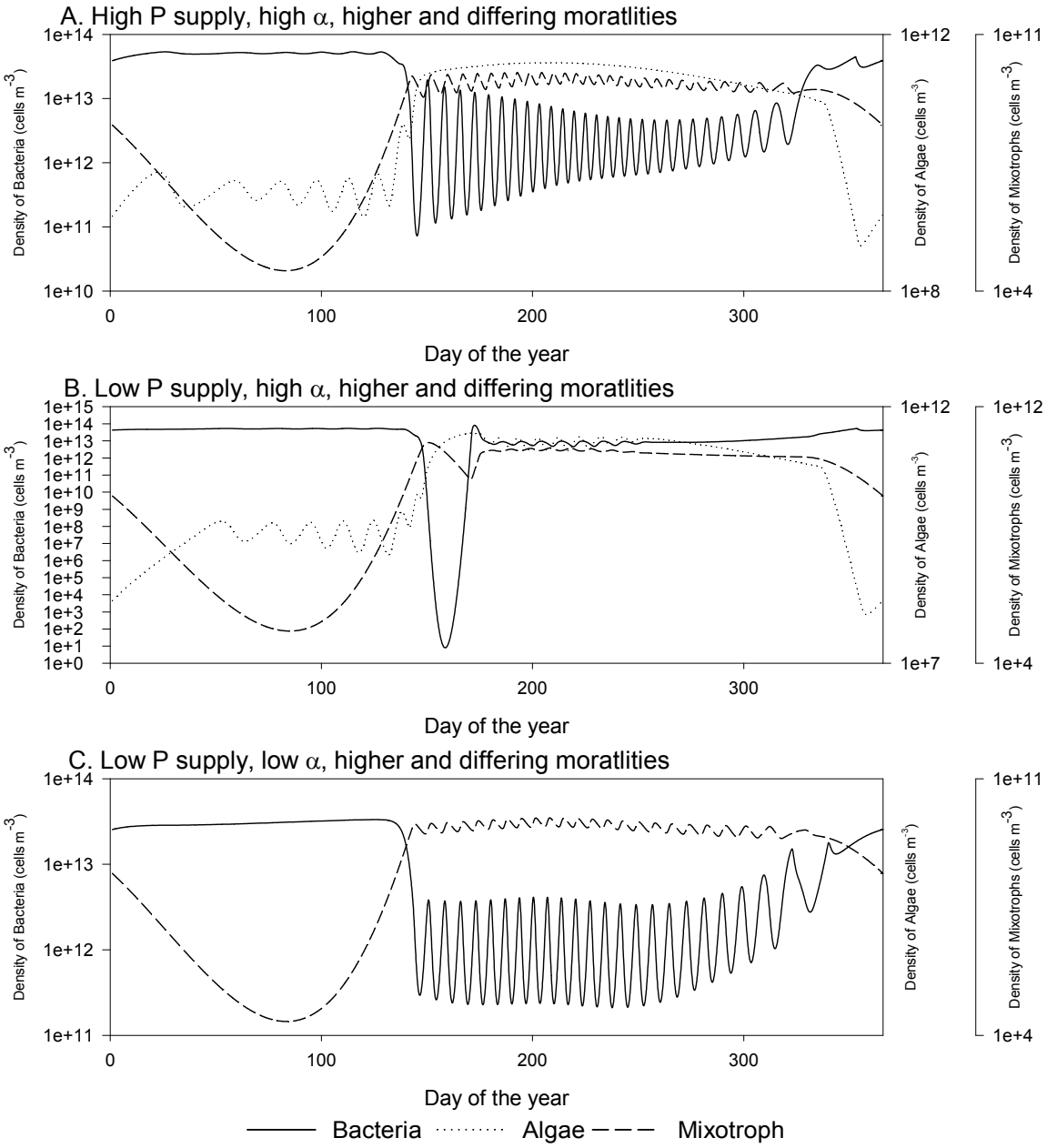

Figure 4.10 Predicted densities for algae, mixotrophs, and bacteria for the differing mortalities scenario through the year. A. High P and low α. B. High P and high α. C. Low P and low α. Note that one combination is missing due to numerical difficulties.

4.4.2 Comparisons of winter and summer

The model predicted a variety of population dynamics depending on the parameters considered and the identity of persisting organisms. These patterns included relatively simple seasonal cycles, high-frequency predator-prey oscillations, and more complex patterns with distinct seasonal minima. To facilitate presenting the model's associated predictions for properties of microbial ecosystems in relation to relative supplies of light and phosphorus, the year was divided into two seasons designated winter and summer. The summer was considered to be days 120 to 270 (approximately May-September), and the rest of the year was considered as winter. The values of predicted quantities during the two seasons were then summarized by their arithmetic mean and standard deviation. All four organisms were not predicted to persist together, so the comparisons were made using simulations with bacteria, algae, and either zooflagellates (designated BAZ) or mixotrophs (designated BAM). These two types of simulations were done for the low P supply and high P supply environments (P_{in} = 0.0003 or 0.0008 mol m^{-3}), equal mortality and differing mortality scenarios, and when the mixotrophs were involved, for low and high α values representing primarily heterotrophic (α = 0.2) and primarily autotrophic (α = 0.9) mixotrophs, respectively. The ecosystem properties of C:P ratios, P flux recycled during bacterivory, and DOC as a percent of primary production were calculated from daily output as described in Chapter 3.

4.4.2.1 Population Densities for BAZ

For all four combinations of P supply and mortality scenario simulated for the BAZ grouping (Figure 4.11), the same trends were found. The algae and zooflagellates increased in density from winter to summer while the bacteria showed a decrease. In all cases the bacteria were always P-limited, and the algae and zooflagellates are always C-limited.

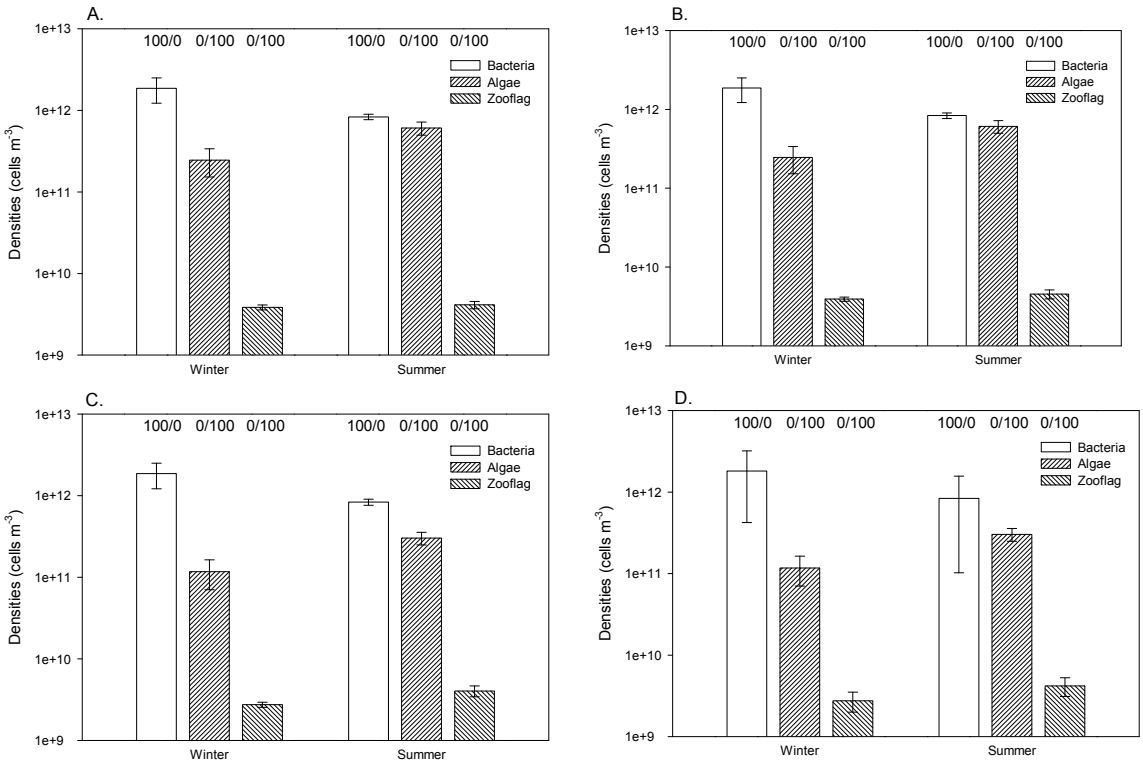

Figure 4.11 Predicted densities of BAZ for winter and summer. The numbers on the figures indicate the percent of the season the organisms were P-limited/C-limited. Standard deviations represent the range of values. A. P supply low and mortalities equal. B. P supply high and mortalities equal. C. P supply low mortalities different. D. P supply high and mortalities different.

4.4.2.2 Population Densities for BAM

For the BAM grouping, not all of the eight combinations of environment and mixotroph type were mathematically tractable, due to excessive stiffness of the differential equations. In all cases that were successfully simulated, bacteria decreased in density from winter to summer, while algae and mixotrophs increased in density (Figure 4.12).

For low P supply (P_{in} = 0.0003 mol m^{-3}) environments, results were obtained successfully only for the equal mortality scenario (Figure 4.12 A,B). When the mixotrophs were mostly heterotrophic (α = 0.2), results were similar to the BAZ environments (Figure 4.11). Algae and zooflagellates increased in density from winter to summer while bacteria decreased. In all cases, bacteria were always P-limited and algae and z 0flagellates were always C-limited, except that algae were P-limited for some time in the summer (Figure 4.12 B). When the mixotrophs were mostly autotrophic (α = 0.9), algae were P-limited during part of the winter, but were more frequently P-limited in the summer (Figure 4.12 A).

Three of the simulations with high P supply (P_{in} = 0.0008 mol m^{-3}) were numerically tractable. When mortalities were equal and the mixotrophs were mostly autotrophic (α = 0.9), the results were very similar to the BAZ cases. Algae and mixotrophs increased in density from winter to summer while bacteria decreased. In all cases, bacteria were always P-limited and algae and mixotrophs were always C-limited. For the two cases where mortalities were different, bacteria were more often C-limited in winter and P-limited in summer (Figure 4.12 D, E). Whether the mixotrophs were mostly autotrophic (α = 0.9) or heterotrophic (α = 0.2) affected population densities, but not patterns of growth limitation. Mixotrophs were more often P-limited in winter and more often C-limited in summer, and had about ten times lower average densities when they were mostly heterotrophic (α = 0.2) compared to when they were mostly autotrophic (α = 0.9). When the mixotrophs were mostly autotrophic, algae were more often P-limited in summer than when the mixotrophs were mostly heterotrophic.

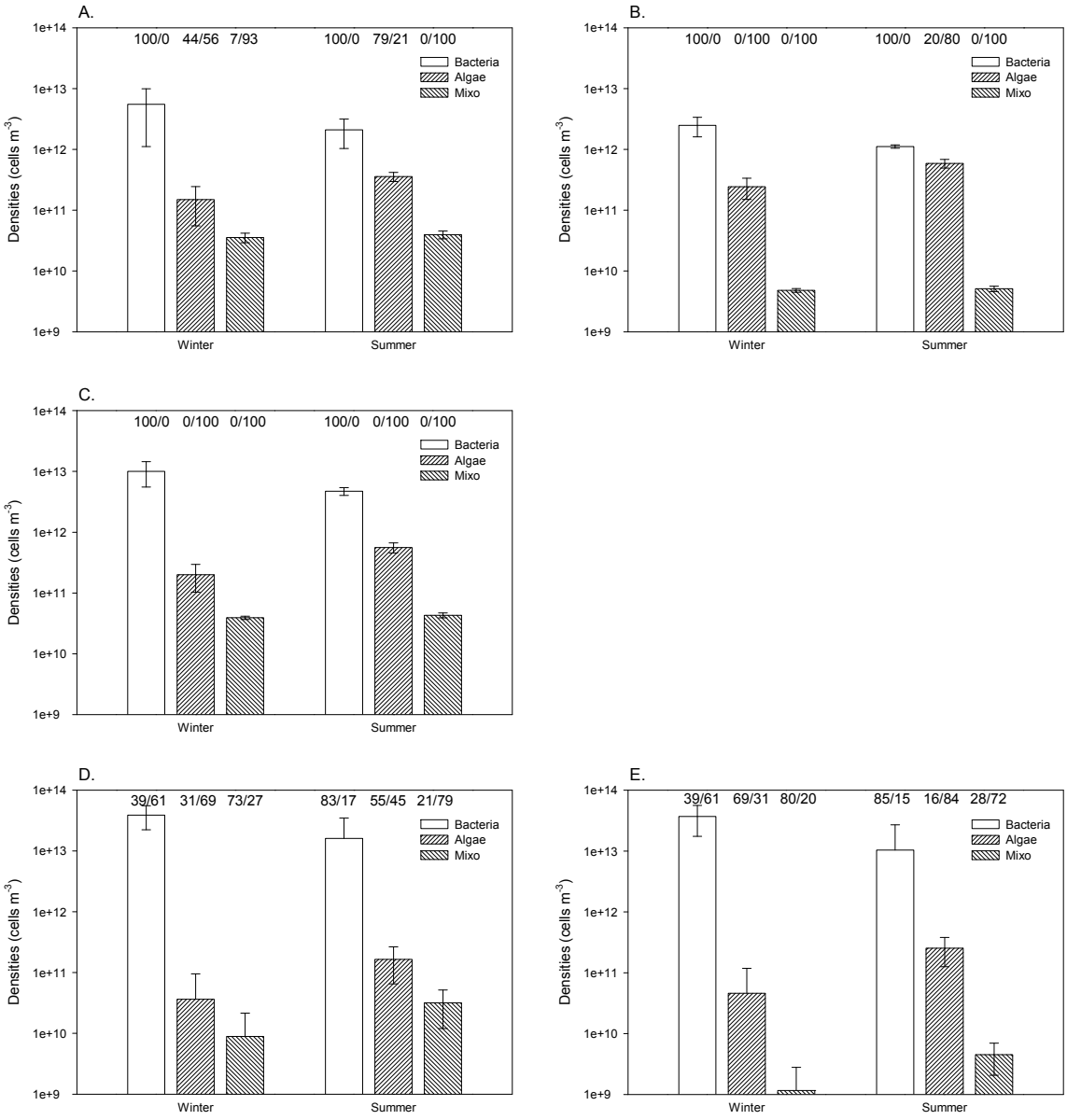

Figure 4.12 Predicted densities for BAM for winter and summer. The numbers on the figures indicate the percent of the season the organism was P-limited/C-limited. Standard deviations represent the range of values. A. P supply low, α high, mortalities equal. B. P supply low,α low, mortalities equal. C. P supply high, α high, mortalities equal. D. P supply high, α high, mortalities different. E. P supply high, α low, mortalities different.

4.4.2.3 Recycled P flux

For the BAZ grouping, recycled P flux (excess P released into the environment from P in bacteria prey that were ingested but not assimilated by consumers) always decreased from winter to summer (Figure 4.13 A). For the BAM groupings, when mortalities were equal the recycled P flux again decreased from winter to summer (Figure 4.13 B). When mortalities were different, recycled P flux increased slightly from winter to summer, but was also highly variable within seasons (Figure 4.13 B).

4.4.2.4 Seston C:P ratios

The seston C:P ratios for all of the conditions examined were predicted to increase from winter to summer (Figure 4.14). Generally, simulations with the equal mortality scenario predicted higher seston C:P ratios than those with different mortalities, which also had higher mortality rates for all organisms. Lower P supply (P_{in} =0.0003 mol m^{-3}) also led to higher predicted seston C:P ratios than did high P supply (P_{in} = 0.0008 mol m^{-3}).

4.5 Discussion

This study has extended a previous theoretical model of mixotrophs embedded in a simple microbial food web to incorporate seasonality. As before, the model includes four different nutritional types: autotrophic algae, heterotrophic zooflagellates and bacteria, and mixotrophs that use both nutritional forms simultaneously. The previous model was set up with steady supply rates and then run to steady state. The current model is, as far as we know, the only seasonal model that incorporates mixotrophy. In this chapter, the modeled physiological rates vary in response to seasonal changes in light and temperature. The densities of organisms and their growth limitations in response to this seasonal forcing were analyzed, along with the ecosystem properties of P flux and the C:P ratios of the organisms. These ecosystem properties were compared to the predictions of the light:P hypothesis of Sterner et al. (1997). The DOC as a percentage of the primary production of the ecosystem was also recorded, but most of the time the producers were C-limited, so no DOC was released and the values were zero.

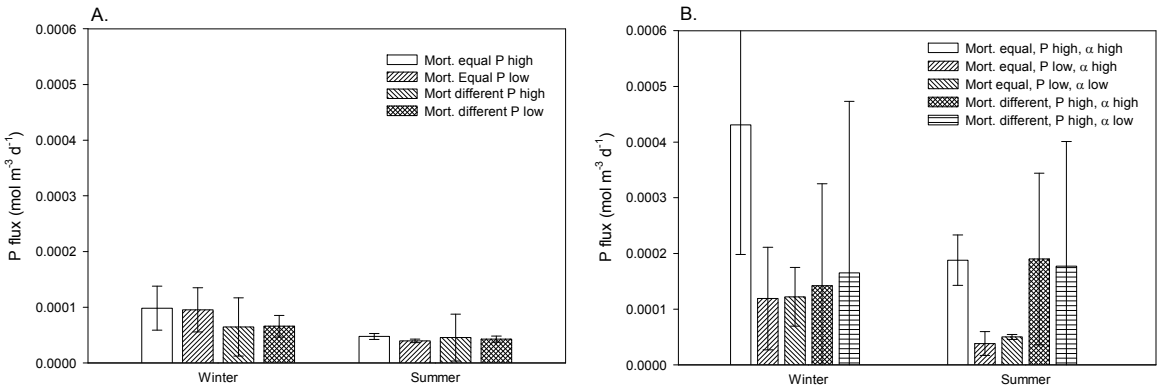

Figure 4.13 Winter and Summer comparison of P flux for A. BAZ and B. BAM. Standard deviations represent the range of values.

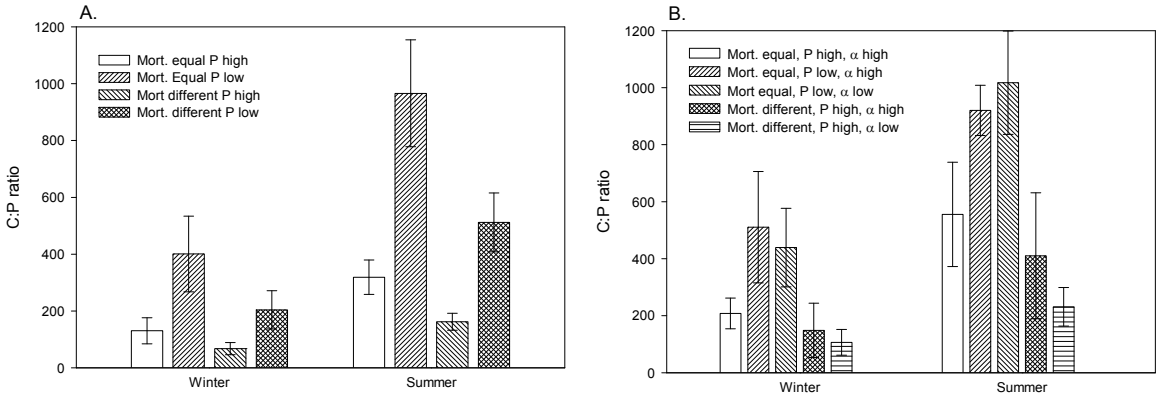

Figure 4.14 Winter and Summer comparison of C:P ratios for A. BAZ and B. BAM. Standard deviations represent the range of values.

Population dynamics and ecosystem properties were predicted for two complex community configurations. One was populated with bacteria, algae, and zooflagellates (BAZ); and the other was populated with bacteria, algae, and mixotrophs (BAM). Predictions were also made for simpler, subset communities of one or two populations. When algae alone are present, they exhibit a seasonal response by increasing in density in the summer and decreasing in density in the winter. This density response is independent of P supply, but does show decreased average and amplitude when mortality is higher. When bacteria alone are present, densities respond to both P supply and mortality, with higher P supply giving higher densities, but stronger seasonal variation when mortality is higher.

When the bacteria and zooflagellates are both present, there are high-frequency predator-prey cycles that are imposed upon the seasonal response. High frequency predator-prey cycles similar to this were found in natural systems (Fenchel 1982). Differing and higher mortalities lead to larger amplitudes than the lower, equal mortality scenario. When three populations are brought together (BAZ), the high-frequency predator-prey cycles are greatly reduced in amplitude or eliminated, regardless of P supply and mortality scenario. The bacteria decrease in density from winter to summer while the algae and zooflagellates increase in density from winter to summer. This occurs while both the algae and zooflagellates are C-limited and the bacteria are P-limited. The light:P hypothesis proposes that the organisms should shift from being more C-limited in winter to more P-limited in summer, but this is not predicted here for this community configuration (BAZ).

In the other complex configuration (BAM), two types of mixotrophs were examined. One was mostly autotrophic, and one was mostly heterotrophic. The mostly autotrophic mixotrophs are able to survive by themselves, without bacterial prey. They exhibit dramatically different population densities depending on the mortality scenario with the differing and higher mortality scenarios showing a large decrease in density through the winter. The mostly heterotrophic mixotrophs must have bacterial prey to survive. When the mixotrophs and bacteria are simulated together, population dynamics depend on the mortality scenario. For the equal mortality

scenarios, the one computationally tractable result shows a decline in bacterial densities that is unrealistic. The differing mortality scenarios give similar responses for each P supply, with a dramatic decrease in density of the mixotrophs in the winter, and an increase in the summer while the bacteria decrease in density from winter to summer. The summer densities show high-frequency predator-prey oscillations for the mixotrophs and bacteria.

The light:P hypothesis predicts that organisms shift from being C-limited in the winter to P-limited in the summer, but the model did not predict this for the BAZ configuration. For the BAM configuration, when the P supply is high, and the mortalities are equal with mixotrophs that are mostly autotrophic, the bacteria are always P-limited, and the algae and mixotrophs are always C-limited. For specific organisms under some circumstances, there are aspects of the light:P hypothesis that agree with the model predictions presented here. The algae follow the prediction of more frequent C-limitation in winter and more frequent P-limitation in summer when the P supply is low and the mortalities are low and equal with a mostly autotrophic mixotroph. For the same environment with a mostly heterotrophic mixotroph, the algae increase the percent of time they are P-limited in the summer compared to winter (from 0 to 20%), but are still frequently C-limited (>50% of the season). When the mortalities are different, bacteria follow the predictions that organisms will be more often C-limited in the winter and more often P-limited in the summer, and the algae sometimes, but the mixotrophs do not. Overall, while some aspects of the light:P hypothesis apply to the predictions of the model explored here, the hypothesis and the model do not always agree.

As organisms shift from being C-limited in the winter to P-limited in the summer, the amount of P released from prey that is not assimilated by consumers, recycled P flux, should decrease from winter to summer, and this is true for the BAZ configuration. The BAM configuration also shows this trend for the equal mortality scenario, but the seasonal trend for the differing mortality scenario is unclear due to large variation within seasons. Additionally, the recycled P flux on average is higher when mixotrophs are present (BAM) than when zooflagellates are present (BAZ). The predictions of the light:P hypothesis and the model agree

well for recycled P flux. The model generates the additional prediction that the presence of mixotrophs, rather than heterotrophic bacterivoirs, strongly impacts recycled P flux.

The model makes very robust predictions about the seston C:P ratio, interpreted as the bulk stoichiometry of all organisms in the community. As light increases in the summer, the sestion C:P ratio increases for every case examined in this study. This agrees with a central proposal of the light:P hypothesis (Sterner et al. 1997). As elaborated in this hypothesis, variations in seston C:P strongly couple the algal and microbial community to the nutrition and population dynamics of zooplankton. The seasonal increase of seston C:P predicted here often far exceeds 200-300, levels which reduce the growth rate (Urabe and Watanabe, 1992) and abundance (DeMott and Gulati, 1999) of herbivores in the genus *Daphnia*. This prediction is important because *Daphnia* species often dominate among herbivorous zooplankton in temperate zone lakes (Sterner 1989).

One glaring problem with this study is the number of simulations that were not mathematically tractable. The model examined here displays stiffness even when running in a constant environment, as in previous chapters, and that problem is stronger when seasonal variations are imposed. For the majority of simulations attempted, results were successfully obtained, and showed that mortality rates often had a profound effect on the results. In fact, the two mortality scenarios explored in this model were chosen because they were found in exploratory work to be in parameter ranges where stiffness was somewhat reduced, so that results could be successfully obtained. There was no parameter combination identified here that would lead to the coexistence of all four types of organisms in seasonal environments. Since all of these nutritional types coexist in natural systems this is a disappointing result. In real systems, mixotrophs and zooflagellates are unlikely to be completely eliminated even when they are uncompetitive. Non-seasonal temporal variation, spatial variation, and immigration from other habitats, among other processes, likely permit diverse microorganisms to persist in natural ecosystems despite competitive disadvantages. Limiting microbial communities to only four types of organisms, as was done here, is of course unrealistic, but necessary to keep the results

comprehensible. Even with these limitations, a comparison of ecosystems with and without mixotrophs can be made and ecosystem properties can also be tracked and compared.

The predictions of this model for the ecosystem properties did not always follow those of the light:P hypothesis. This was especially evident in the growth limitations of the organisms, where exceptions to the expected prevalence of P-limitation in summer arose in some cases. In contrast, recycled P flux during bacterivory did follow predictions by decreasing in the summer when C:P ratios of the organism should climb according to the light:P hypothesis. The C:P ratios were indeed the most robust of the predictions of the light:P hypothesis. The predictions of the model explored here thus followed the predictions of the light:P hypothesis at an ecosystem level, but not at an organismal level. By comparing the results of the BAZ and BAM environments, we have additionally predicted that the use of multiple resources by the mixotrophs leads to changes in the growth limitations of other organisms, and to an increase in the recycled P flux in the microbial food web. Therefore, the inclusion of mixotrophs in other theoretical models for planktonic ecosystems may have a profound impact on their predictions, just as was seen here.

CHAPTER 5

A MODEL FOR *P. PARVUM* WITH MIXOTROPHY

5.1 Introduction

Aquatic microorganisms have diverse nutritional strategies. Phototrophs utilize the sun's energy to create food by photosynthesis. Heterotrophs consume dissolved organic matter or other organisms. One other strategy, mixotrophy, is to utilize both phototrophy and heterotrophy. Mixotrophy as a nutritional form and mixotrophs in general are gaining in notoriety since most, if not all, harmful algal species (HAS) are mixotrophs (Burkholder 2008). Since predicting blooms of HAS, called harmful algal blooms (HAB), can be beneficial to managers of aquatic resources, mathematical models for predicting HAB that do not include mixotrophy may lead to inaccuracy in predictions. One of these HAS of interest to resource managers in Texas is *Prymnesium parvum*.

Prymnesium parvum is commonly known as "golden algae" in Texas and is responsible for numerous fish kills in the southwestern U.S. (Southard et al. 2010) and elsewhere (Edvardsen and Paasche 1998, Johnsen et al. 2010). *P. parvum* typically forms harmful algal blooms (HABs) in Texas in the winter. Using laboratory cultures, Baker et al. (2007, 2009) determined that *P. parvum* displays rapid growth at relatively warm temperatures. This property was incorporated into mathematical models for *P. parvum* growth in Texas (Grover et. al. 2010). These models were based on conventional approaches for modeling in water quality studies (Chapra 1997), and designed to predict algal dynamics given input data on commonly measured limnological conditions. The models included up to five algal populations with two limiting resources, and allelopathic effects. However, the models all assumed that *P. parvum* grows strictly as an autotroph. None of the models provided satisfying predictions of *P. parvum* dynamics when using

input data from a Texas reservoir, since all of them predicted a winter decline precisely at the time when annual maxima were observed.

The existing models treat a lake as a chemostat, whose dilution rate is estimated from hydrological data. Limiting resources are nitrogen and phosphorus, whose supply is estimated from observations of total nitrogen and phosphorus. Growth rates depend on temperature, light and salinity, while grazing mortality is estimated from observations of zooplankton abundance. One model represents only the population of *P. parvum*, while others represent one or four competing populations of other algae. The model that represents only the population of *P. parvum* was designated PP0. Observational data from Lake Granbury were collected by D.L. Roelke and colleagues from 10 stations arranged along the length of the lake, and were spatially averaged to obtain input data and observations of *P. parvum* dynamics for evaluating model predictions.

In this chapter, we construct a model which adds mixotrophy to a much simplified version of the PP0 model. This model was not created to explore theoretical implications of mixotrophy for aquatic ecosystems, but rather to attempt to model a specific occurrence of *P. parvum* bloom dynamics in Texas. Therefore, it takes a simpler approach to representing mixotrophy than was attempted in the models presented in previous chapters. This also gives the advantage of simplifying the numerical calculations and eliminating problems of stiffness that plagued the differential equations of previous models. One aspect of this simplified approach to mixotrophy is to treat it as an additive effect to the autotrophic growth that was previously modeled for *P. parvum.* This likely gives the *P. parvum* population more of an advantage than would be expected in a natural system, where diminishing returns to mixotrophic nutrition might be expected, but we are trying to determine whether adding mixotrophy to the prior model would produce results that more accurately predict observed population dynamics, rather than trying to create a perfectly accurate and general model. The model developed here only examines one limiting resource, here taken to be phosphorus, since Lake Granbury has a fairly high N:P ratio

(Grover et al. 2010, Roelke et al. 2010a) In order to allow for mixotrophy, the model includes, in a simple way, a dynamic population of bacteria as a prey species for *P. parvum*.

The modeling exercise presented here attempts to ascertain whether incorporating mixotrophy can correct the principal flaw of previous models – their tendency to predict a winter decline of *P. parvum* when instead a maximum is observed. To do this, several features of the model are designed to give *P. parvum* a strong contribution of mixotrophy to population growth, especially in winter. The parameters describing ingestion of bacterial prey are set to values that are high compared to some published observations, and ingestion is assumed to be up-regulated in response to low P availability and low light. The goal was to determine first whether mixotrophy could boost the predicted winter growth of *P. parvum*, giving it every possibility to do so, and then if so, to evaluate whether the resulting model was plausible in other aspects.

5.2 Model Formulation

The model examined here consists of three ordinary differential equations to explore the effects of mixotrophy on *Prymnesium parvum* dynamics. Notation is summarized in Table 5.1. The model tracks the densities of *P. parvum* and their edible bacterial prey along with the concentration of a limiting inorganic resource here taken to be phosphorus.

$$\frac{dN}{dt} = D(N_{in} - N) + \mu N - mN \tag{5.1}$$

$$\mu = \frac{\mu_{max} R}{K_R + R} + \frac{\iota_{max} B}{(K_B + B) Y_{RB}} e Y_{RP} \tag{5.2}$$

The change in density of *P. parvum* (N_P , cells / liter) through time has three terms (Eq. (5.1)). The first term is a standard chemostat supply term with dilution (*D*) times the difference between an inflow of *P. parvum* cells (N_{in}) and the current *P. parvum* density. This term allows for immigration of *P. parvum* in the inflow, though we have primarily analyzed cases where such immigration does not occur ($N_{in} = 0$). Setting N_{in} to a low value prevents transient extinction of *P. parvum* in cases where seasonal variations are large, but such extinction did not generally occur for the conditions examined here. The second term in Eq. (5.1) is the change in density due

to growth. The P-limited growth rate of *P. parvum* (Eq. (5.2)) is the sum of rates based on two sources of P. One source is uptake of dissolved P (at concentration *R*, μmol / liter) and the other is ingestion of bacterial prey (at density *B*, cells / liter). Growth in relation to dissolved P is a Monod function with μ_{max} being the maximal growth rate and K_R the half-saturation constant. The growth rate based on ingestion of bacteria is also a Monod function with ι_{max} as the maximal ingestion rate of bacterial cells per day per *P. parvum* and K_B the half-saturation constant for the bacteria. Dividing this ingestion function by the yield for bacteria (Y_{RB}) gives us the amount of P obtained per bacterial cell ingested. This is then multiplied by the yield of *P. parvum* cells per amount of P (Y_{RP}) and an efficiency (*e*) that is the proportion of P from ingested bacteria that is converted into *P. parvum*. The final term in Eq. (5.1) is the loss due to mortality at a per capita rate *m*.

$$\frac{dB}{dt} = a(B_{max} - B) - N_P \frac{\iota_{max} B}{K_B + B} - DB \tag{5.3}$$

The change in edible bacterial density (*B*) through time (Eq.(5.3)) also has three terms. The first term is like a standard chemostat supply term with *a* being a turnover, or growth rate of edible bacteria times the difference between a maximal bacterial density (B_{max}), similar to a carrying capacity, and the current density (*B*). This simple form was adopted to avoid complicated dynamics and possible numerical problems that could arise with a more realistic description of bacterial growth. The second and third terms are decreases due to ingestion from *P. parvum* and dilution.

$$\frac{dR}{dt} = D(R_{in} - R) - \frac{\mu_{max} R}{(K_R + R)Y_{RP}} N_P + \frac{r m_P N_P}{Y_{RP}} + N_P(1-e)\frac{\iota_{max} B}{(K_B + B)Y_{RB}} \tag{5.4}$$

The change in the concentration of P (Eq. (5.4)) has four terms. The first is a standard chemostat supply term with the dilution rate (*D*) times the difference between supplied P (R_{in}) and current P (*R*). The next term is the loss due to the uptake of P and its conversion to cells during growth of *P. parvum.* The third term is the return of P due to the mortality of *P. parvum.*

This term has a recycling efficiency (*r*) that determines the proportion of P that is returned to the dissolved state. The final term is the return to the dissolved state of the proportion of P from ingested bacteria that is not converted to *P. parvum*.

Table 5.1 Symbols

Symbol	Description	Value	Units
N	Density of *P. parvum*	variable	cells/liter
B	Density of edible bacteria	variable	cells/liter
R	Phosphate	variable	µmol P/liter
D	Dilution rate	input	/day
R_{in}	Phosphate supply	input	µmol P/liter
r	Recycling efficiency of *P. parvum*	input	dimensionless
B_{max}	Maximum density of edible bacteria	f(B_0(t))	cells/liter
a	Turnover rate of bacteria	f(T)	/day
μ_{max}	Maximum *P. parvum* growth rate	f(T,I,σ)	/day
μ	Growth rate of *P. parvum*	f(T,σ,I,R,S)	/day
ι_{max}	Maximum ingestion rate	f(T,σ,I,R,S)	bacteria cells /day/Prym. cell
K_R	Half-saturation constant for phosphorus	0.009	µmolP/liter
m	Mortality of *P. parvum*	0.1	/day
e	Conversion efficiency of *P. parvum*	0.5	dimensionless
N_{in}	Supply of *P. parvum*	0	cells/liter
Y_{RB}	Yield of bacteria from P	4.03×10^8	cells/µmol P
K_B	Half-saturation constant for ingestion of bacteria	5×10^8	cells/liter
Y_{RP}	Yield coefficient for P in *P. parvum*	7.2×10^8	cells/µmol P

5.2.1 Parameters

Parameters with constant values are listed in Table 5.1 with their values. Parameters were assigned values based on data gathered during studies on Lake Granbury (Roelke et al. 2010b). Several parameters are shared with a previously published model and were assigned the same values (Grover et al., 2010). Parameters listed with the word 'input' are read from an array of daily values for Lake Granbury (constructed from observations as described in Grover et al., 2010). Other quantities in Table 5.1 are functions, which in turn depend on input and on additional parameters.

The first of these functions is the maximum density of edible bacteria (B_{max}). This was taken as an input parameter based on total bacterial densities observed during the sampling events described in Grover et al. (2010). To obtain values for every day of the year, linear interpolation was used between sampling dates over one year. It was then assumed arbitrarily that since possibly not all bacteria are edible to *P. parvum*, $B_{\max}$ would be ½ of the observed, interpolated total density. The turnover rate of bacteria (*a*) was assumed to be equal to the empirical temperature-dependent population growth rate found in other Texas reservoirs (Chrzanowski and Grover, 2001b), given by the expression $\max(0, 0.032T - 0.1611)$. The maximal *P. parvum* growth rate based on P (Eq. (5.5)) is taken directly from the previous models (Grover et al. 2010, based on Baker et al. 2009). It is a function of temperature (*T*), light (*I*), and salinity (σ).

$$\mu_{\max}(\sigma, I, T) = \max\left\{0, \beta_0 + \beta_1(\sigma - \sigma_{\text{ref}}) + \beta_2 e^{\left[0.7\left(\frac{T-T_{\text{ref}}}{T_{\text{ref}}}\right)\right]} + \beta_3(I - I_{\text{ref}})\right.$$
$$+ \beta_4(\sigma - \sigma_{\text{ref}})^2 + \beta_5 e^{\left[1.4\left(\frac{T-T_{\text{ref}}}{T_{\text{ref}}}\right)\right]} + \beta_6(I - I_{\text{ref}})^2 \qquad (5.5)$$
$$\left. + \beta_7(\sigma - \sigma_{\text{ref}}) e^{\left[0.7\left(\frac{T-T_{\text{ref}}}{T_{\text{ref}}}\right)\right]}\right\}$$

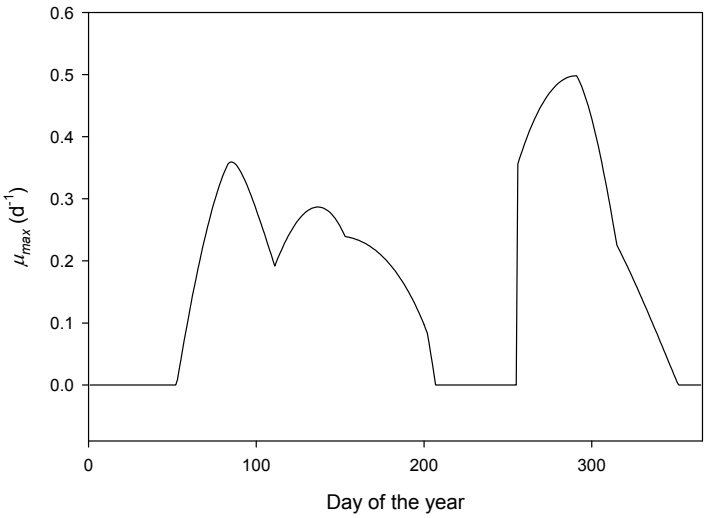

Figure 5.1 Maximum growth rate for *P. parvum* by day of the year for autotrophic growth based on P

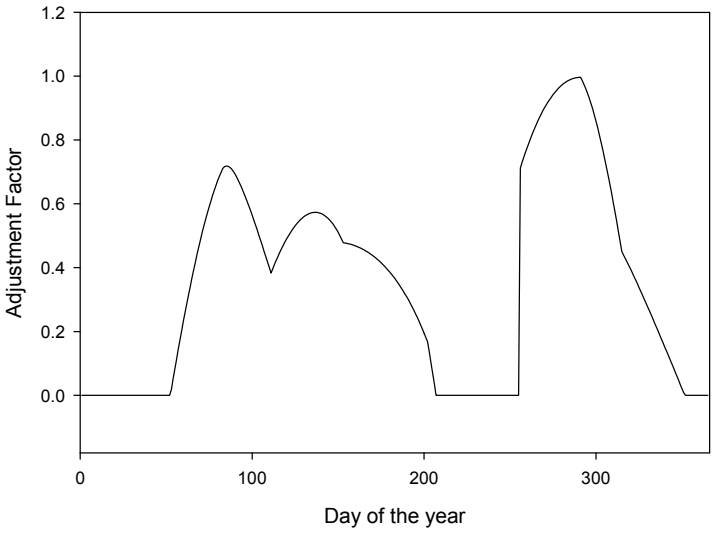

Figure 5.2 Function F1(T, I, σ) that modifies ingestion rate due to temperature, light, and salinity by day of the year. Note scale difference with Figure 5.1.

The parameters β_i were set to the values used in the previous models of *P. parvum* (Grover et al. 2010).

5.2.1.1 Initial Bacterial Ingestion Rate

The maximum ingestion rate (i_{max}) under optimal conditions was assumed to be 100 bacterial cells consumed per *P. parvum* cell per day (Nygaard and Tobiesen, 1993; Legrand et al., 2001). This rate was reduced by a product of three functions (f_i) taking values between 0 and 1 to account for reduced ingestion under various conditions (Eq.(5.6)). The maximum bacterial ingestion rate is a function of temperature, light, and salinity like the autotrophic growth.

$$i_{max} = 100 \times f_1(T, I, \sigma) \times f_2(I) \times f_3(R) \tag{5.6}$$

The first of these functions ($f_1(T, I, \sigma)$) is a rescaling of the maximum growth rate function (Eq.(5.5), Figure 5.1) into the range of 0 to 1 (Figure 5.2). The second function ($f_2(I)$) decreases with irradiance (Figure 5.3 A)

$$f_2(I) = -0.35 \arctan(0.02(I - 200)) + 0.5 \tag{5.7}$$

This function reduces mixotrophic growth based on ingestion of bacteria, as irradiance increases through a range of 100 – 400 μE m^{-2} s^{-1}. In simulations, the array of daily irradiances from Grover et al. (2010) was used to determine the value of this function. The third function ($f_3(R)$) is a decreasing function of P (Figure 5.3 B)

$$f_3(R) = -0.33 \arctan(1.4(R - 3)) + 0.55 \tag{5.8}$$

This function reduces mixotrophy when dissolved P is high, assuming that *P. parvum* regulates mixotrophy in a manner similar to the closely related haptophyte *Chrysochromulina polylepis* (Stibor and Sommer, 2003). The number of bacterial cells consumed by P. parvum each day is graphed in Figure 5.4.

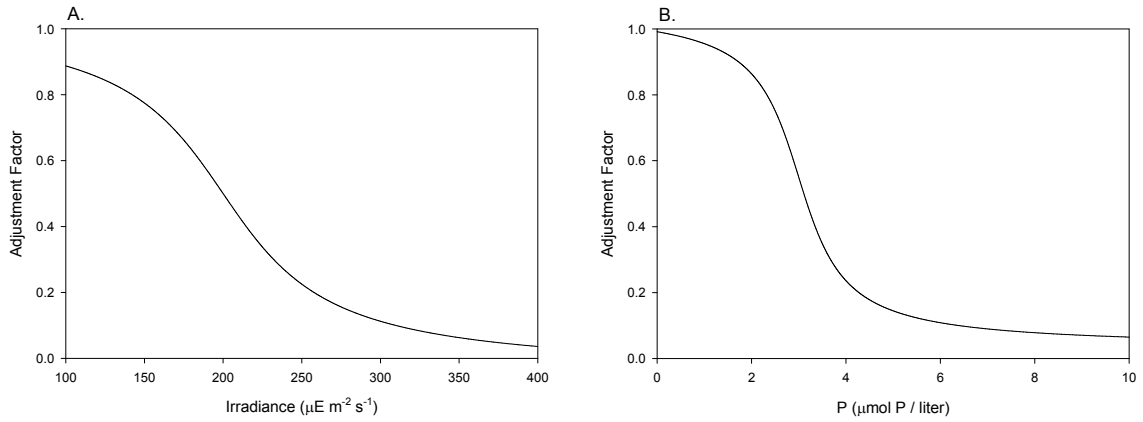

Figure 5.3 Functions that modify maximum ingestion rate A. due to irradiance and B. due to P

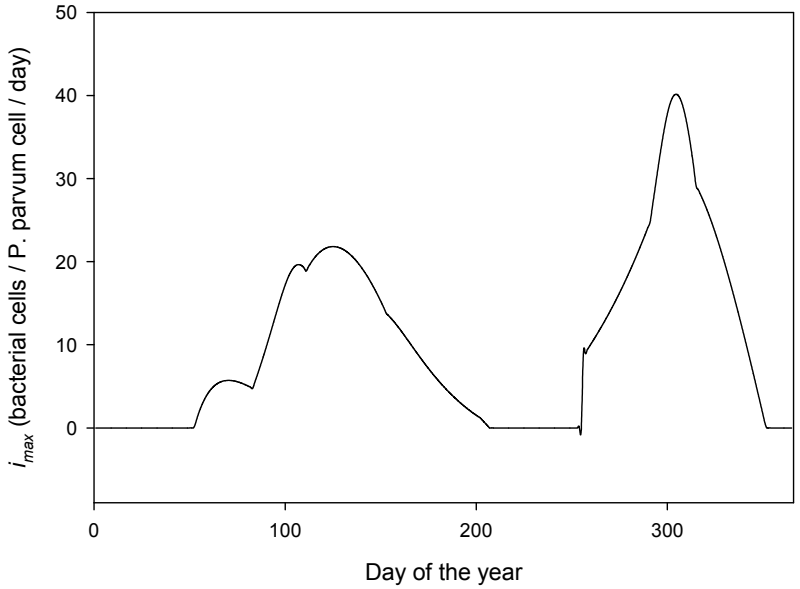

Figure 5.4 Maximum ingested cells by *P. parvum* per day by day of the year using the Initial Bacterial Ingestion Rate

5.2.1.2 Modified Bacterial Ingestion Rate

One final modification was made to the model. The *P parvum* population declines in the summer. There have been arguments that mixotrophy is a response to adverse conditions(Nygaard and Tobiesen 1993). Since *P. parvum* is mostly autotrophic, feeding may be a response to a decrease in nutrients when there is not enough light to carry out enough photosynthesis (Carvalho and Grane'li 2010). Therefore, the ingestion of bacteria was made to be dependent on light level (Eq. (5.9)). This causes *P. parvum* to ingest fewer bacteria in the bright summer and more bacteria in the dark winter. To give the mixotrophs an unrealistic advantage, a multiplier was created for a maximum ingestion amount that was arbitrarily chosen to be 100 bacterial cells per day per *P. parvum* cell. (The actual figure is closer to 17.)

$$i_{max} = 100 \times (1 - \frac{I_{day}}{I_{\max}}) \tag{5.9}$$

The multiplier was made relative to the maximum light level for the year by dividing the light level for each day by the maximum light level for the year. This is then subtracted from one. This makes the multiplier zero at the maximum light level for the year and closer to one for the lowest light level for the year. The maximum ingestion rate and light levels for the year are graphed in Figure 5.5.

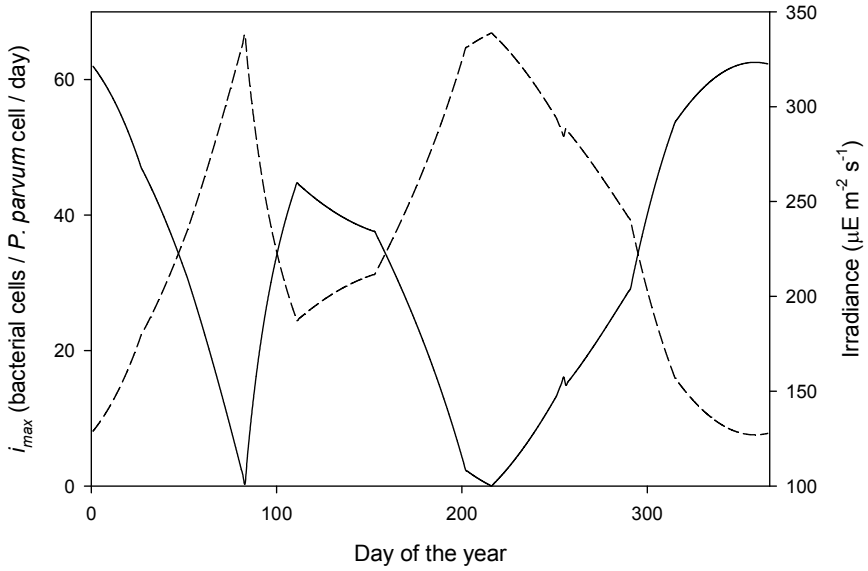

Figure 5.5 Maximum ingested cells by *P. parvum* per day using the Modified Bacterial Ingestion Rate. (Solid line – imax Dashed line – Irradiance)

5.3 Numerical Calculations

5.3.1 Steady State Analysis

Though this model was written with the idea that values from the input array would change every day for time-variable simulations, the first analyses addressed steady states using average values from the input array over one year as constant parameters (Table 5.2).

Solutions for the steady state were found both numerically and analytically. The analytic solutions were calculated using Mathematica's Solve function while the numeric solutions were found using MATLAB. Analytical solutions for the steady state are summarized in Table 5.3.

Table 5.2 Steady state parameters.

Description	Value	Units
Phosphorus (R_{in})	1.62	µmol P / liter
Light (I)	231	$\mu E\ m^{-2}\ s^{-1}$
Temperature (T)	20	°C
Dilution (D)	0.04	d^{-1}
Salinity (σ)	2	psu
Recycling (r)	0.5	dimensionless
B_{max}	1.71E+09	cells / liter
i_{max}	20.81576	cells / *P.parvum* /day
turnover (a)	0.4789	d^{-1}
$\mu_{max}(T,I,\sigma)$	0.373763	d^{-1}

Table 5.3 Analytical steady state solutions.

Variable	Analytical Solution
N (cells / liter)	1.67617×10^{10}
B (cells / liter)	1.17543×10^{6}
R (µmol P / liter)	0.00312755

The same two methods were used to explore the values of the parameters that affect the growth of *P. parvum* and the density of bacteria (i_{max}, K_B, e, Y_{RB}, a, and B_{max}). (Sensitivity analyses for other parameters, which were carried over from previous models, were reported in Grover et al., 2010). The Matlab solver ode23s was used for these simulations to cope with stiffness that arose for some parameter values. There were also some parameter values for which Mathematica algorithms could not find solutions. When there were analytical and numerical solutions, they agreed well.

5.3.2 Analysis of Seasonal Dynamics

Daily environmental data (temperature, light, salinity, irradiance, and phosphorus) was fed into the solver each day for one year. This same data was then used for five years, and the results are presented as the values obtained for the fifth year. The model was run with bacteria alone, *P. parvum* alone, and *P parvum* with bacteria.

Equation (5.2) describes the growth rate of *P. parvum* as the sum of an autotrophic part and a heterotrophic part. Seasonality in the autotrophic component of growth is controlled by the function μ_{max}. This is the function described by Baker et al. (2009) and is governed by temperature, light, and salinity. These quantities vary seasonally and corresponding variations of growth rate throughout the year are shown in Figure 5.1. Autotrophic growth is reduced to zero by low temperature in winter, and by low salinity in summer. Seasonality in the mixotrophic component of growth similarly arises from the initial description of maximum ingestion rate because it shares a similar dependence on temperature and salinity. The seasonal variation of the maximum ingestion rate is shown in Figure 5.4. Note that in this case mixotrophic growth, like autotrophic growth, goes to zero in winter due to a strong effect of low temperature portrayed by Eq. (5.5).

5.4 Results

5.4.1 Steady States

As the maximal ingestion rate (i_{max}) increases, the density of the bacteria decreases while the *P. parvum* population receives a small and diminishing benefit (Figure 5.6). As the half-saturation constant for ingestion of bacteria (K_B) increases, *P. parvum* decreases linearly but slightly, while the bacteria increase linearly about ten-fold (Figure 5.7). As the yield coefficient relating bacteria to phosphorus (Y_{RB}) increases, the density of the bacteria increases and the *P. parvum* density decreases by about 100-fold (Figure 5.8). Note that the yield coefficient is an inverse measure of the P content of bacteria, thus an inverse measure of their contribution to growth of *P. parvum* by mixotrophy. The density of *P. parvum* shows an increase as the turnover rate of bacteria (*a*) increases and the bacteria show a very slight increase (Figure 5.9). There is an increase in the density of bacteria as maximal density (B_{max}) first increases, but this quickly becomes constant with further increases, while the *P. parvum* density increases more steadily (Figure 5.10). Variations in the efficiency of mixotrophic growth (*e*) do not affect the steady state *P. parvum* and bacteria populations, but the dissolved P concentration (*R*) decreased as efficiency increased (Figure 5.11). With the exception of Y_{RB}, all of the parameter variations produced little change in the steady state concentration of dissolved P, but as Y_{RB} increases, dissolved P increases (Figure 5.12).

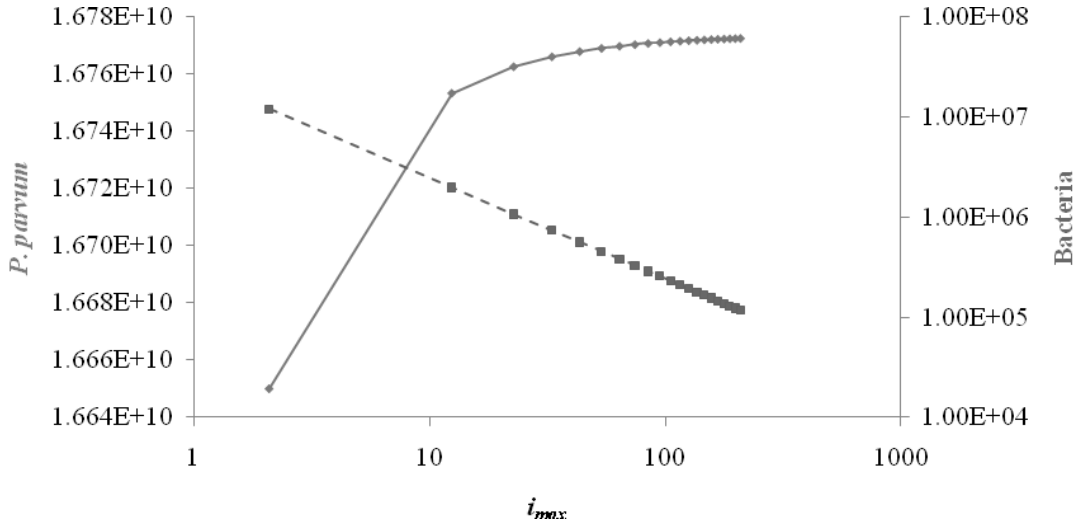

Figure 5.6 *P. parvum* (solid) and Bacteria (dashed) densities in response to the maximum ingestion rate (i_{max}). Note that *P. parvum* is linearly scaled while i_{max} and Bacteria are log scaled.

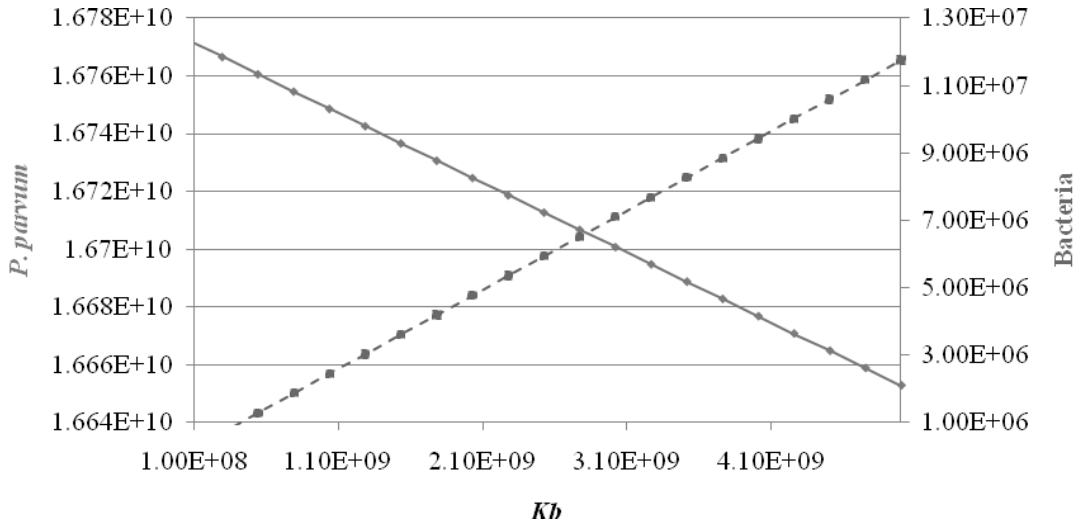

Figure 5.7 *P. parvum* (solid) and Bacteria (dashed) densities in response to the half saturation constant for ingestion of bacteria (K_b). Note that all axes are linearly scaled.

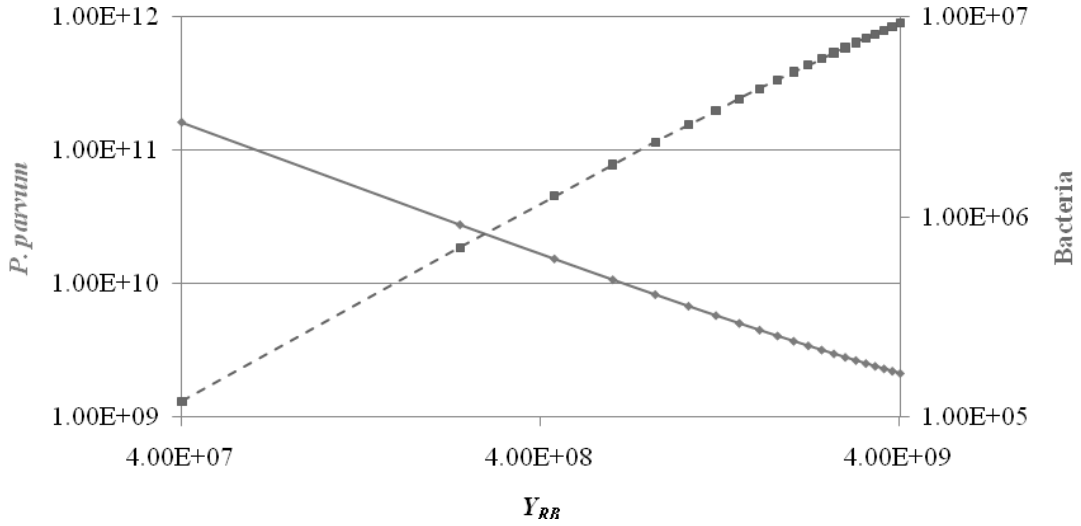

Figure 5.8 *P. parvum* (solid) and bacteria (dashed) densities in response to the yield coefficient of bacteria from P (Y_{RB}). Note that all of the axes are log scaled.

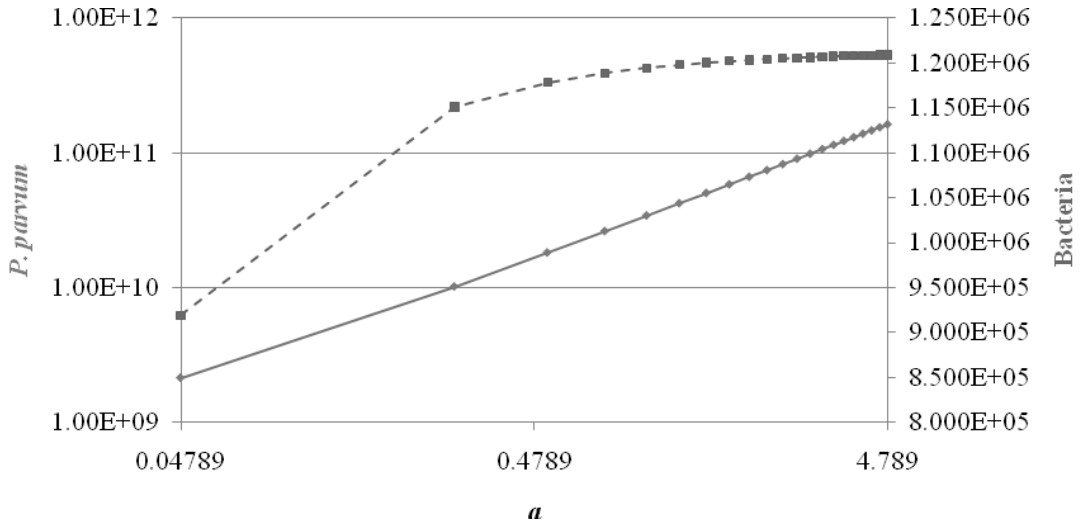

Figure 5.9 *P. parvum* (solid) and bacteria (dashed) densities in response to turnover rate for bacteria (a). Note that the *P. parvum* density (solid line) and the turnover rate are on log scales, while the bacteria (dashed line) are on a linear scale

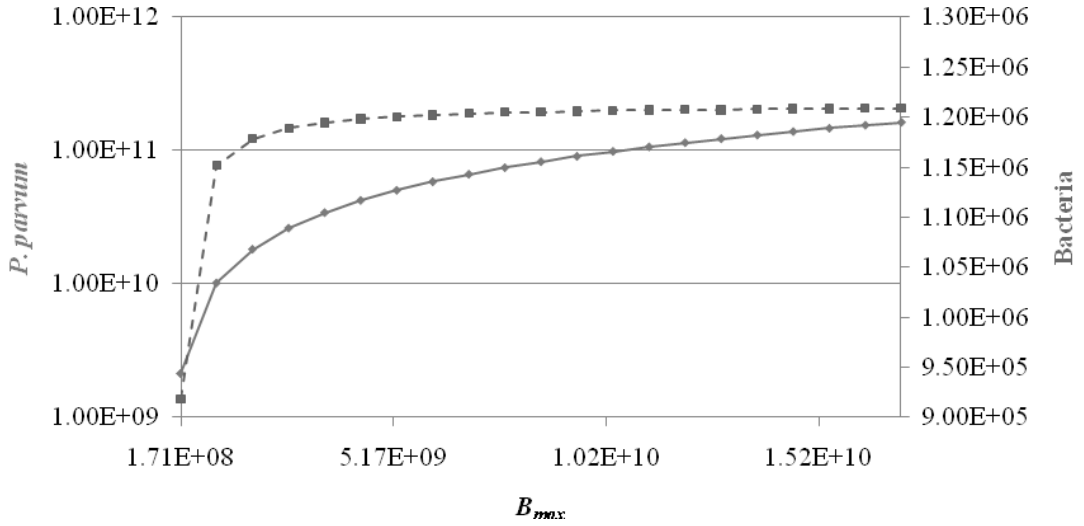

Figure 5.10 *P. parvum* (solid) and bacteria (dashed) densities in response to the maximum density of edible bacteria (B_{max}). Note that the *P. parvum* densities (solid line) are on a log scale, but B_{max} and the bacteria (dashed line) are on a linear scale

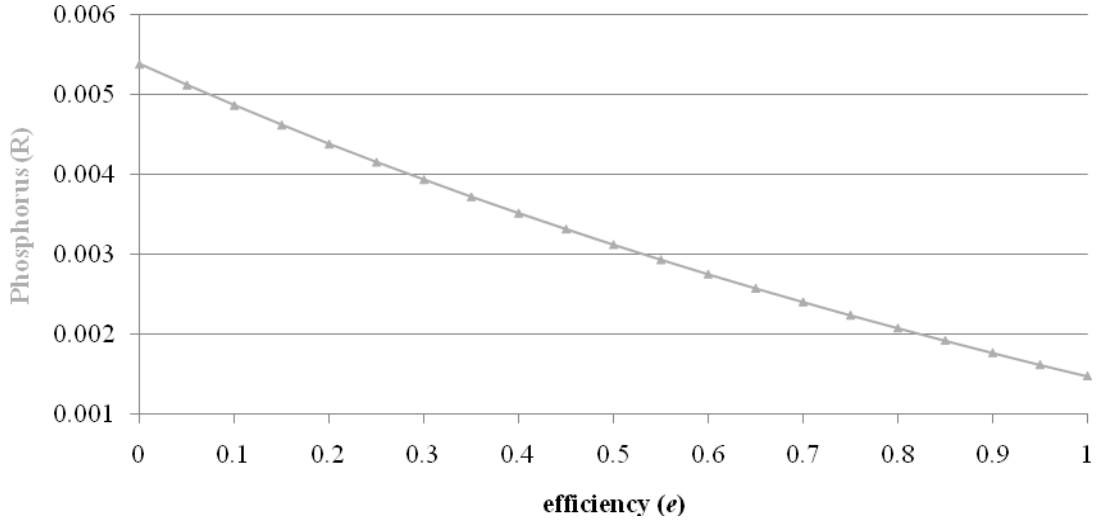

Figure 5.11 Dissolved P concentration in response to efficiency of mixotophic growth (*e*)

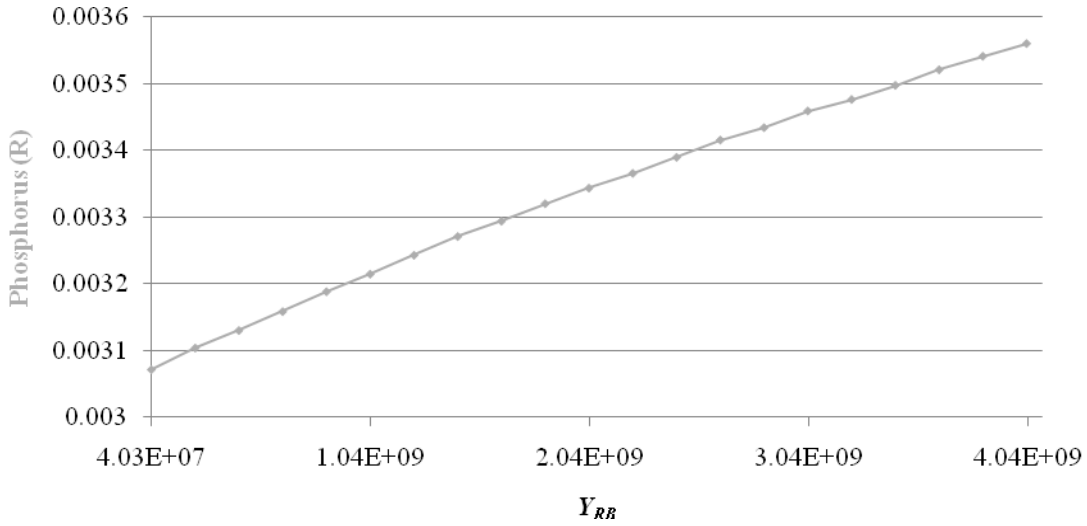

Figure 5.12 Dissolved P in response to the yield of bacteria from P.

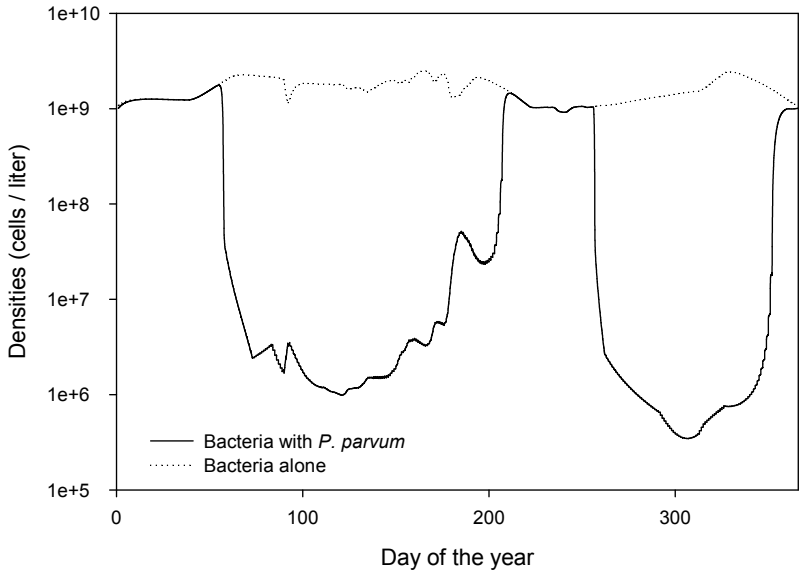

Figure 5.13 Densities of bacteria with and without *P. parvum* through the year for the reformulated model.

5.4.2 Seasonal Dynamics

The bacteria alone have a fairly constant predicted population density through the year. When *P. parvum* are present, the bacteria show large reductions in densities in the summer and early winter (Figure 5.13).

The *P. parvum* density for the fifth year of running the model for five years is shown in Figure 5.14. The P. parvum densities showed large sharp decreases in density during days 350-50 and 200-250. After these sharp declines, the densities rapidly increase to show higher and lightly changing population densities in the summer and early winter. Without the bacteria, the densities of the P. parvum through the year showed a greater range in values (Figure 5.14). The length of the declines increased with declining densities from about days 290-60 and 175-250. Recoveries from minima also took longer. Finally, overall densities were always lower when the P. parvum were without bacteria than when they were present.

Using the alternative description of maximum ingestion rate to produce strong mixotrophic growth in winter, leads to a seasonal pattern with strong mixotrophic growth in winter as intended, but also strong growth during a period in spring when irradiance was low due to turbid water associated with rainy weather (Figure 5.15). However, both descriptions of mixotrophy predict reduced mixotrophic growth in late summer – due to low salinity in the original description and due to high light in the alternative description. The alternative, strongly light-dependent description of the maximal ingestion rate decreases the extent of these winter and summer minima. However, there is still an annual minimum during winter, so that even with a deliberately overestimated consumption rate, the winter minimum does not disappear.

Some further changes to some of the other parameters were pursued to see if they could appreciably change the predicted seasonal dynamics of the *P. parvum* population. There were four parameters, yield coefficient of bacteria from P (Y_{Rb}), turnover rate for the bacteria (a), half-saturation constant for ingestion of bacteria (K_b), efficiency of mixotrophic growth (e), that were varied from 1/10 of their original value to ten times their original value. The results were summarized in Table 5.4. Although parameter changes could substantially alter the population

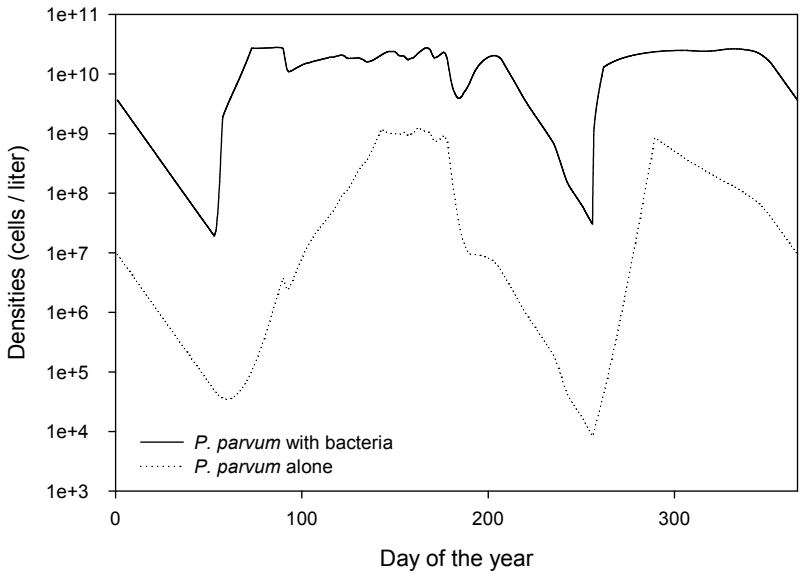

Figure 5.14 Density of P. parvum with and without bacteria.

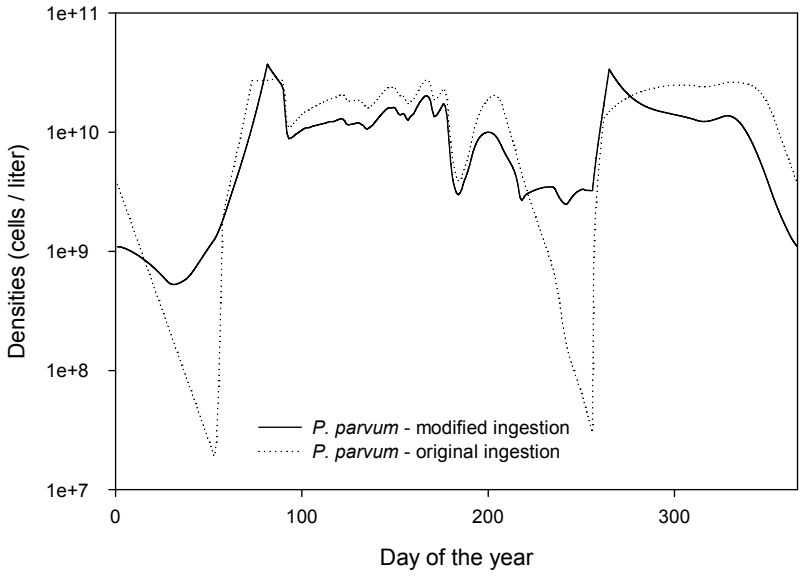

Figure 5.15 Comparison of *P. parvum* densities using modified ingestion and as originally formulated

Table 5.4 Comparison of parameter changes to *P. parvum* density

Parameter that increases	Changes to P. parvum density
yield coefficient of bacteria from P (Y_{Rb})	Decreased
turnover rate for the bacteria (a)	Increased
half-saturation constant for ingestion of bacteria (K_b)	Little change
efficiency of mixotrophic growth (e)	Little change

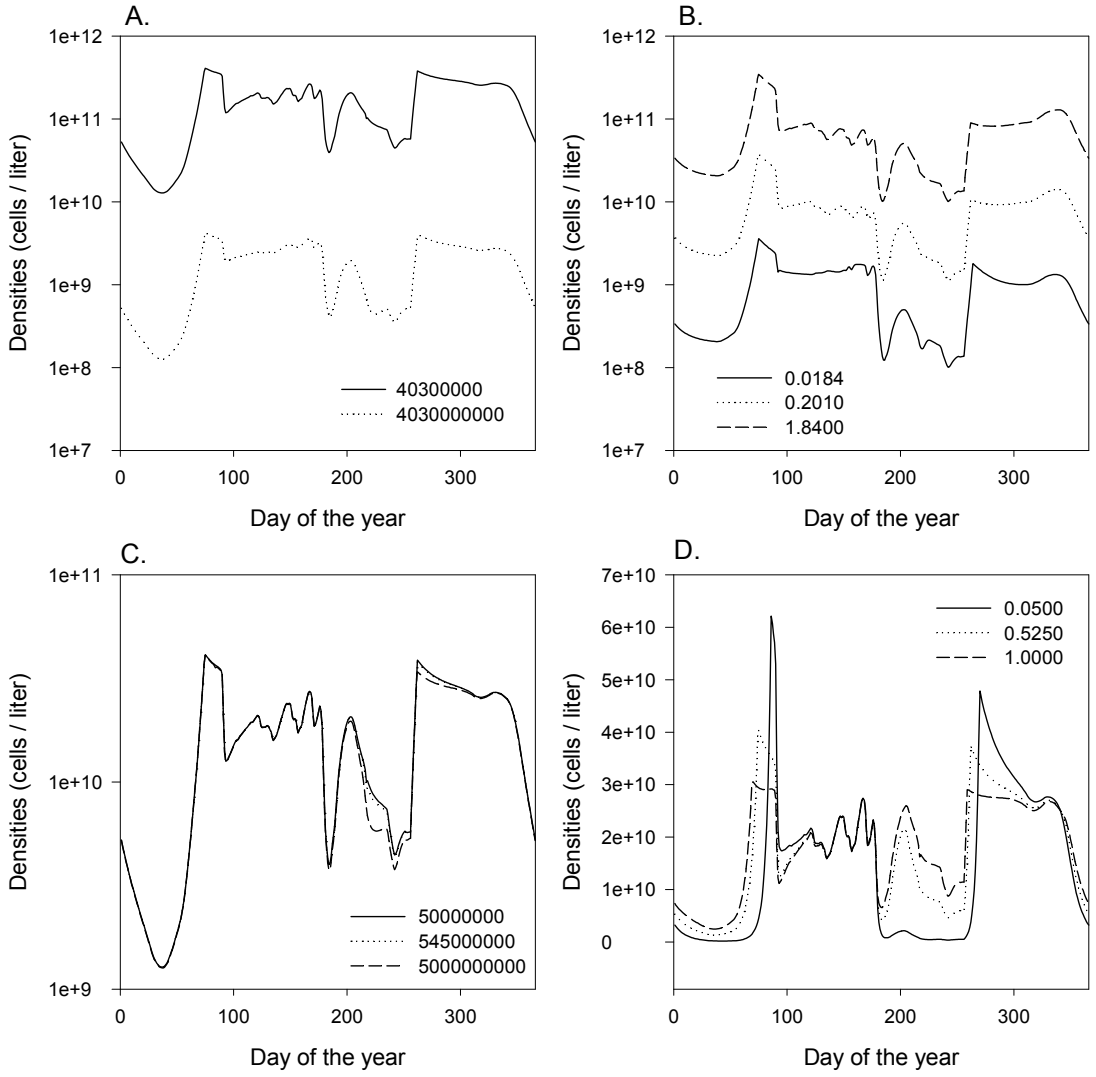

Figure 5.16 Seasonal effects of increasing model parameters of A. yield coefficient of bacteria from P (Y_{Rb}), B. turnover rate for the bacteria (a), C. half-saturation constant for ingestion of bacteria (K_b), D. efficiency of mixotrophic growth (e).

densities predicted for *P. parvum*, they did not change the seasonal pattern much (Figure 5.16). For all the parameter values explored, an annual minimum was predicted to occur in winter.

5.5 Discussion

This study examined the consequences of adding mixotrophy to a model for *Prymnesium parvum*, a harmful algal species that forms blooms in Texas in the winter. The model used here was based on a previous model (Grover et al. 2010) that has *P. parvum* growing phototrophically and alone, without competitors. The previous model predicted a winter decline when natural populations in Texas show winter blooms. The model examined here has *P. parvum* growing as a mixotroph, using both phototrophic and heterotrophic nutritional modes, with a dynamic prey population of bacteria and one limiting resource (phosphorus). The mixotrophy for P*. parvum* in this model had bacterivory as providing additive nutrition, in addition to that of photrophy. This possibly gives *P. parvum* as modeled here an unrealistic advantage from mixotrophy, in an attempt to overcome the winter loss predicted by the previous model. Numerical simulations were done for steady state and seasonally forced systems. The densities of the organisms and the effects of changing parameters were examined.

5.5.1 Steady State

The steady state analysis of sensitivity to parameters varied only those specifically introduced to model mixotrophic growth, and varied them one-at-a-time with other parameters set to default values. The population density of *P. parvum* was not sensitive to the three parameters describing mixotrophic ingestion and growth rates, ι_{max}, K_B, and e. As is often the case in chemostat models, these growth rate parameters probably do more to determine the rate of approach to steady state than the ultimate value reached, which is often controlled more by resource supply. The three parameters governing the rate of supply of bacteria (a, B_{max}) and the nutrient available from them (Y_{RB}) strongly affected the steady state density of *P. parvum*. Of these three parameters, there is empirical information to constrain a and Y_{BR}.

However, B_{max} is essentially unknown. It corresponds to the maximum density of edible bacteria that would occur in the habitat without mixotrophic ingestion. Under many conditions in

aquatic habitats, total bacterial density can be reasonably estimated from observations, but the fraction of the total bacteria that is edible to *P. parvum* is unknown. In addition, *P. parvum* may be able to ingest particulate matter released by lysis of cells targeted by its toxins (as observed for ciliates by Tillman 2003). So the mixotrophic resource base available to *P. parvum* may extend beyond bacteria. To some extent, this can be accounted by increasing the value of B_{max}. But a thorough empirical description of resources available to mixotrophic *P. parvum* is not yet available.

5.5.2 Seasonal

In Figure 5.1, the growth rate of *P. parvum* is zero for days 350-50 and 200-250. This is when previous mathematical models such as PP0 predict large decreases in *P. parvum* densities, in the winter and fall (Figure 5.17). These large sharp decreases in density make the model not very useful for predicting *P. parvum* in Texas. The new version of model PP0 with mixotrophy results in higher densities than the original PP0 model. Given that this model treats mixotrophy as an additive to the original growth this is not surprising. However, the model is plagued with the same difficulty as the PP0 model, the steep drops in density during the winter while the natural population has an increase in the winter.

The hypothesis for this model was that the incorporation of mixotrophy to the existing PP0 model as an additive effect of bacterivory would eliminate winter declines in *P. parvum* density predicted by the current model, and thus generate more realistic predictions of natural populations. In several ways, mixotrophy was modeled with unrealistic advantages for growth of *P. parvum*, especially in winter. Mixotrophy was additive to phototrophic growth, and the ingestion of bacteria was almost ten times greater than indicated from the literature (Carvalho and Grane'li 2010). This did indeed boost the density of the mixotrophs, but did not eliminate the decline in density during winter (Figure 5.17). The ingestion of bacteria by the *P. parvum* was also made to be reciprocal to light level so that the mixotrophs would ingest more bacteria in the dark of winter. This did raise the minima of predicted population density, but did not eliminate them (Figure 5.17).

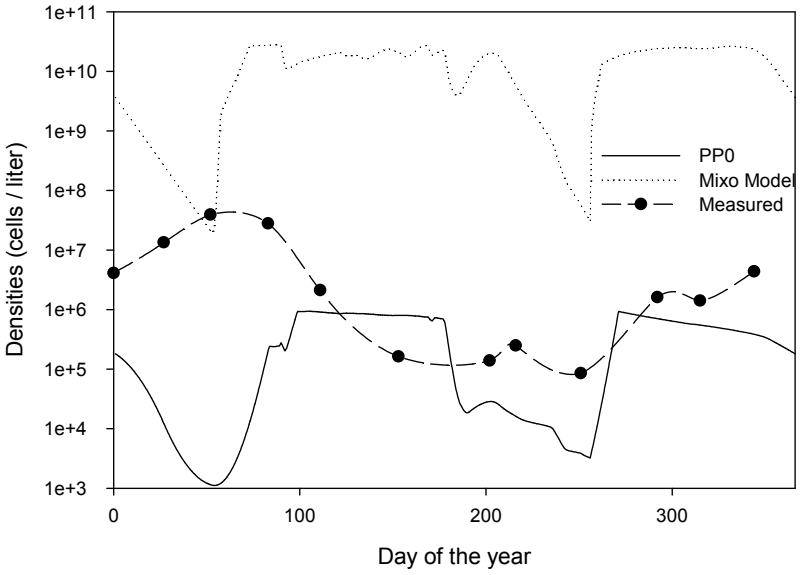

Figure 5.17 Comparison of PP0, this model that includes mixotrophy, and measured values for *P. parvum* densities through the year.

This model incorporating mixotrophy is thus unable to account for the winter increase in the *P. parvum* population in Texas. Even with extraordinary parameter changes, it cannot avoid the predicted winter decline in density of *P. parvum*. The model is based on growth responses to temperature and salinity generated from Baker et al. (2007, 2009). So far, the only way to change the predictions of the PP0 and related models is to change these growth responses (Grover et al. 2010). Though the problem of modeling *P. parvum* blooms in Texas was not solved with this study of mixotrophy, we have eliminated one of the simpler routes to incorporating this process into predicting *P. parvum* blooms in Texas. Possibly, a more sophisticated description of mixotrophy would prove more helpful (e.g. Flynn and Mitra 2009). Alternatively, other processes may be more influential on bloom formation than the growth physiology of *P. parvum*. There has been some success with mathematical modeling that stresses spatial dynamics and hydrology as factors in bloom formation (Grover et al. 2010), and field observations support a strong role for hydrology (Roelke et al. 2010a, b).

CHAPTER 6

CONCLUSION

In order to explore aspects of mixotrophy, four studies were undertaken. The first study involved a model that had four dynamic populations of organisms that included phototrophic algae that utilize photosynthesis, heterotrophic bacteria that take up inorganic nutrients from the environment, heterotrophic zooflagellates that consume bacteria, and mixotrophs that combine phototrophy and heterotrophy in response to a parameter α that is the proportion that the mixotroph utilizes photosynthesis. The mixotrophs were placed in a variety of environments to explore coexistence with the other nutritional types and to determine the most successful type of mixotroph in terms of the α parameter. The second study used the previously developed model, but fixed the α parameter at two characteristic values representing primarily phototrophic and primarily heterotrophic mixotrophs, and then varied the environmental parameters controlling resource supplies. Simulations of the resulting scenarios were run to a steady state with constant environmental conditions. Results were examined in terms of coexistence of all four nutritional types, growth-limiting nutrients, and the ecosystem properties of total C:P of the organisms, excess P released by consumption, and DOC production. The third study then elaborated the model to include seasonal variation in light and temperature and their effects on nutrient uptake, growth, and attack rates. The results of the numerical simulations were examined for seasonal variations in the densities of the organisms, their coexistence, and seasonal effects on the aforementioned ecosystem properties. The final study created a much revised model of *P. parvum* dynamics from one of the current models for *P. parvum* growth that incorporated mixotrophy and a dynamic population of bacterial prey. The seasonal densities of these populations and the effects of altering parameters that affected mixotrophy were explored.

The first study addressed the coexistence of microorganisms pursuing diverse nutritional strategies, using the first model of mixotrophs that embeds these organisms in a realistic, dynamic microbial food web and explicitly represents the categories of resources minimally required for autotrophic and heterotrophic growth (Crane and Grover 2010). In the range of model environments explored, at least three different types of organisms were predicted to persist, and with high supply of both P and light, all four types of organisms were predicted to persist for some ranges of the mixotrophy parameter α.

Mixotrophy was favored when nutrients were limiting. Persistence of mixotrophs was predicted predominantly when P supply was low, or when high P supply was accompanied by environmental characteristics producing high light supply. Moreover, predicted population densities of mixotrophs increased as α increased, peaking near α of 0.9. Thus, in terms of abundance, the most successful mixotrophs were predicted to be primarily autotrophic, supplementing photosynthesis with bacterivory. The coexistence of all four organisms in this model was generally predicted with enough available light. This model extended the reach of theoretical models commonly applied to microbial food webs, and specifically to mixotrophs. This model thus lays a foundation for addressing open questions concerning the ecosystem and geochemical roles of mixotrophs.

The second study extended the first study and included ecosystem and geochemical roles of mixotrophs. It focused more on the environmental parameters governing resource supplies and the responses of populations and ecosystem properties for two distinct types of mixotrophs, primarily heterotrophic and primarily phototrophic. Coexistence of all four organisms was possible and even likely, and coexistence was favored when mostly autotrophic mixotrophs were in shallow environments. The second study also examined ecosystem properties and geochemical roles of mixotrophs, especially as they pertain to the light:P hypothesis (Sterner et al. 1997). The ecosystem properties were: seston C:P, proportion of photosynthesis released as DOC, and recycling of P by phagotrophic consumers. According to the light:P hypothesis, the

C:P of the seston should show a direct correspondence with light:P. Increasing light and holding P supply constant did slightly increase the predicted bulk C:P ratio of the organisms, a proxy for seston, and the predicted C:P ratio also decreased with increasing depth. These results agreed with the light:P hypothesis. However, when light was held constant and P supply was increased (decreasing the light:P ratio), the C:P ratio predicted by this model did not decrease, contradicting the expectations of the light:P hypothesis. The C:P ratio did increase for the lowest P supplies examined, and then decreased for the highest levels. This increase, which contradicted the light:P hypothesis, occured when the algae were predicted to be P-limited. With higher P-supply, algae became light-limited, and the predicted C:P ratios declined, in agreement with the light:P hypothesis.

The model generally reflected the predictions of this hypothesis as long as the P supply was not profoundly limiting. Coexistence of all four types of organisms was possible across the range of incident light examined, and across a broad range of higher values for P supply. However, such coexistence was only predicted at shallow depths and the attendant P flux of deeper ecosystems were altered by the lack of mixotrophs. This model thus suggests that the composition of nutritional strategies in microbial ecosystems can have a profound influence on P flux. Coexistence of microbial populations pursuing different nutritional strategies was commonly predicted. Moreover, the ecosystem properties expected under the light:P hypothesis were supported by the predictions of this model, with the noted exceptions involving severely P-limited habitats. This study shows the hypothesis remains a reasonable way to look at aquatic ecosystems, when mixotrophs and their mechanisms of interaction with other microorganisms are explicitly incorporated. More generally, this study suggests theoretically that mixotrophs are abundant under wide ranges of resource supplies and leave a signature on the properties of aquatic ecosystems.

Ecosystem properties were again explored in the third study which extended the previous theoretical model of mixotrophs embedded in a simple microbial food web to incorporate seasonality. The current model is, as far as we know, the only seasonal model that incorporates

mixotrophy. The modeled physiological rates varied in response to seasonal changes in light and temperature. The densities of organisms and their growth limitations in response to this seasonal forcing were analyzed, along with the ecosystem properties of P flux and the C:P ratios of the organisms. The DOC as a percentage of the primary production of the ecosystem was also recorded, but most of the time the producers were C-limited, so no DOC was released and the values were zero.

Population dynamics and ecosystem properties were predicted for two complex community configurations. One was populated with bacteria, algae, and zooflagellates (BAZ); and the other was populated with bacteria, algae, and mixotrophs (BAM). Predictions were also made for simpler, subset communities of one or two populations. When three populations were brought together (BAZ), the high-frequency predator-prey cycles of zooflagaellates and bacteria were greatly reduced in amplitude or eliminated by the presence of algae, regardless of P supply and mortality scenario. The light:P hypothesis proposes that the organisms should shift from being more C-limited in winter to more P-limited in summer. For specific organisms under some circumstances, there are aspects of the light:P hypothesis that agreed with the model predictions. Overall, while some aspects of the light:P hypothesis apply to the predictions of the model explored here, the hypothesis and the model did not always agree. Another property, recycled P flux, should decrease from winter to summer. The predictions of the light:P hypothesis and the model agreed well for recycled P flux. The model generated the additional prediction that the presence of mixotrophs, rather than heterotrophic bacterivores, strongly impacts recycled P flux. The model makes very robust predictions about the seston C:P ratio, interpreted as the bulk stoichiometry of all organisms in the community and consistently agreed with the predictions of the light:P hypothesis.

The predictions of this model did not always follow those of the light:P hypothesis. This was especially evident in the growth limitations of the organisms, where exceptions to the expected prevalence of P-limitation in summer arose in some cases. In contrast, recycled P flux during bacterivory did follow predictions by decreasing in the summer when C:P ratios of the

organism should climb according to the light:P hypothesis. The C:P ratios were indeed the most robust of the predictions of the light:P hypothesis. The predictions of the model explored here thus followed the predictions of the light:P hypothesis at an ecosystem level, but not at an organismal level. By comparing the results of the BAZ and BAM environments, we have additionally predicted that the use of multiple resources by the mixotrophs leads to changes in the growth limitations of other organisms, and to an increase in the recycled P flux in the microbial food web. Therefore, the inclusion of mixotrophs in other theoretical models for planktonic ecosystems may have a profound impact on their predictions.

The fourth study examined the inclusion of mixotrophy to an existing model for *Prymnesium parvum* (Grover et al. 2010). The largely reformulated model has *P. parvum* growing as a mixotroph, using both phototrophic and heterotrophic nutritional modes, with a dynamic prey population of bacteria and one limiting resource (phosphorus). The mixotrophy for *P. parvum* in this model has bacterivory as providing additive nutrition, in addition to that of phototrophy. This gave the modeled *P. parvum* an unrealistic advantage from mixotrophy. The previous model had *P. parvum* growing only phototrophically and showed a winter loss when the natural population shows winter blooms. Numerical simulations were done for steady state and seasonally forced systems. The densities of the organisms and the effects of changing parameters were examined.

The hypothesis for this model was that the incorporation of mixotrophy to the existing model as an additive effect of bacterivory would eliminate winter declines in *P. parvum* density predicted by the current model, and thus generate more realistic predictions of natural populations. Mixotrophy was modeled with unrealistic advantages for growth of *P. parvum*, especially in winter. This did indeed boost the density of the mixotrophs, but did not eliminate the decline in density during winter as compared to summer. The ingestion of bacteria by the *P. parvum* was also made to be reciprocal to light level so that the mixotrophs would ingest more bacteria in the dark of winter. This did raise the minima of predicted population density, but did not eliminate them.

This model incorporating mixotrophy was thus unable to account for the winter increase in the *P. parvum* population in Texas. Even with extraordinary parameter changesthe winter decline in density of *P. parvum* occurred. Though the problem of modeling *P. parvum* blooms in Texas was not solved with this study of mixotrophy, one of the simpler routes to incorporating this process into predicting *P. parvum* blooms in Texas was eliminated.

Through the four studies described above, we have explored many aspects of mixotrophy using mathematical models. The model created here gives a framework for theoretical explanations of aspects of mixotrophy. Giver the other parameter ranges explored here, the most successful mixotrophs are those that are mostly phototrophic and supplement their nutritional needs with heterotrophy. These types of mixotrophs are also able to coexist with a variety of organisms, though mixotrophy can at times give a competitive advantage to an organism in nutrient poor environments and allow them to outcompete other organisms. Because of their overlapping use of resources, they can have a large impact on the nutrient cycling of ecosystems. Through their nutrient cycling, they can even change the nutrient limitations of other organisms. The inclusion of this nutritional form in mathematical models of ecosystems has the potential to be important. While the inclusion of mixotrophy to explain *P. parvum* was not very successful, this may suggest more about the importance of mixotrophy to *P. parvum* than to ecosystem models.

Just as the knowledge of mixotrophy has evolved from a curiosity to a recognition of a common nutritional form in protists, knowledge of mixotrophy in higher plants is evolving. Its perception is changing from a peculiar adaptation to nutrient-poor environments to one that is common. It has now been identified in carnivorous plants and orchids, both denizens of nutrient poor environments, and in other plants that inhabit the forest floor (Jones 1999, Selose 2009). There are even orchids that have taken this nutritional form to the extreme and can survive for years without photosynthesis as mycoheterotrophs (Abadie et al. 2006). Mixotrophy from higher plants may have a large effect on the nutrients in some forest ecosystems. The important role

of mixotrophy as a nutritional form in the functioning of aquatic ecosystems is now being recognized. Could it also be just as important in the terrestrial ecosystems of higher plants?

REFERENCES

Abadie, Jean-Claued, Ulle Puttsep, Gerhard Gebauer, Antonella Faccio, Paola Bonfante, Marc-Andre Selosse, 2006. *Cephalanthera longifolia* (Neottieae, Orchidaceae) is mixotrophic: a comparative study between green and nonphotosynthetic individuals. Can. J. Bot. 84, 1462-1477.

Abrams, P. A., 1999. Is predator-mediated coexistence possible in unstable systems? Ecology 80(2), 608-621.

Abrams, P. A., Holt, R. D., 2002. The impact of consumer–resource cycles on the coexistence of competing consumers. Theor. Pop. Biol. 62, 281–295.

Azam, F., Fenchel, T., Field, J. G., Gray, J. S., Meyer-Rei1, L. A., Thingstad, F., 1983. The Ecological Role of Water-Column Microbes in the Sea. Mar. Ecol. Prog. Ser. 10, 257-263.

Baker, Jason W., James P. Grover, Bryan W. Brooks, Fabiola Uren˜a-Boeck, Daniel L. Roelke, Reagan Errera, Richard L. Kiesling, 2007. Growth and toxicity of *Prymnesium parvum* (Haptophyta) as a function of salinity, light, and temperature. J. Phyc. 43, 219-227.

Baker, Jason W., James P. Grover, Ratheesh Ramachandrannair, Cody Black, Theodore W. Valenti, Jr., Bryan W. Brooks, and Daniel L. Roelke. 2009. Growth at the edge of the niche: An experimental study of the harmful alga Prymnesium parvum. Limnol. Oceanogr., 54(5), 1679–1687.

Berger, S. A., Diehl, S., Kunz, T.J., Albrecht, D., Oucible, A.M., Ritzer, S., 2006. Light supply, plankton biomass, and seston stoichiometry in a gradient of lake mixing depths. Limnol. Oceanogr. 51(4), 1898-1905.

Bratbak, G., Thingstad, T. F., 1985. Phytoplankton-bacteria interactions: an apparent paradox? Analysis of a model system with both competition and commensalism. Mar. Ecol. Prog. Ser. 25: 23-30.

Burkholder, JoAnn M., Patricia M. Glibert, Hayley M. Skelton. 2008. Mixotrophy, a major mode of nutrition for harmful algal species in eutrophic waters. Harmful Algae 8, 77–93.

Butterwick, C., S. I. Heaney, and J. F. Talling. 2005. Diversity in the influence of temperature on the growth rates of freshwater algae, and its ecological relevance. Freshwater Biology 50, 291–300.

Carter, N., 1937. New or interesting algae from brackish water. Arch. Protistenk. 90: 1–68.

Carvalho, Wanderson F., and Edna Grane´li. 2010. Contribution of phagotrophy versus autotrophy to *Prymnesium parvum* growth under nitrogen and phosphorus sufficiency and deficiency. Harmful Algae 9, 105–115.

Chapra S. C., 1997. Surface Water Quality Modeling. McGraw-Hill, New York.

Chase, J. M., Abrams, P.A., Grover, J.P., Diehl, S., Chesson, P., Holt, R.D., Richards, S.A., Nisbet, R. M., Case, T. J., 2002. The interaction between predation and competition: A review and synthesis. Ecol. Lett. 5, 302–315.

Chrzanowski, T. H., Grover, J.P., 2001a. The light : nutrient ratio in lakes: a test of hypothesized trends in bacterial nutrient limitation. Ecology Letters 4: 453-457.

Chrzanowski, T. H., Grover, J.P., 2001b. Effects of mineral nutrients on the growth of bacterio- and phytoplankton in two southern reservoirs. Limnol. Oceanogr. 46(6), 1319-1330.

Codeço, C. T., Grover, J. P., 2001. Competition along a spatial gradient of resource supply: A microbial experimental model. Am. Nat. 157(3), 300-315.

Crane, Kenneth W. and James P. Grover. Coexistence of mixotrophs, autotrophs, and heterotrophs in planktonic microbial communities. 2010. Journal of Theoretical Biology 262, 517–527.

Cropp, Roger and John Norbury. 2009. Simple predator–prey interactions control dynamics in a plankton food web model. Ecological Modelling 220, 1552–1565.

DeMott, W. R., and R. D. Gulati. 1999. Phosphorus limitation of Daphnia: Evidence from a long term study of three hypereutrophic Dutch lakes. Limnology and Oceanography 44: 1557-1564.

Diehl, S., 2007. Paradoxes of enrichment: Effects of increased light versus nutrient supply on pelagic producer-grazer systems. Am. Nat. 169(6), E173-E191.

Dolan, J. R., 1997. Phosphorus and ammonia excretion by planktonic protists. Mar. Geol. 139, 109-122.

Domaizon, Isabelle, Sylvie Viboud, Dominique Fontvieille, 2003. Taxon-specific and seasonal variations in flagellates grazing on heterotrophic bacteria in the oligotrophic Lake Annecy - importance of mixotrophy. FEMS Microbiology Ecology 46, 317-329.

Edvarsen, B. and Paasche, E., 1998. Bloom dynamics and physiology of *Primnesium* and *Chrysochromulina* Physiological Ecology of Harmful Algal Blooms, Springer, Berlin (1998).

Elser, James J. and Jotaro Urabe. 1999. The stoichiometry of consumer-driven nutrient recycling: theory, observations, and consequences. Ecology, 80(3), 735–751.

Eppley, Richard W., 1972. Temperature and phytoplankton growth in the sea. Fishery Bulletin, 70(4) 1063-1085.

Fehling, J., Stoecker, D., Baladuf, S. L., 2007. Photosynthesis and the eukaryotic tree of life. In: Falkowski, P. G., Knoll, A. H. (Eds.), Evolution of Primary Producers in the Sea. Elsevier Academic Press, Boston, pp. 75-107.

Fenchel, T., 1982. Ecology of Heterotrophic Microflagellates. IV. Quantitative Occurrence and Importance as Bacterial Consumers. Mar. Ecol. Prog. Ser. 9: 3 5 4 2.

Fenchel, T., 1986. The ecology of heterotrophic microflagellates. Adv. Microb. Ecol. 9, 57-97.

Flynn, K. J., Mitra, A., 2009. Building the “perfect beast”: modeling mixotrophic plankton. J. Plankton. Res. 31: 965-992.

Gao, Meng, Honghua Shi, Zizhen Li, 2009. Chaos in a seasonally and periodically forced phytoplankton–zooplankton system. Nonlinear Analysis: Real World Applications 10, 1643–1650.

Goldman, J.C., Dennett, M.R., 2000. Growth of marine bacteria in batch and continuous culture under carbon and nitrogen limitation. Limnol. Oceanogr. 45(4), 789-800.

Gotham, I. J., Rhee, G., 1981. Comparative kinetic studies of phosphate-limited growth and phosphate uptake in phytoplankton in continuous culture. J. Phycol. 17(3), 257-265.

Graham, L.E., Wilcox, L.W., 2000. Algae. Prentice Hall, Upper Saddle River, NJ.

Grover, J.P., 2000. Resource competition and community structure in aquatic microorganisms: Experimental studies of algae and bacteria along a gradient of organic carbon to inorganic phosphorus supply. J. Plankton Res. 22(8), 1591–1610.

Grover, J. P., 2003. The impact of variable stoichiometry on predator-prey interactions: a multinutrient approach. Am. Nat. 162, 29-43.

Grover, J. P., 2004. Predation, competition, and nutrient recycling: A stoichiometric approach with multiple nutrients. J. Theor. Biol. 229, 31–43, doi:10.1016/j.jtbi.2004.03.001.

Grover, James P., 2009. Is storage and adaptation to spatial variation in resource availability? Am. Nat. 173(2).

Grover, James P., Jason W. Baker, Daniel L. Roelke, and Bryan W. Brooks, 2010. Current status of mathematical models for population dynamics of Prymnesium parvum in a Texas reservoir. Journal of the American Water Resources Association, 46(1):92-107. DOI: 10.1111 / j.1752-1688.2009.00393.x

Hackett, J. D., Yoon, H.S., Butterfield, N.J., Sanderson, M.J., Bhattacharya, D., 2007. Plastid endosymbiosis: Sources and timing of major events. In: Falkowski, P. G., Knoll, A. H. (Eds.), Evolution of Primary Producers in the Sea. Elsevier Academic Press, Boston, pp. 109-132.

Hammer, Astrid C. and Jonathan W. Pitchford, 2005. The role of mixotrophy in plankton bloom dynamics, and the consequences for productivity. Journal of Marine Science, 62: 833-840.

Huisman, J., Jonker, R.R., Zonneveld, C., Weissing, F.J., 1999. Competition for light between phytoplankton species: experimental tests of mechanistic theory. Ecology 80(1), 211-222.

Huisman, J., Weissing, F.J., 1994. Light-limited growth and competition for light in well-mixed aquatic environments: An elementary model. Ecology 75(2), 507-520.

Huisman, Jef, and Sommeijer, Ben, 2002. Population dynamics of sinking phytoplankton in light-limited environments: simulation techniques and critical parameters. Journal of Sea Research 48, 83-96.

Huppert, Amit, Bernd Blasius, Ronen Olinky, Lewi Stone, 2005. A model for seasonal phytoplankton blooms. Journal of Theoretical Biology 236, 276–290.

Hutchinson, G. Evelyn, 1944. Limnological studies in Connecticut. VII. A critical examination of the supposed relationship between phytoplankton periodicity and chemical changes in lake waters. Ecology, 25(1) 3-26.

Johnsen, Torbjørn M., Wenche Eikrem, Christine D. Olseng, Knut E. Tollefsen, and Vilhelm Bjerknes, 2010. *Prymnesium parvum*: The Norwegian Experience. Journal of the American Water Resources Association (JAWRA), 46(1) 6-13. DOI: 10.1111／j.1752-1688.2009.00386.

Jones, H.L.J., 1997. A classification of mixotrophic protists based on their behaviour. Freshw. Biol. 37, 35-43.

Jones, Harriet L. J., 1999. Mixotrophic protists: the microscopic equivalent to the carnivorous plant?. Botanical Journal of Scotland, 51(1), 15-22.

Jones, R.I., 2000. Mixotrophy in planktonic protists: An overview. Freshw. Biol. 45, 219-226.

Kamjunke, Norbert, Tanja Henrichs, and Ursula Gaedke, 2007. Phosphorus gain by bacterivory promotes the mixotrophic flagellate *Dinobryon spp.* during re-oligotrophication. Journal of Plankton Research 29(1) 39–46.

Katechakis, A., Stibor, H., 2006. The mixotroph *Ochromonas tuberculata* may invade and suppress specialist phago- and phototroph plankton communities depending on nutrient conditions. Oecologia 148, 692–701.

Kooijman, S. A. L. M., Andersen, T., Kooi, B.W., 2004. Dynamic energy budget representations of stoichiometric constraints on population dynamics. Ecology 85(5), 1230-1243.

Kooijman, S. A. L. M., Auger, P., Poggiale, J.C., Kooi, B.W., 2003. Quantitative steps in symbiogenesis and the evolution of homeostasis. Biol. Rev. 78, 435–463.

Legrand, C., N. Johansson, G. Johnsen, K. Y. Borsheim, E. Graneli, 2001. Phagotrophy and Toxicity Variation in the Mixotrophic Prymnesium patelliferum (Haptophyceae). Limnology and Oceanography, 46(5), 1208-1214.

Levin, S.A., 1970. Community equilibria and stability, and an extension of the community exclusion principle. Am. Nat. 104(939), 413-423.

Litchman, E. 2007. Resource Competition and the Ecological Success of Phytoplankton. In Evolutionof Primary Producers in the Sea, ed. P. G. Falkowski and A. H. Knoll, 75-107. Boston : Elsevier Academic Press.

Morris, Donald P. and William M. Lewis, Jr.,1992. Nutrient limitation of bacterioplankton growth in Lake Dillon, Colorado. Limnol Oceanogr., 37(6), 1179-1192.

Nygaard, K., and A. Tobiesen. 1993. Bacterivory in Algae: A Survival Strategy During Nutrient Limitation. Limnology and Oceanography 38(2):273-279.

Porter, K.G., Sherr, E.B., Sherr, B.F., Pace, M., Sanders, R.W., 1985. Protozoa in planktonic food webs. J. Protozool. 32(3), 409-415.

Raven, J.A., 1997. Phagotrophy in Phototrophs. Limnol. Oceanogr. 42(1), 198-205.

Reynolds, Colin S., 1980. Phytoplankton assemblages and their periodicity in stratifying lake systems. Holarctic Ecology 3:3.

Riemann, B., Søndergaard, M., 1986. Bacteria. In: Riemann, B., Søndergaard, M. (Eds.), Carbon dynamics in eutrophic, temperate lakes. Elsevier Science Publishers, Amsterdam, pp. 127-197.

Roelke, Daniel L., Leslie Schwierzke, Bryan W. Brooks, James P. Grover, Reagan M. Errera, Theodore W. Valenti, Jr., and James L. Pinckney, 2010a. Factors Influencing Prymnesium parvum Population Dynamics During Bloom Initiation: Results from In-Lake Mesocosm Experiments. Journal of the American Water Resources Association, 46(1):76-91. DOI: 10.1111 / j.1752-1688.2009.00392.x

Roelke, Daniel L., George M. Gable, Theodore W. Valenti, James P. Grover, Bryan W. Brooks, James L. Pinckney. 2010b. Hydraulic flushing as a Prymnesium parvum bloom-terminating mechanism in a subtropical lake. Harmful Algae 9, 323–332.

Rothhaupt, K.O., 1996. Laboratory experiments with a mixotrophic chrysophyte and obligately phagotrophic and photographic competitors. Ecology 77(3), 716-724.

Selosse, Marc-Andre´ and Me´ lanie Roy, 2009. Green plants that feed on fungi: facts and questions about mixotrophy. Trends in Plant Science 14(2), 64-70.

Shampine, L. F., Reichelt, M.W., 1997. The MATLAB ODE suite. SIAM J. Sci. Comput. 18(1), 1-22.

Sommer, U., A. M. Gliwicz, W. Lampert, and A. Duncan, 1986. The PEG-model of seasonal succession of planktonic events in fresh waters. Arch. Hydrobiol. 106:433-47.

Southard, Gregory M., Loraine T. Fries, and Aaron Barkoh, 2010. Prymnesium parvum: The Texas Experience. Journal of the American Water Resources Association, 46(1):14-23. DOI: 10.1111/j.1752-1688.2009.00387.x

Sterner, R. W. 1989. The role of grazers in phytoplankton succession. Pages 107-169 in: Sommer, U. (ed.). Plankton Ecology: Succession in Plankton Communities. Springer-Verlag, Berlin.

Sterner, Robert W.,1993. Daphnia growth on varying quality of *Scenedesmus*: mineral limitation of zooplankton. Ecology, 74(8) 235 1-2360.

Sterner, Robert W. and Dag O. Hessen, 1994. Algal nutrient limitation and the nutrition of aquatic herbivores. Annu. Rev. Ecol. Syst., 25:1-2.

Sterner, Robert W., James J. Elser, Everett J. Fee, Stephanie J. Guildford, Thomas H. Chrzanowski, 1997. The light:nutrient ratio in lakes: The balance of energy and materials affects ecosystem structure and process. The American Naturalist, 150(6), 663-684.

Stibor, Herwig and Ulrich Sommer, 2003. Mixotrophy of a Photosynthetic Flagellate viewed from an Optimal Foraging Perspective. Protist, 154, 91–98.

Stickney, H.L., R.R. Hood, D.K. Stoecker, 2000. The impact of mixotrophy on planktonic marine ecosystems. Ecological Modelling 125, 203–230.

Stoecker, D.K., 1998. Conceptual models of mixotrophy in planktonic protists and some ecological and evolutionary implications. Eur. J. Protistol. 34(3), 281-290.

Stoecker, D.K. 1999. Mixotrophy among Dinoflagellates. Journal of Eukaryn Microbiology. 46(4):397-401.

Thingstad, T. F., Havskum, H., Garde, K., Riemann, B., 1996. On the strategy of "eating your competitor": A mathematical analysis of algal mixotrophy. Ecology 77(7), 2108-2118.

Thingstad, T.F. 1987. Utilization of N, P, and organic C by heterotrophic bacteria. I. Outline of a chemostat theory with a consentient concept of “maintenance” metabolism. Mar. Ecol. Prog. Ser. 35, 99-109.

Tilman, D., 1982. Resource Competition and Community Structure. Princeton University Press, Princeton.

Tittel, J., Bissinger, V., Zippel, B., Gaedke, U., Bell, E., Lorke, A., Kamjunke, N., 2003. Mixotrophs combine resource use to outcompete specialists: Implications for aquatic food webs. Proc.Natl. Acad. Sci. 100(22), 12776–12781.

Troost, T.A., Kooi, B.W., Kooijman, S.A.L.M., 2005a. Ecological specialization of mixotrophic plankton in a mixed water column. Am. Nat. 166(3), E45-E61.

Troost, T.A., Kooi, B.W., Kooijman, S.A.L.M., 2005b. When do mixotrophs specialize? Adaptive dynamics theory applied to a dynamic energy budget model. Math. Biosci. 193, 159–182, doi:10.1016/j.mbs.2004.06.010.

Urabe, J., and Y. Watanabe. 1992. Possibility of N or P limitation for planktonic cladocerans: An experimental test. Limnology and Oceanography 37: 244-251.

Vadstein, O., 2000. Heterotrophic planktonic bacteria and cycling of phosphorus: phosphorus requirements, competitive ability, and food web interactions. Adv. Microb. Ecol. 16, 115-167.

Zubkov, M.V., Tarran, G.A., 2008. High bacterivory by the smallest phytoplankton in the North Atlantic Ocean. Nature 455, 224-227.

BIOGRAPHICAL INFORMATION

K. W. Crane received his B.S. degree in Biology in 1993 from the University of Texas at Austin. He later received secondary teaching certificates in composite science, mathematics, and computer science. He spent many years teaching high school and while doing so, earned a master's degree in Interdisciplinary Science in 2002 with the fields of biology and math from The University of Texas at Arlington. He later returned to combine these two fields into research in mathematical models to earn his Ph.D. His main focus was on the incorporation of mixotrophy into theoretical ecosystem models. He will return to teaching and continue his research in theoretical ecology.